

Recent soft QCD results from ATLAS and CMS

Valentina Cairo

On behalf of the ATLAS and CMS collaborations

LHCP 2019

Puebla, Mexico

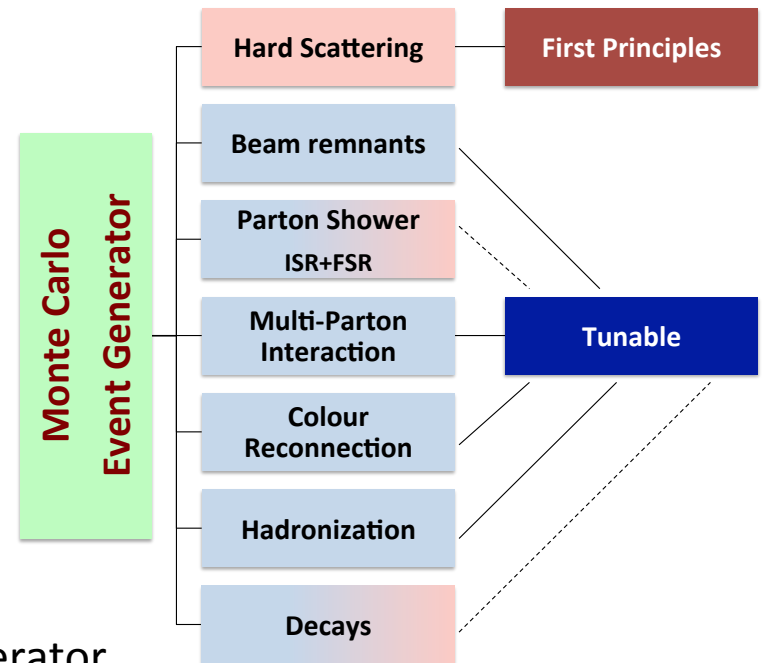
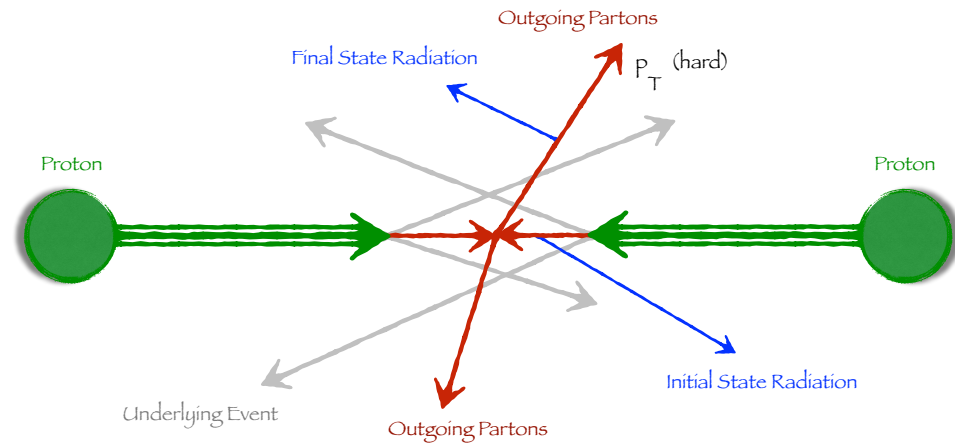
May 20th – 25th 2018



NATIONAL
ACCELERATOR
LABORATORY

Introduction

- Hard QCD events: tiny fraction of the **total pp cross-section**, which is **dominated by soft events** (peripheral processes) → while hard QCD processes can be studied by means of perturbative approaches, this is not possible for the soft QCD events
- The development of **Monte Carlo (MC) event generators** began shortly after the discovery of the partonic structure of hadrons and the formalisation of QCD as the theory of strong interactions → Models have to be developed with a set of **tunable parameters** to describe the hadron-level properties of final states dominated by soft QCD

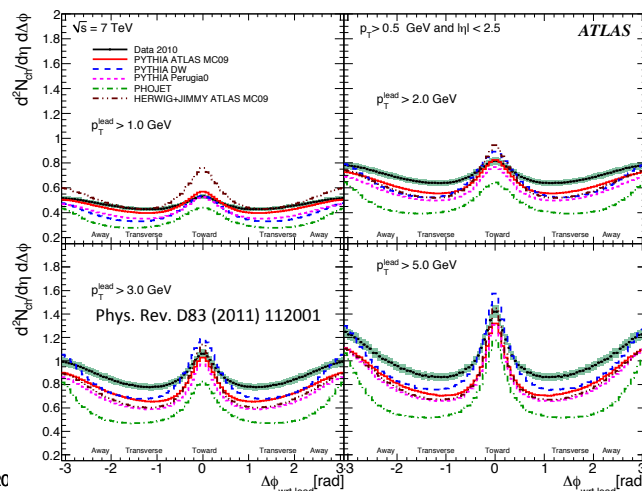
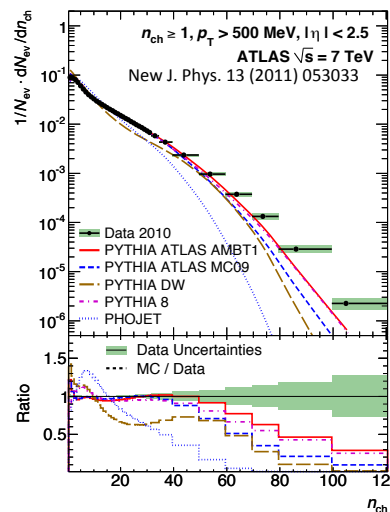
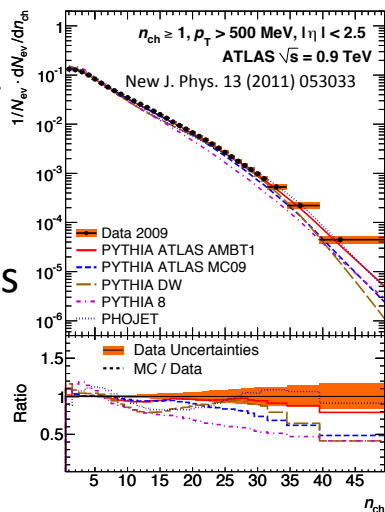


Soft QCD measurements are:

- **Crucial for the tuning** of the Monte Carlo event generator
- **Essential to understand** and correctly simulate any other more **complex phenomena**
- **Mostly track-based, so also ideal to study tracking performance** in the “early” stage of a new data taking...

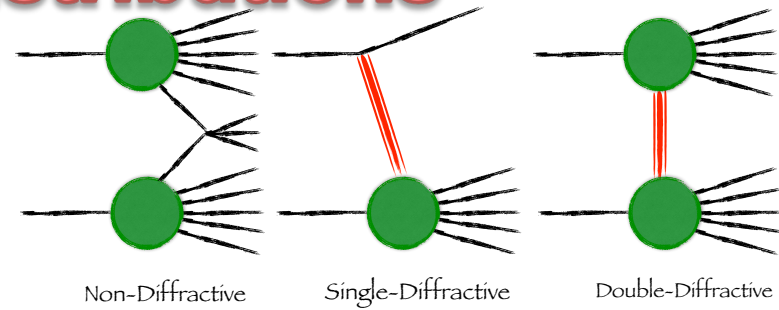
What do we talk about today?

The LHC experiments offer a broad range of soft QCD measurements, all ATLAS and CMS results can be found at the following webpages: [ATLAS](#), [CMS](#)

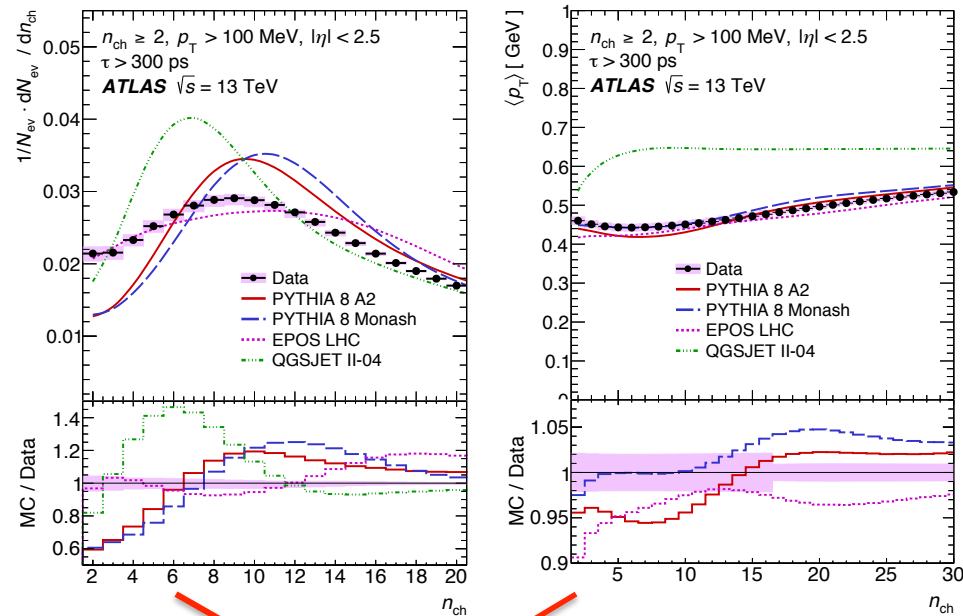


- **Run 1 Summary: higher min bias and underlying event activity in data than that predicted by Monte Carlo models tuned to pre-LHC data**
- Today: Some recent highlights (recently published in most cases) are selected here (mainly based on my personal taste) which revolve around:
 - **Charged-particle multiplicity (only en-passant)**
 - Low p_T 13 TeV minimum bias in ATLAS and 5.44 TeV Xe-Xe results from CMS
 - **Single Diffractive Cross-Section**
 - First LHC results from both ATLAS+ALFA and CMS+Totem (8 TeV)
 - **Underlying Event**
 - Mainly with a leading Z-boson (measured by both ATLAS and CMS)
 - Also at forward pseudorapidities with CMS+CASTOR
 - **Double Parton Scattering**
 - In 4 lepton final state, in ATLAS
 - In same-sign WW events in CMS

Charged-particle distributions



[Eur. Phys. J. C \(2016\) 76:502](#)

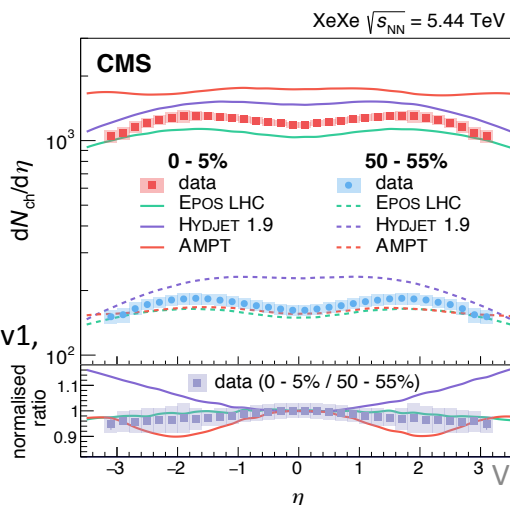


Low n_{ch} not well modelled, large contribution from diffraction

EPOS LHC gives the best predictions of charged particle multiplicities both in proton and heavy ion collisions!

- Inclusive charged-particle measurements in pp collisions provide insight into the **strong interaction** in the low energy, **non-perturbative QCD region**
- Main source of background when more than one interaction per bunch crossing
- Perturbative QCD can not be used for peripheral interactions
 - ND described by QCD-inspired phenomenological models (tunable)
 - SD and DD hardly described and little data available** (back to this in a tiny bit)
- Goal: Measure spectra of unfolded primary charged particles** (inclusive measurement – do not apply strong model dependent corrections)

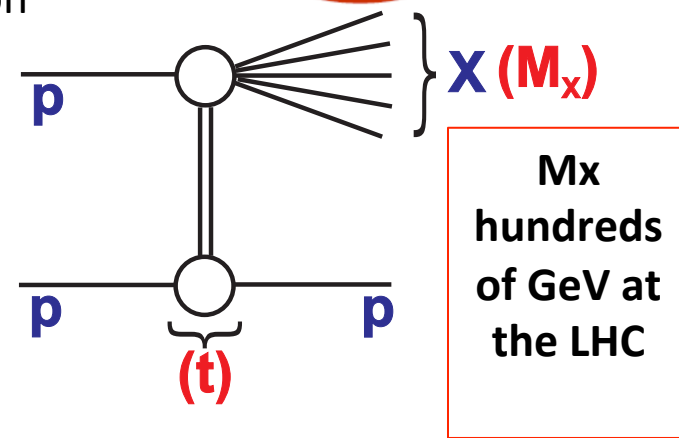
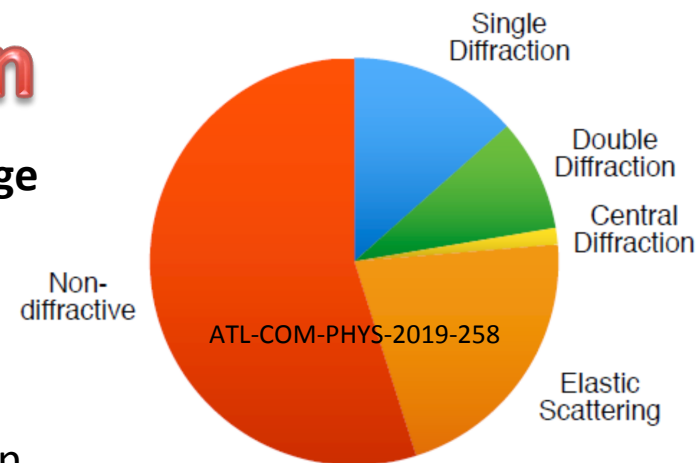
Measured in heavy ion collisions too, for instance in 5.44 TeV Xe-Xe collisions by CMS



arXiv:1902.03603v1, submitted to PLB

Single-Diffractive Cross-Section

- Single diffractive dissociation $\sim 10\%$ of the total XS: **exchange of a net colour-singlet strongly interacting object, a Pomeron**
- Universal Pomeron for total, elastic and diffractive processes has a long history of investigation
- Important ingredient in understanding low Bjorken- x region of proton structure, cosmic ray air showers, and even the string theory of gravity
- Experimentally, diffractive events can be selected by:
 - **large rapidity gaps** \rightarrow not able to distinguish SD, DD and ND and to access the squared 4-momentum transfer t and energy loss ξ of the proton
 - **scattered proton** \rightarrow direct access to t and suppression of other contributions
- ATLAS and CMS measured diffractive cross-sections through large rapidity gaps and recently released the **first SD differential cross-section measurements through direct detection of the intact proton in the forward detectors ALFA and TOTEM**
 - 8 TeV dedicated dataset (July 2012, $\mu < 0.08$, $\beta^* = 90$ m)

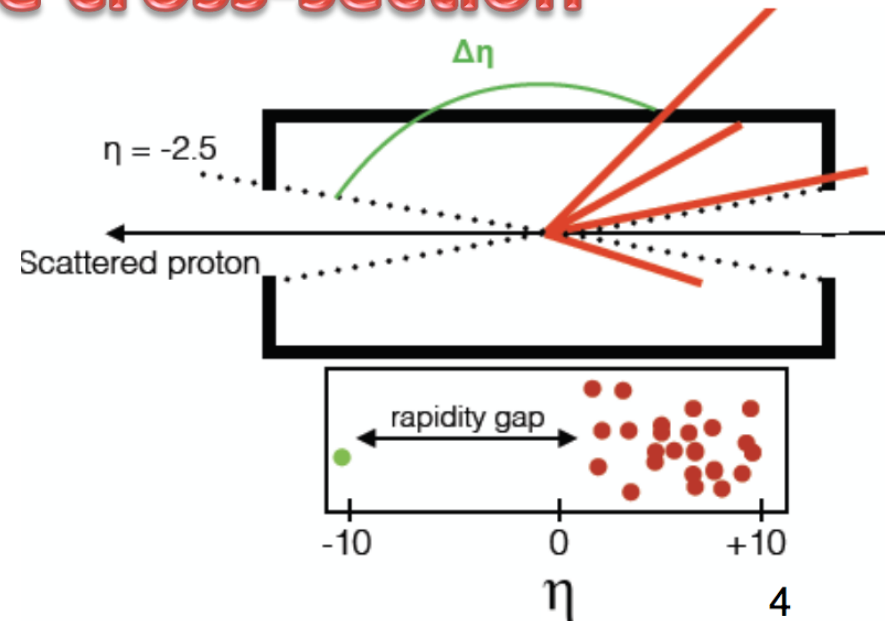


$t < 1 \text{ GeV}^2 \rightarrow$ the intact proton scatters through a very small angle ($10\text{-}100 \mu\text{rad}$)

Small fractional energy loss
 $\xi = M_x^2/s$

Hadron level cross-sections: σ vs t , ξ , $\Delta\eta$

- **Py8 A3 as default, Py8 A2 as alternative**
- Both tunes use the **H1 2006 Fit B** diffractive parton densities as an input to model the hadronisation in the diffractive channels.
- **Herwig7** compared to Py8 for uncertainties from hadronisation properties of the dissociation system X



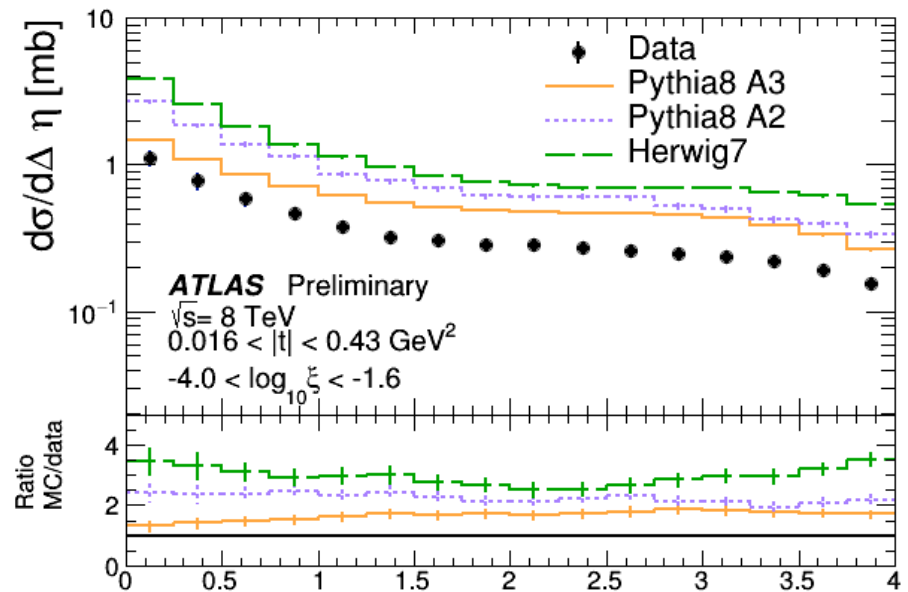
Background from non-SD pp collisions:

- **Single source** \rightarrow correlated signals in ALFA and the ID (estimated from MC)
- **Overlay Background** \rightarrow coincidences of a signal in ALFA with an uncorrelated signal in the ID (data-driven estimate, contributes the largest uncertainty)

Selection:

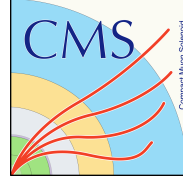
L1 trigger: MBTS(A/C) and ALFA(C/A)
 ALFA: exactly one reconstructed proton
 MBTS: at least 5 counters above threshold
 ID: at least 1 track with $p_T > 200$ MeV & $|\eta| < 2.5$
 Reconstructed vertex

Fiducial region: $0.016 < |t| < 0.43$ GeV²,
 $-4.0 < \log_{10}(\xi) < -1.6$, ($80 < MX < 1270$ GeV)

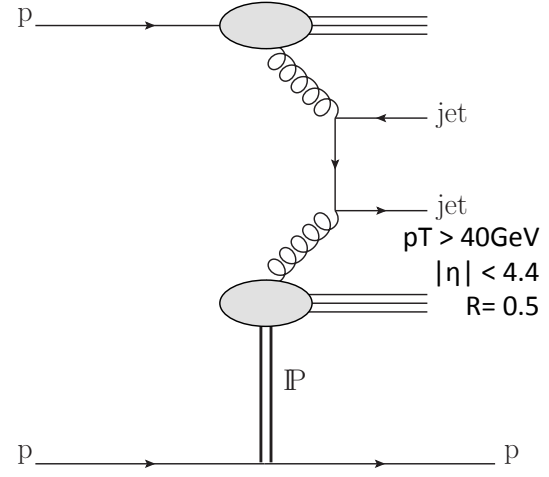


All models overestimate the XS! $\Delta\eta$ 6

Diffractive di-jet cross-section



- **SD in di-jet events:** $d\sigma/dt$, $d\sigma/d\xi$ and $R(x)$ (ratio between SD and inclusive di-jet XS) (measured in large η gaps by ATLAS at 7 TeV ([Phys. Lett. B 754 \(2016\) 214](#)))
- Trigger **simultaneously in CMS and TOTEM**
- **Main background:** overlap of a pp collision in CMS and an additional track in the RP stations
- Dominant uncertainties: **jet energy scale** and **horizontal dispersion**

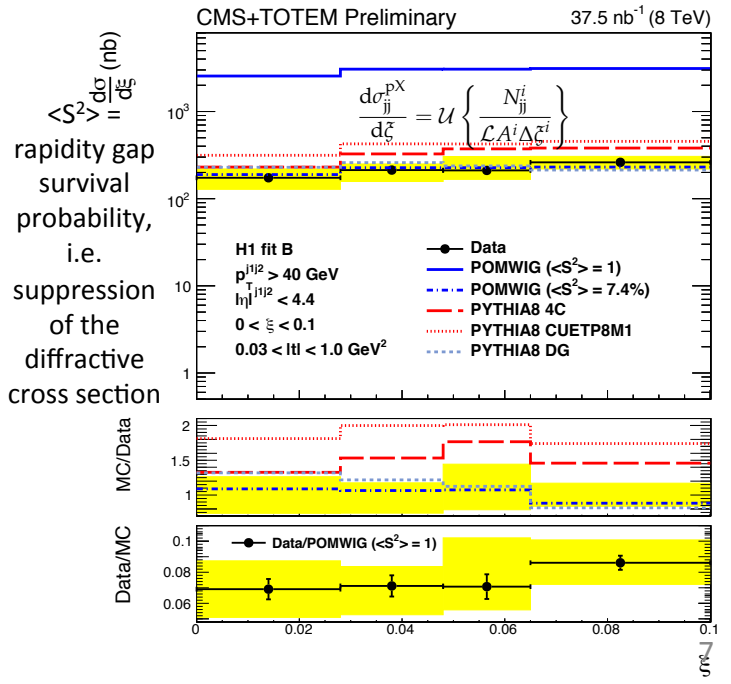
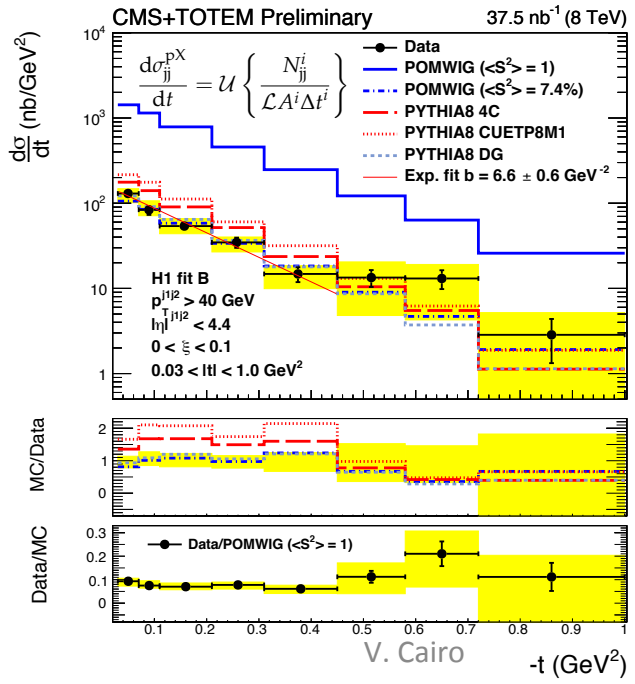


$$\sigma_{jj}^{pX} = 21.7 \pm 0.9 \text{ (stat)} \pm_{-3.3}^{+3.0} \text{ (syst)} \pm 0.9 \text{ (lumi) nb}$$

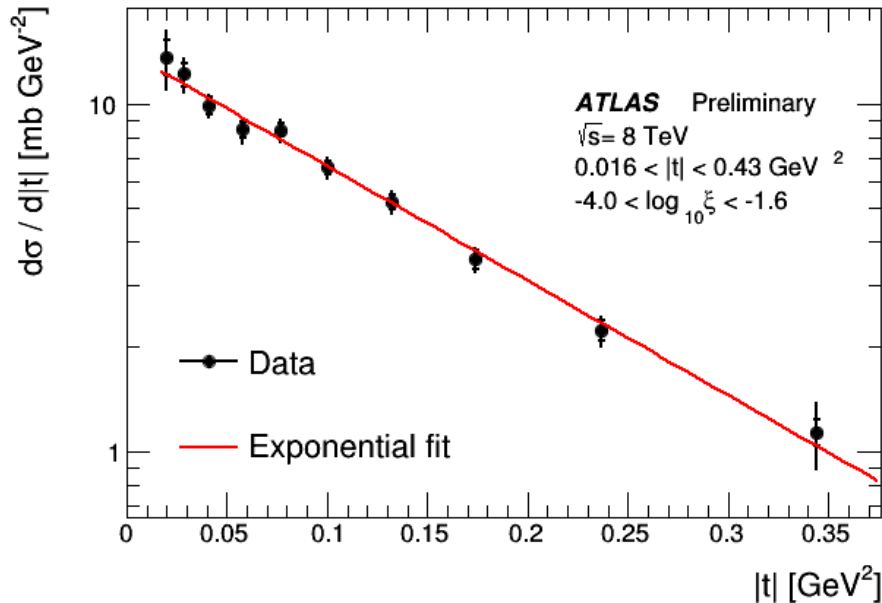
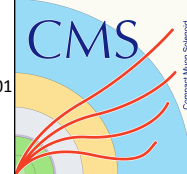
Py8 DG $\sigma_{jj}^{pX} = 23.7 \text{ nb}$

POMWIG: sum of Pomeron (pIP, $\sigma_{pIP} = 256\text{nb}$), Reggeon (pIR, $\sigma_{pIR} = 31\text{nb}$) and Pomeron-Pomeron (IPIP, $\sigma_{IPIP} = 6.8\text{nb}$) exchange contributions. NLO dPDF

PYTHIA8: only Pomeron (pIP) contribution ($\sigma_{pIP} = 280 \text{ nb}$). LO dPDF

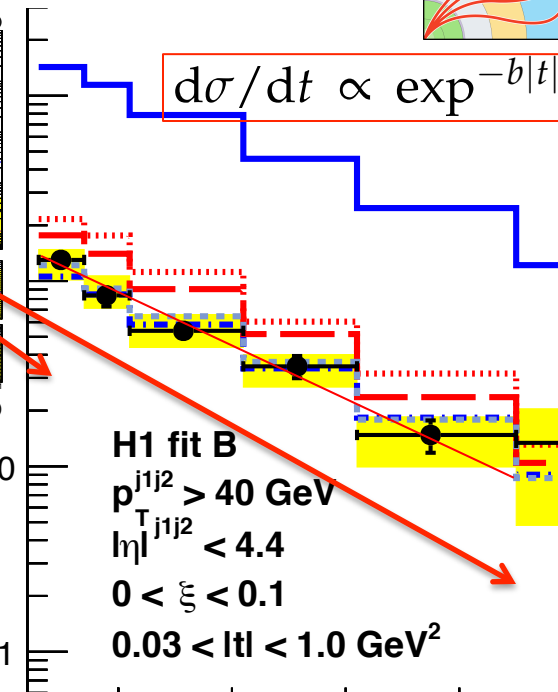
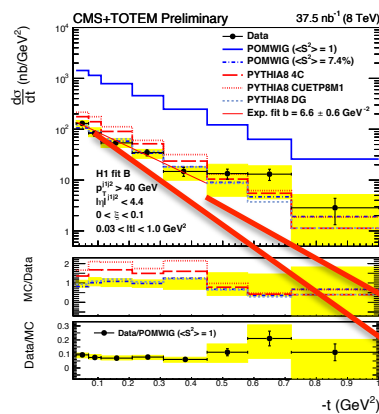


SD Cross-Sections comparison



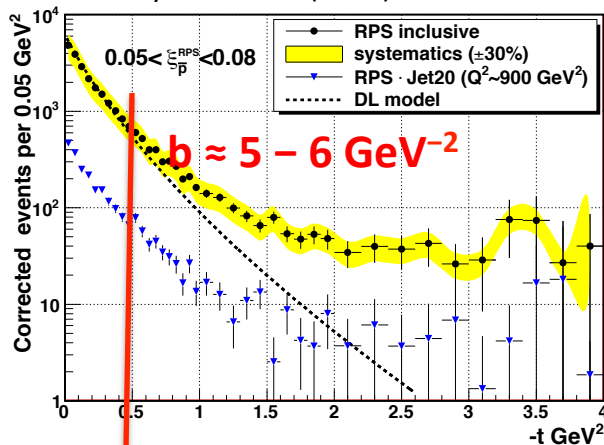
$$B = 7.60 \pm 0.23(\text{stat.}) \pm 0.22(\text{syst.}) \text{ GeV}^{-2}$$

Py8 A3: 7.10 GeV⁻² (1.6σ compatibility), Py8 A2: 7.82 GeV⁻² (0.7σ compatibility)



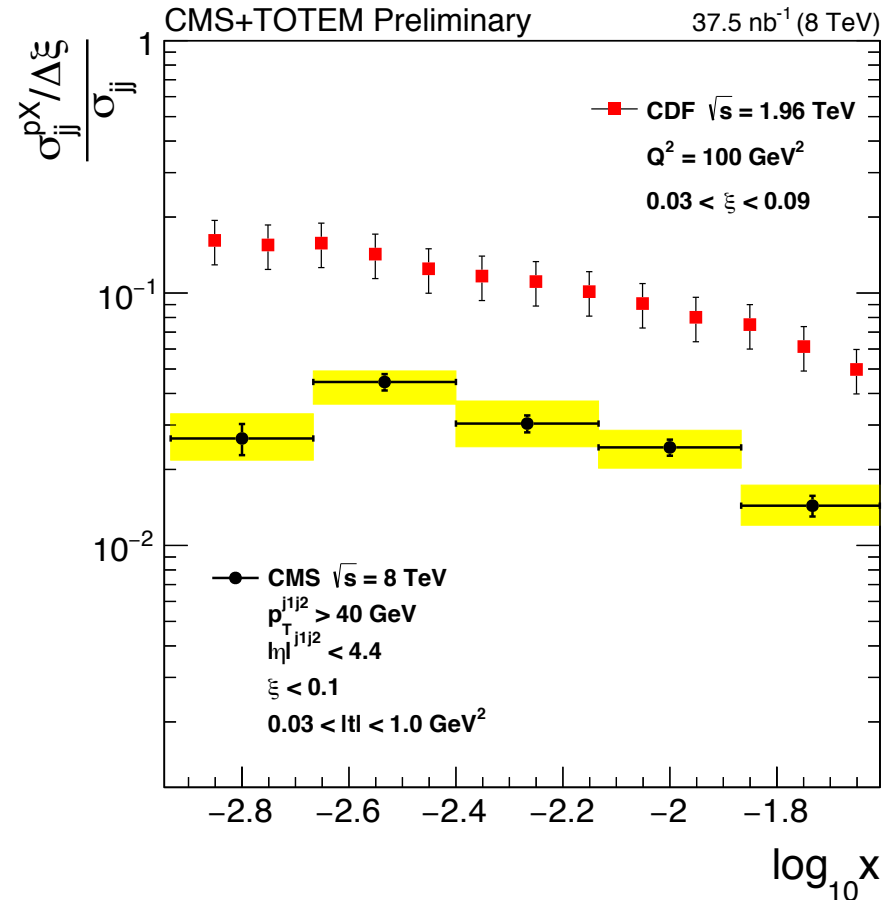
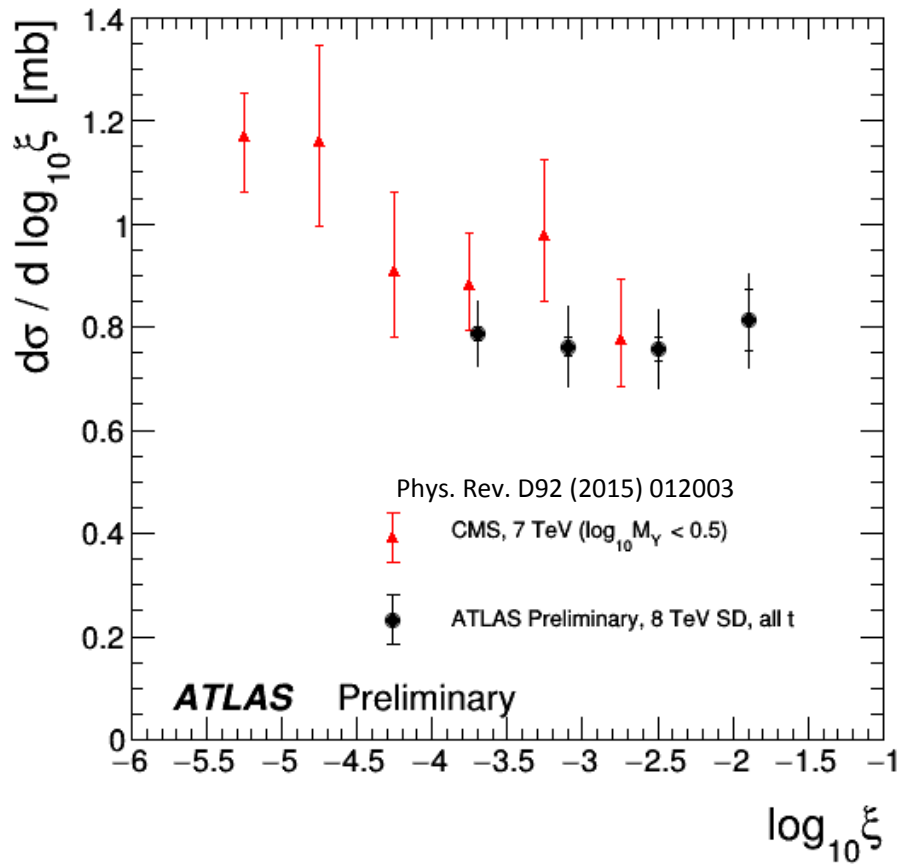
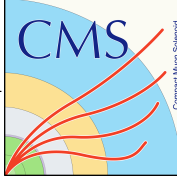
$$b = 6.6 \pm 0.6 (\text{stat}) \pm_{-0.8}^{+1.0} (\text{syst}) \text{ GeV}^{-2}$$

Phys.Rev. D86 (2012) 032009



- Larger uncertainties in CMS wrt ATLAS, but also larger t range
- CMS exp.slope not significantly larger than that from CDF in the small- $|t|$ region
 - The current data do not yet show conclusive evidence for a flattening of the t distribution in the larger $|t|$ region

SD Cross-Sections comparison



A decrease of the ratio of diffractive to non-diffractive cross sections with \sqrt{s} has also been observed by CDF by comparing data at 630 and 1800 GeV

The Underlying Event

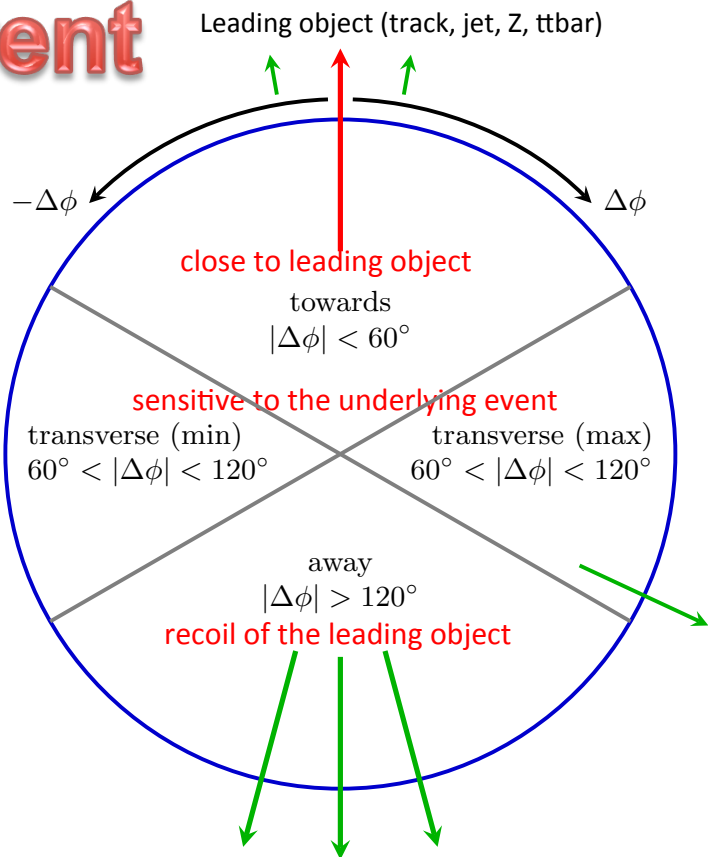


Photos by F. Cairo, *Musée du Louvre*

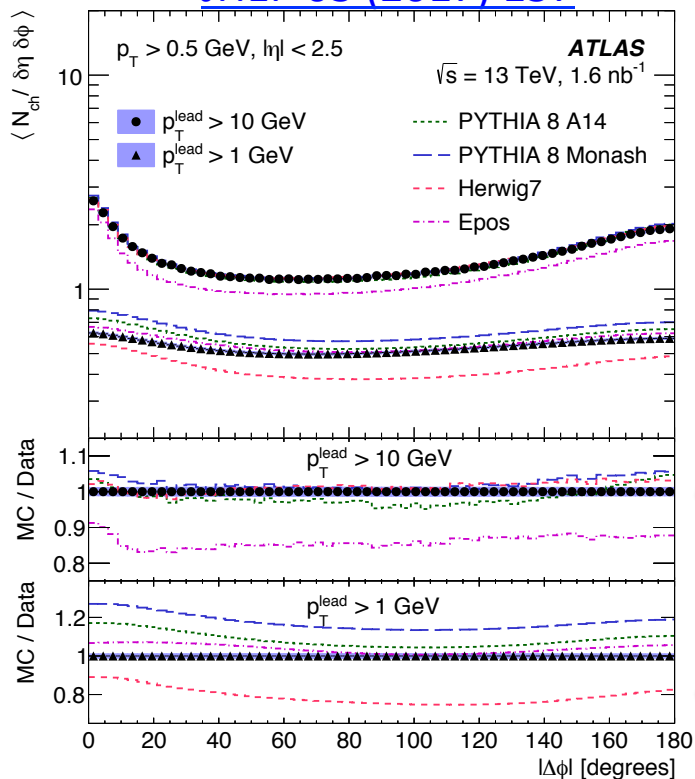
Underlying Event

Underlying Event (UE): activity accompanying any hard scattering in a collision event:

- Partons not participating in a hard-scattering process (beam remnants)
- multiple parton interactions (MPI)
- Initial and final state gluon radiation (ISR, FSR)



JHEP 03 (2017) 157

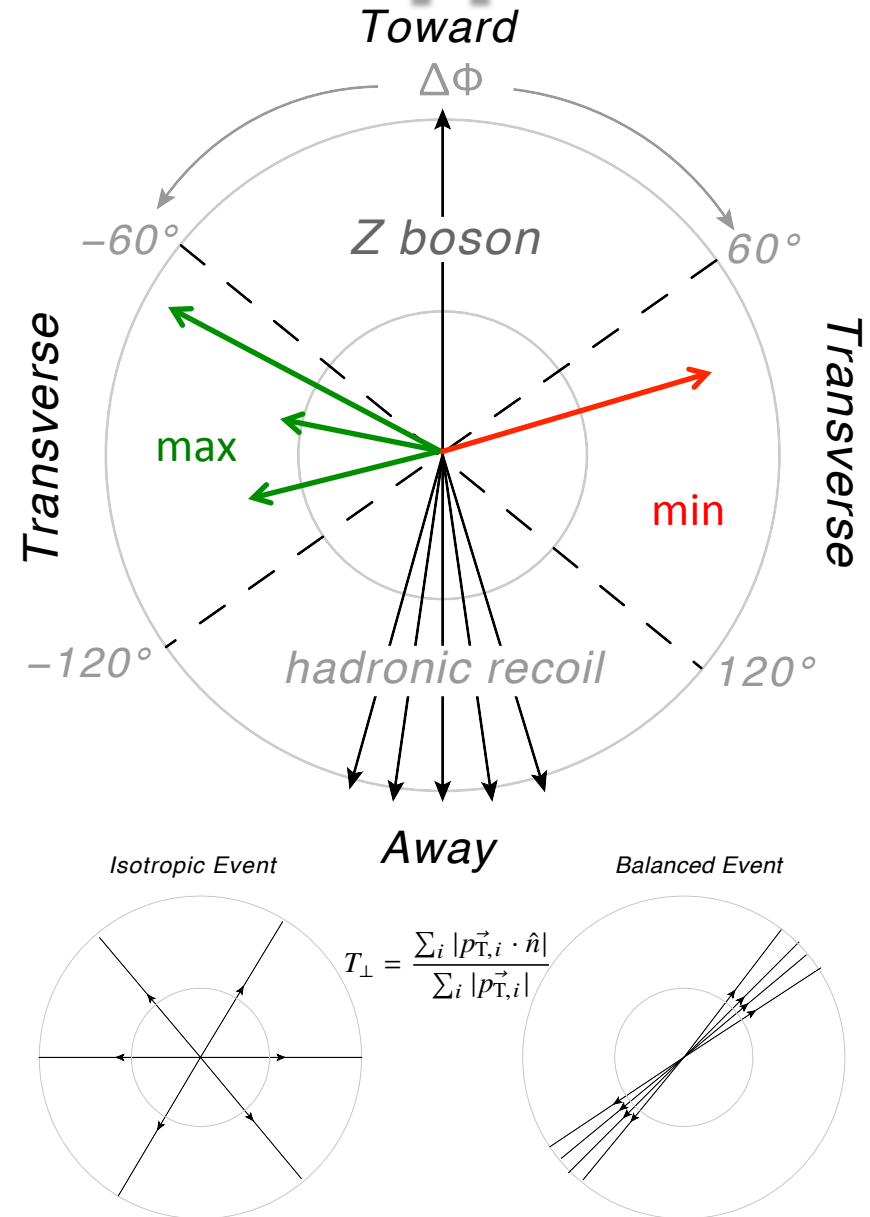


- **First 13 TeV ATLAS analysis based on leading track:**
 - **Same dataset and same event and track selection as the MinBias analysis** with an additional request: leading track with a p_T of at least 1 GeV

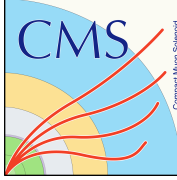
Transition from relatively isotropic minimum-bias scattering to the emergence of hard partonic scattering structure and hence a dominant axis of energy flow

Underlying Event in $Z \rightarrow \mu\mu$

- Processes with leptonic final states like **Z events** are **experimentally clean** and **theoretically well understood**, allowing reliable identification of the particles from the underlying event
- The **absence of QCD FSR** permits a study of different kinematic regions with varying transverse momenta of the Z boson due to harder or softer ISR
- The final state Z boson is well-identified and colour neutral, so that **interaction between the final state leading particle and the UE is minimal**
- Low-thrust** ($T_{\perp} \leq 0.75$): sensitive to MPI
- Trans-min**: distinguish UE from extra jet activity (from HS)

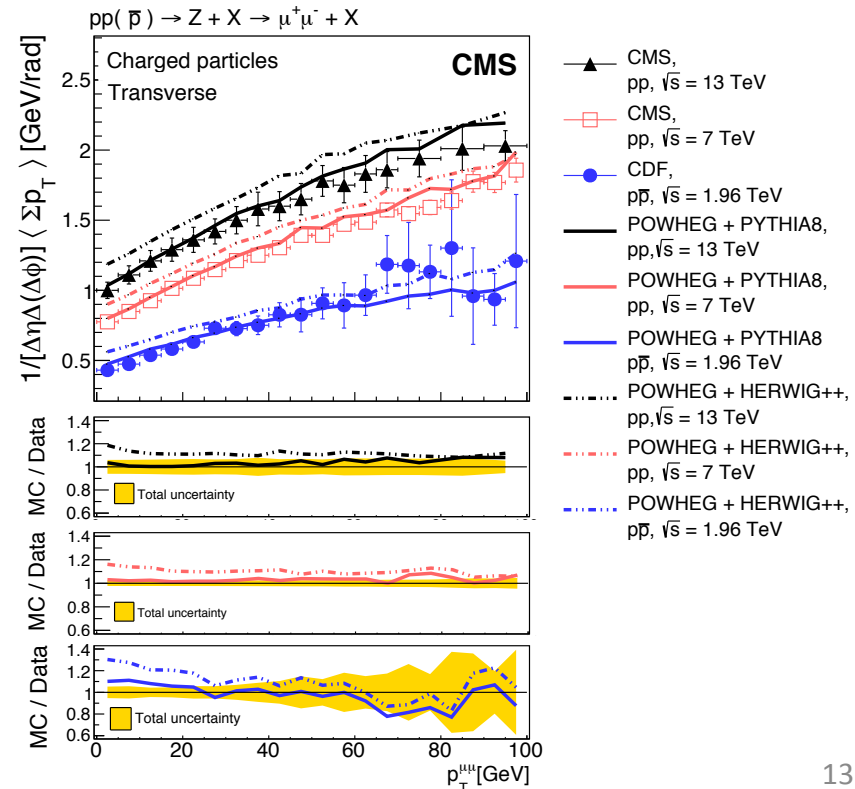
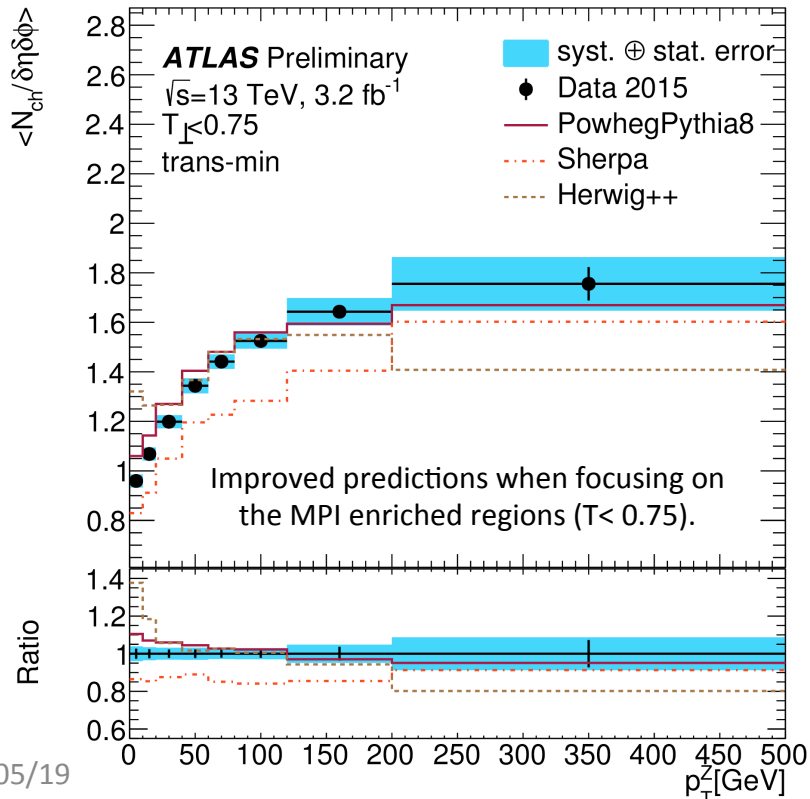


Underlying Event in $Z \rightarrow \mu\mu$

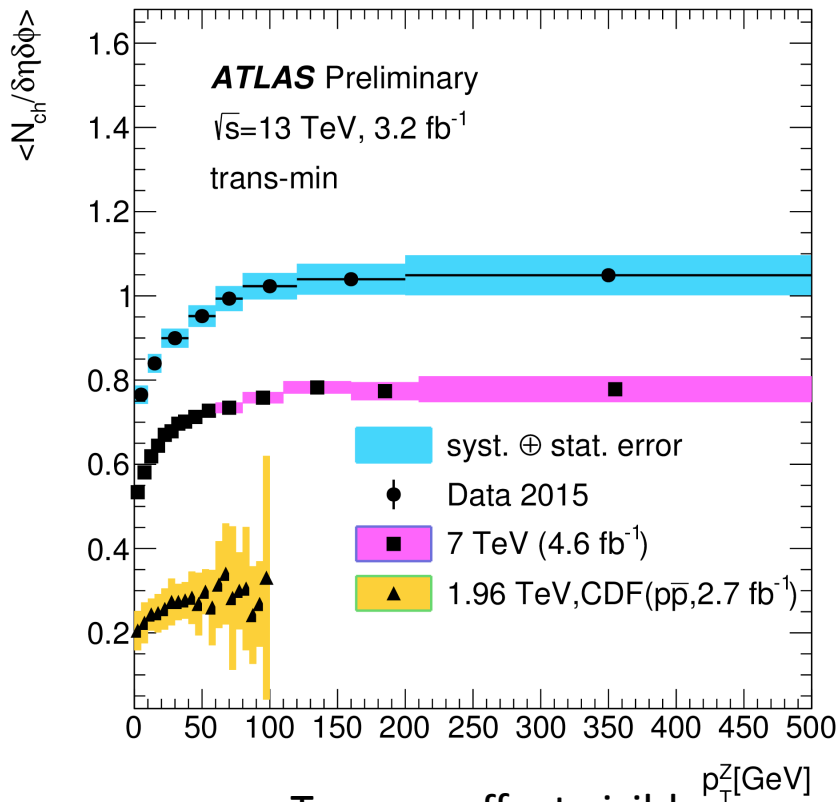


- Tracks $p_T > 0.5$ GeV and $|\eta| < 2$ (2.5) in CMS (ATLAS)
- $p_T > 20$ GeV (CMS, lead), 10 GeV (CMS, sublead), 25 GeV (ATLAS)
- $81 < m_{ll} < 101$ (CMS), $66 < m_{ll} < 116$ (CMS)
- Background from top and dibosons $< 1\%$ (mainly at low p_T^Z) for both ATLAS and CMS. MJ data-driven in ATLAS $< 0.1\%$

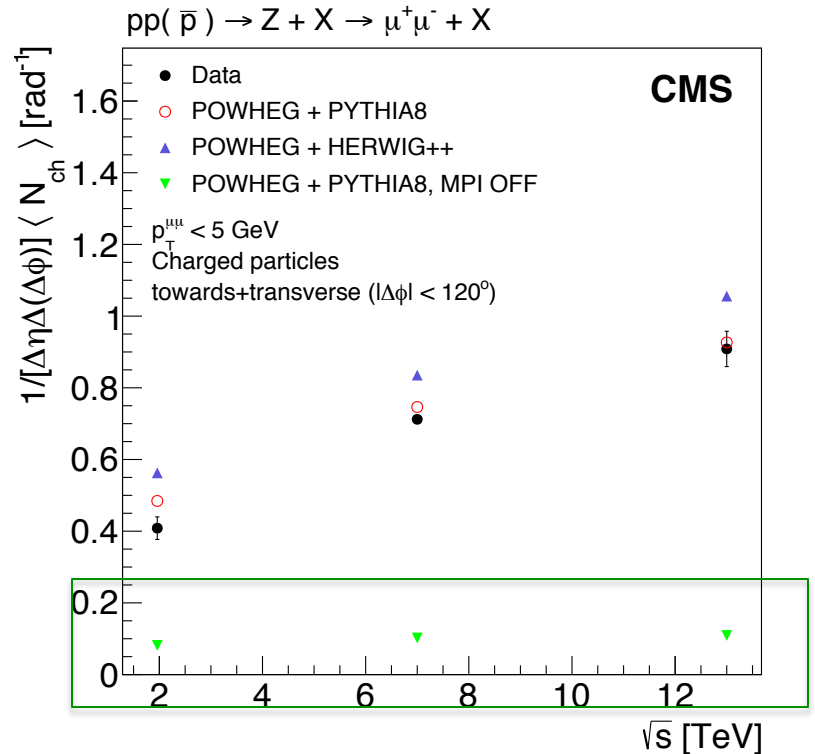
- **CMS:** 2D iterative unfolding, with a response matrix constructed with LO MADGRAPH + PYTHIA8 (CUET8PM1 tune) (for signal simulation NLO MC@NLO)
- **ATLAS:** iterative unfolding in bins of p_T^Z and thrust, with a response matrix constructed with NLO Powheg (CTEQ6L1) + Pythia8 (AZNLO tune) (same as for signal simulation)
- **Largest systematic uncertainties from model dependence and tracking efficiency**



Underlying Event in $Z \rightarrow \mu\mu$

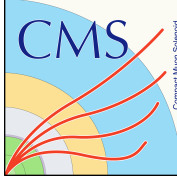


- Turn-on effect visible
- Increase in the underlying event activity with \sqrt{s}



- The comparison of the distributions **with and without MPI** indicates that the ISR and FSR contributions, which increase slowly with center-of-mass energy, are small.

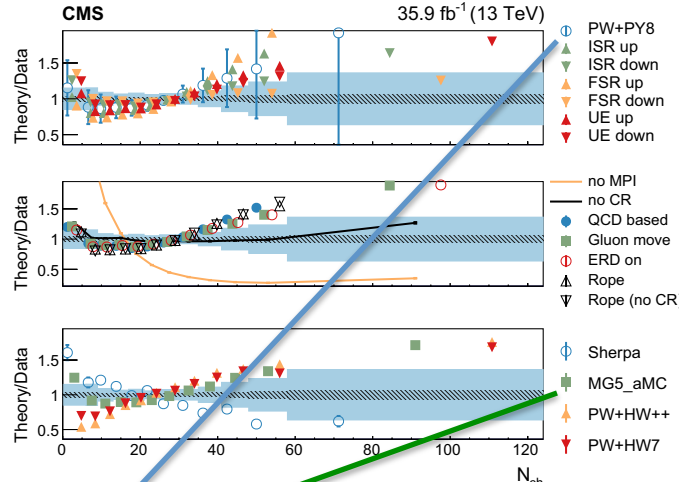
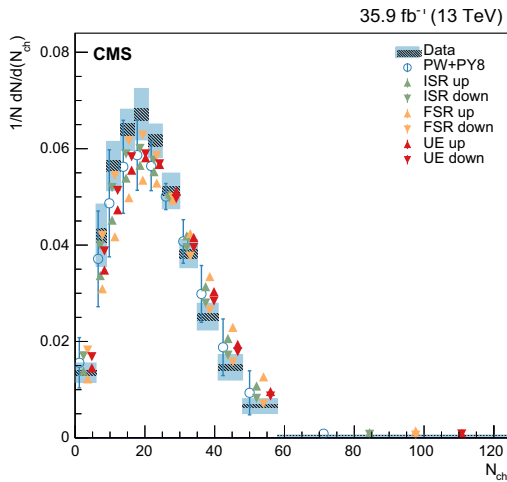
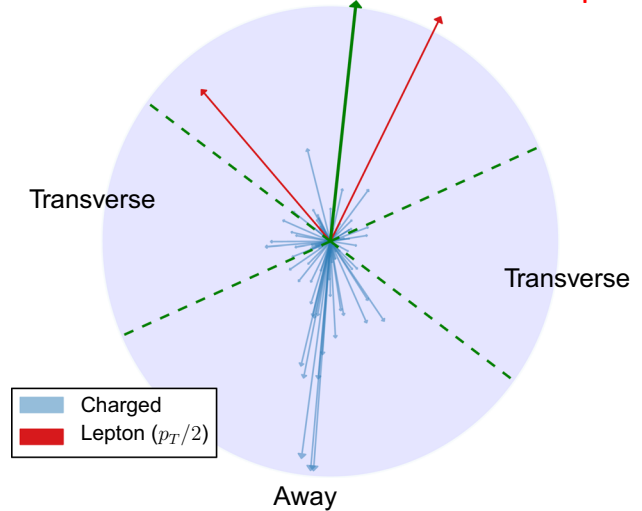
New handles to better understand the evolution of ISR, FSR, and MPI contributions separately, as functions of the event energy scale and the collision energy.



Underlying Event in Top-pairs

- CMS characterized for the first time **UE in ttbar events** (with $t \rightarrow Wb$), factorization scale above 2x the top mass
- Many variables investigated (N_{ch} , p_T , aplanarity, sphericity, etc) as well as their profiling for various event categories

CMS Simulation $t\bar{t} \rightarrow (e\nu b)(\mu\nu b)$ (13 TeV)
Toward, $\vec{p}_T(\ell\ell)$ **>90% purity**

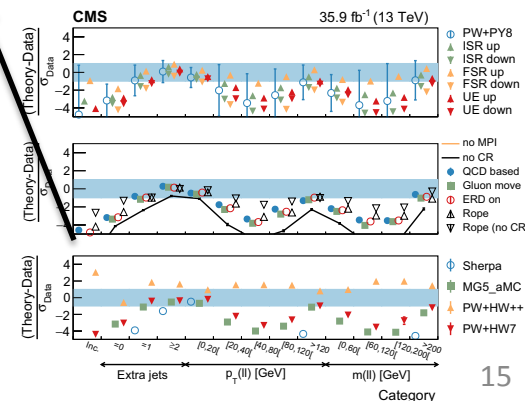
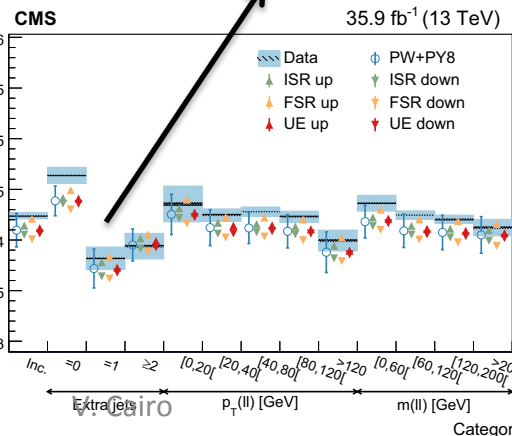


Shape variables are sensitive to event categorizations
→ more isotropic event when no additional jets are present and more sensitivity to CR

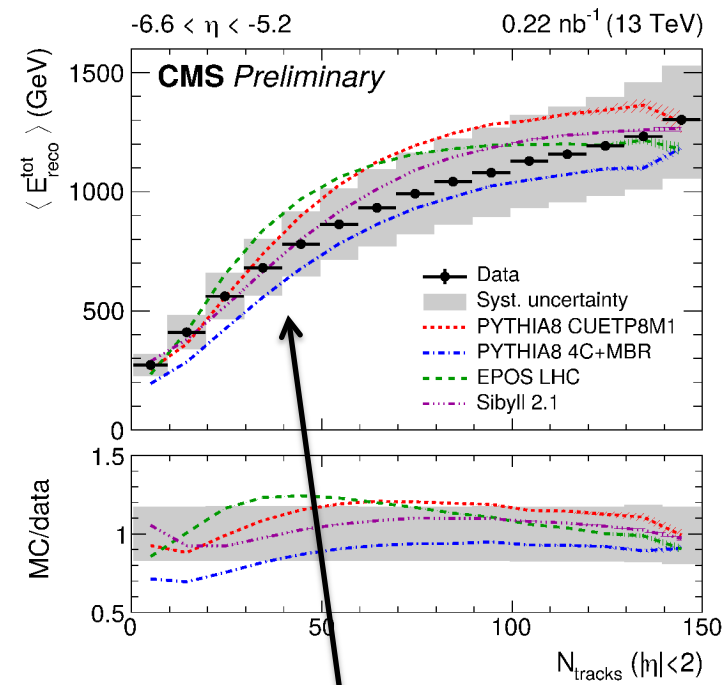
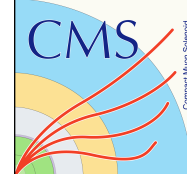
O(20) charged particles, average p_T and p_z both being ≈ 2 GeV, vectorially summing to a recoil of about 10 GeV.

No sizable dependence on Matrix element generator (similar predictions from PW+Py8 and MG5_aMC), but large dependence on PS.

Data favor predictions from PW+Py8 (CUETP8M2T4 tune), disfavor MPI and CR switched off, PW+H7, PW+H++ and Sherpa. The usage of NLO matrix element (MG5_aMC) has a negligible effect

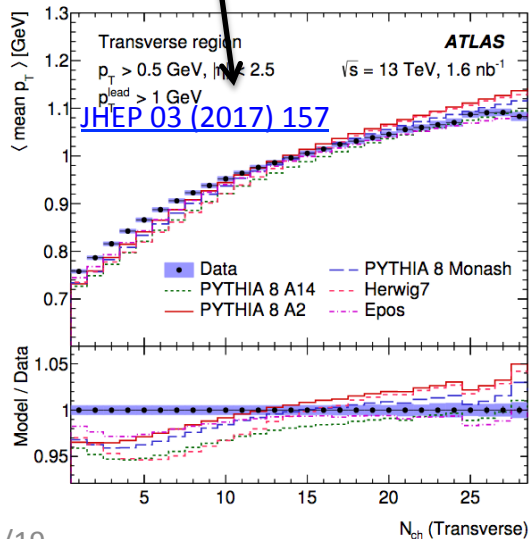


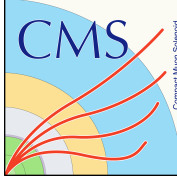
UE at forward rapidities



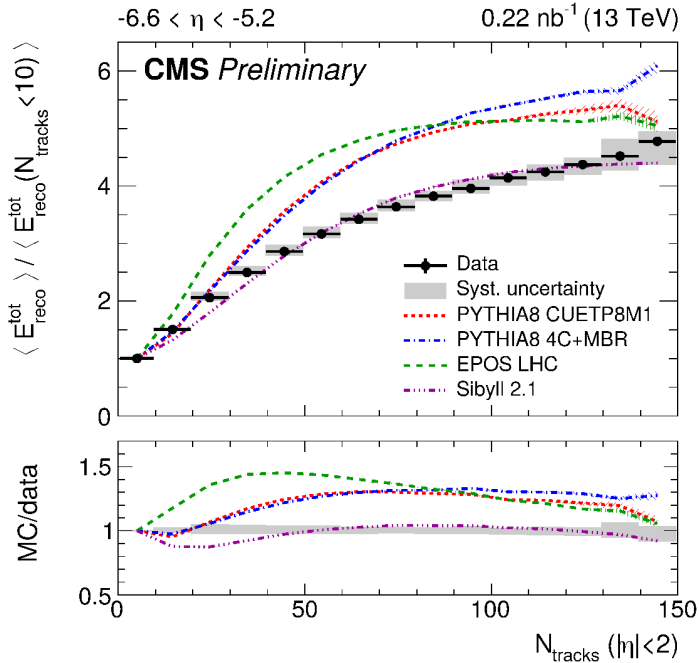
Energy carried by particles produced in the very forward region covered by is a **powerful probe of UE**: first correlation of hadron activity at very forward and central rapidities

- **Average total energy** as well as its hadronic and electromagnetic components are measured with CMS+CASTOR at $-6.6 < \eta < -5.2$ in pp collisions at 13 TeV and presented as a function of the multiplicity of charged particle tracks in the region $|\eta| < 2$
- Statistical uncertainty $< 2\%$, dominated by systematic uncertainties (mainly energy scale)
- Average total energy increases with multiplicity, **consistent with the UE at central rapidities**
- **The model parameter tunes for the underlying event, as determined at central rapidities, are consistent with the very forward data within experimental uncertainties.**
- Py8 4C+MBR and SIBYLL 2.3c underestimate data at low Nch
- Py8 CP5 predicts average energies larger than those observed at intermediate Nch

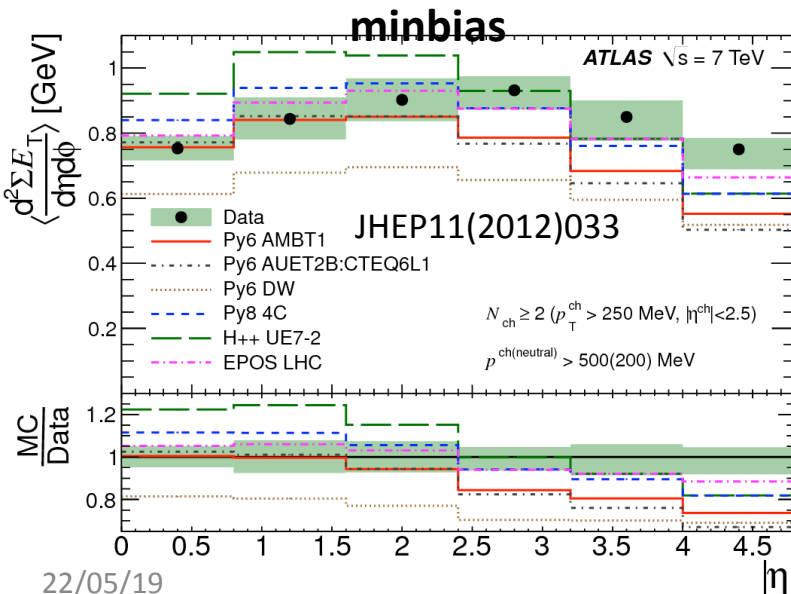




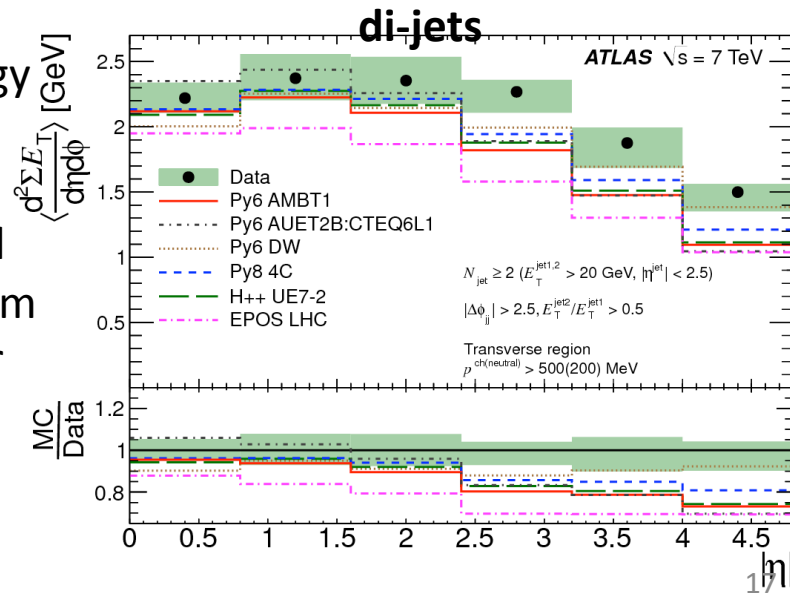
UE at forward rapidities



- Distributions normalised to the first Nch bin ($N_{\text{ch}} < 10$) \rightarrow systematic uncertainty reduced
- **Relative increase is steep at low multiplicities and becomes softer at higher multiplicities.**
- Py 8 tunes have very similar shapes, inconsistent with that observed in the data (worst for Py8 CP5, optimised for UE at central rapidity)
- All the other generators see a saturation at about Nch 80, not visible in data
- Worst predictions from **EPOS LHC**



Previous energy flow results from ATLAS showed good predictions from **EPOS LHC** for minbias like events



Double parton scattering

- One source of the underlying-event activity is MPI
- In high-energy pp interactions, where the density of low-x partons is high, there is enough energy to produce hard multi-parton interactions
- The simplest example is hard **double-parton scattering (DPS)**: two partons from each proton interact with each other leading to perturbative final states.
- Twofold interest in studying DPS:
 1. the probability of it and the potential correlations between the products of these two perturbative interactions provide valuable information about the dynamics of the partonic structure of the proton.
 2. DPS processes may also constitute a background to reactions proceeding through single-parton scattering (SPS).

$$pp \rightarrow A + B + X$$

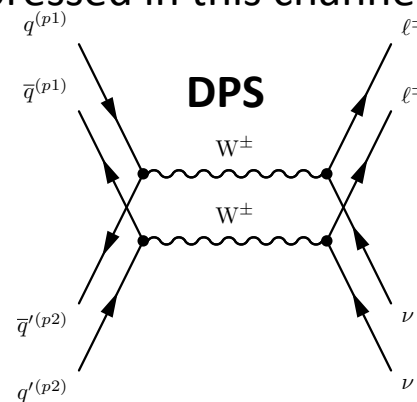
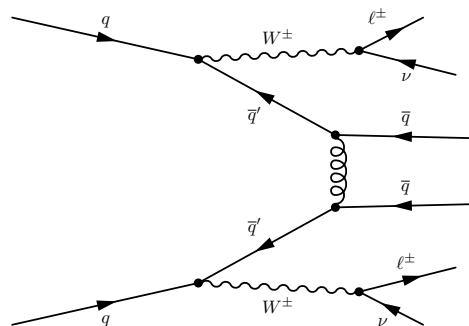
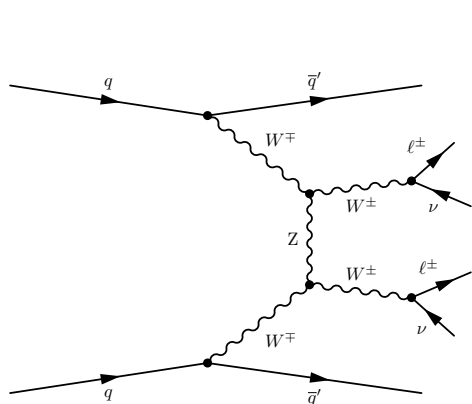
symmetry factor
 $k = 1$ if $A = B$
 or
 $k = 2$ if $A \neq B$

$$\sigma_{DPS}^{AB} = \frac{k}{2} \frac{\sigma_{SPS}^A \sigma_{SPS}^B}{\sigma_{eff}}$$

Production cross-section of state A and B in a single-parton scattering

effective transverse overlap area containing the interacting partons
 (measured to be around 15 mb)

- ATLAS: 8 TeV, 20 fb⁻¹, inclusive 4l production**, decay products of two Z^(*) bosons produced in two distinct parton–parton scatterings within the same pp interaction
 - Drell–Yan production driven by qq annihilation, most of the previously explored DPS processes driven by gg scattering, and the final state of four charged leptons constitutes the golden channel for the studies of Higgs boson properties, $H \rightarrow Z^{(*)} Z^{(*)} \rightarrow 4l$
- CMS: 13 TeV, 77 fb⁻¹, same sign WW**, focus on WW leptonic decay in two muons $\mu^\pm\mu^\pm$ or an electron-muon ($e^\pm\mu^\pm$) pair (subdominant contributions from leptonic τ decays)
 - No additional jets at LO \rightarrow background from SPS is suppressed in this channel
 - Signal: LO Py8 and, for cross checks, with Hw++



two leptons: $e^\pm\mu^\pm$ or $\mu^\pm\mu^\pm$

$p_T^{\ell_1} > 25 \text{ GeV}$, $p_T^{\ell_2} > 20 \text{ GeV}$

$|\eta_e| < 2.5$, $|\eta_\mu| < 2.4$

$p_T^{\text{miss}} > 15 \text{ GeV}$ Reduces MJ

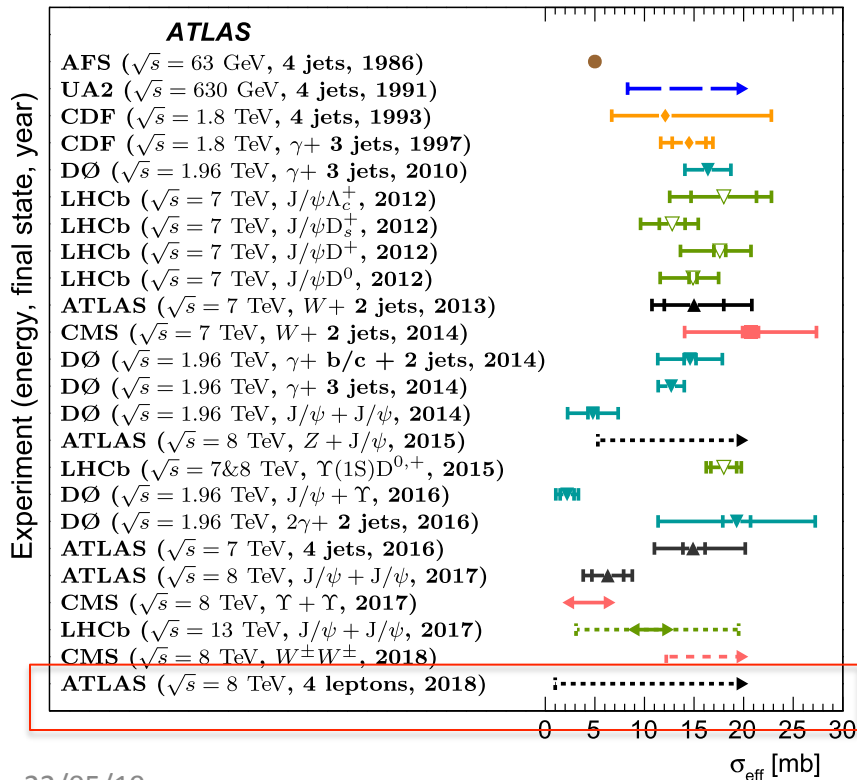
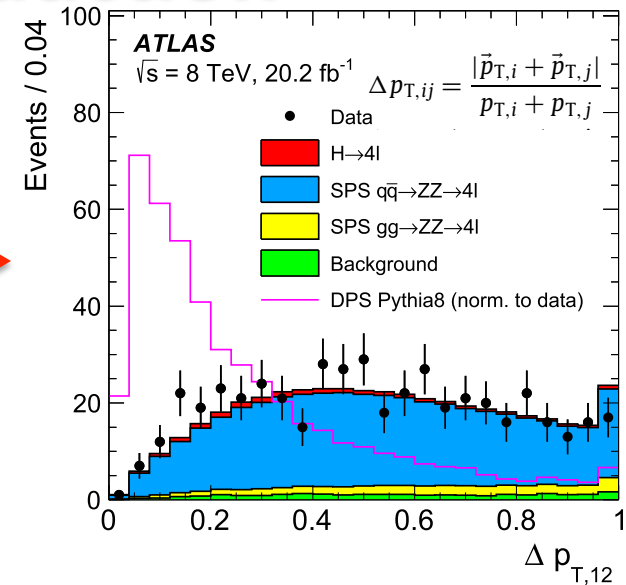
$N_{\text{jets}} < 2$ ($p_T > 30 \text{ GeV}$ and $|\eta| < 2.5$) Reduces top

$N_{\text{b-tagged jets}} = 0$ ($p_T > 25 \text{ GeV}$ and $|\eta| < 2.4$)

veto on additional e, μ , and τ_h

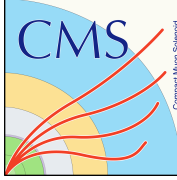
DPS in inclusive 4l production

- In the **DPS** 4l final states, the 2l of each dilepton will tend to be balanced in p_T and back-to-back in ϕ , due to the dominance of low- p_T $Z^{(*)}$ production
- In the **SPS** case, the **leading and sub-leading pairs are expected to balance each other in p_T**
- $\Delta p_{T,12}$, $\Delta\phi_{13}$, Δy_{13} , and Δ_{1234} used to train an ANN to extract the signal



- No signal of double-parton scattering is observed and an upper limit on the fraction of the DPS contribution to the inclusive four-lepton final state of 0.042 is obtained at 95% CL

- This translates into a **lower limit of 1.0 mb on the effective cross section**



DPS in same-sign WW

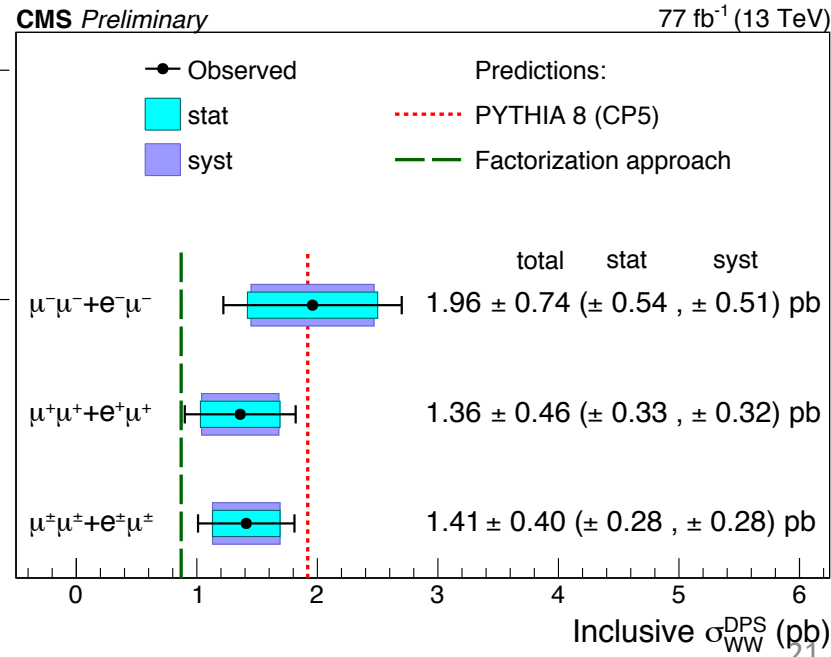
- **Dominant backgrounds from:**
 - **WZ** (very similar kinematics to that of the signal, i.e. no hadronic activity in form of high p_T jet, but Lorentz boost sharing along z-axis for WZ) -> from MC
 - **non prompt leptons** (kinematics differences larger, but also much larger cross-sections) -> data-driven (contributes the largest uncertainty)
- 11 variables to train 2 BDTs -> 2D classifier with 15 bins to optimize the constraining power of the maximum likelihood fit
- Signal process enhanced in the l^+l^+ configuration, background processes more symmetric between the two charges -> classification into two charge configurations increases sensitivity

Suffers from large uncertainties related to the UE tuning

	obtained value	significance (standard deviations)
$\sigma_{DPS WW, exp}^{PYTHIA8}$	1.92 pb	5.4
$\sigma_{DPS WW, exp}^{factorized}$	0.87 pb	2.5
$\sigma_{DPS WW, obs}$	1.41 ± 0.28 (stat) ± 0.28 (syst) pb	3.9
σ_{eff}	$12.7^{+5.0}_{-2.9}$ mb	-

Suffers from imprecise knowledge of σ_{eff}

First experimental evidence of the DPS WW process



Heavy Ion programme

Plenty of interesting results not covered here due to lack of time:

- **ATLAS**: Azimuthal anisotropy of charged particles in Pb+Pb
 - arxiv:1808.03951 Eur. Phys. J. C 78 (2018) 997
- **ATLAS**: Multiparticle azimuthal correlations in pp, p+Pb, and Pb+Pb
 - arxiv:1705.04176 Eur. Phys. J. C 77 (2017) 428
 - <http://atlas.cern/updates/physics-briefing/exploring-nature-ridge-small-systems>
- **ATLAS**: Femtoscopy with charged pions in 5.02 TeV p+Pb (made it to the cover of PRC)

- **CMS**: $dN/d\eta$ in XeXe collisions
 - <http://cms-results.web.cern.ch/cms-results/public-results/publications/HIN-17-006/index.html>
- **CMS**: $dE_T/d\eta$ in pPb collisions
 - <http://cms-results.web.cern.ch/cms-results/public-results/publications/HIN-14-014/index.html>
- **CMS**: Elliptic flow in XeXe
 - <http://cms-results.web.cern.ch/cms-results/public-results/publications/HIN-18-001/index.html>

- See also talks on “Recent results on collectivity and correlations in HI collisions from ATLAS/CMS” by Dominik Derendarz (**ATLAS**) and Javier Alberto Murillo Quijada (**CMS**)

Summary

- The LHC and its experiments allow for **extensive tests of soft QCD**
- Generator predictions very much improved since Run 1, but still visible discrepancies wrt data, in particular for the underlying event at larger momentum transfer
- Soft QCD is crucial for many more complex analyses, e.g. precision measurements:
 - UE and CR: very large uncertainties on the **top mass measurement** (Eur. Phys. J. C (2018) 78:891)

	2D approach		1D approach	Hybrid	
	δm_t^{2D} [GeV]	δJSF^{2D} [%]	δm_t^{1D} [GeV]	δm_t^{hyb} [GeV]	δJSF^{hyb} [%]
Underlying event	-0.10 ± 0.08	+0.1	$+0.01 \pm 0.05$	-0.07 ± 0.07	+0.1
Early resonance decays	-0.22 ± 0.09	+0.8	$+0.42 \pm 0.05$	-0.03 ± 0.07	+0.5
Color reconnection	$+0.34 \pm 0.09$	-0.1	$+0.23 \pm 0.06$	$+0.31 \pm 0.08$	-0.1
Total systematic	0.75	1.1	1.10	0.62	0.8
Statistical (expected)	0.09	0.1	0.06	0.08	0.1
Total (expected)	0.76	1.1	1.10	0.63	0.8

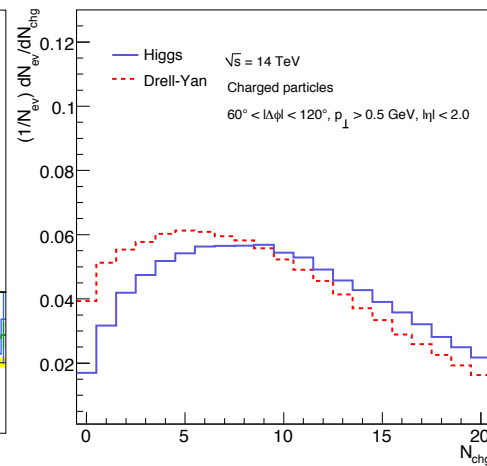
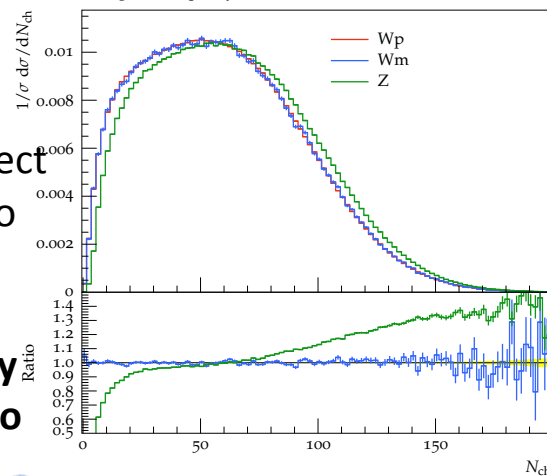
- ATLAS used the AZNLO Tune for the measurement of m_W , as it describes best the hadronic recoil distribution (tuned on $p_T Z$)

- Can UE-models tuned on **Z boson** events, also correctly describe the UE for **W bosons**?

- MC based studies showed large differences

- Besides the W and Z differences, we can expect a very different UE in Higgs production due to the different initial state (gg/qq)

<https://indico.cern.ch/event/712572/contributions/2996559/>
Charged multiplicity of events



While the existing soft measurements already challenge the models, plenty of possibilities to guide theory with new measurements!

Thanks for your attention!



F. Cairo, From Conn(II)ecting the dots

Valentina Cairo

Extra Slides

Quantum Chromodynamics

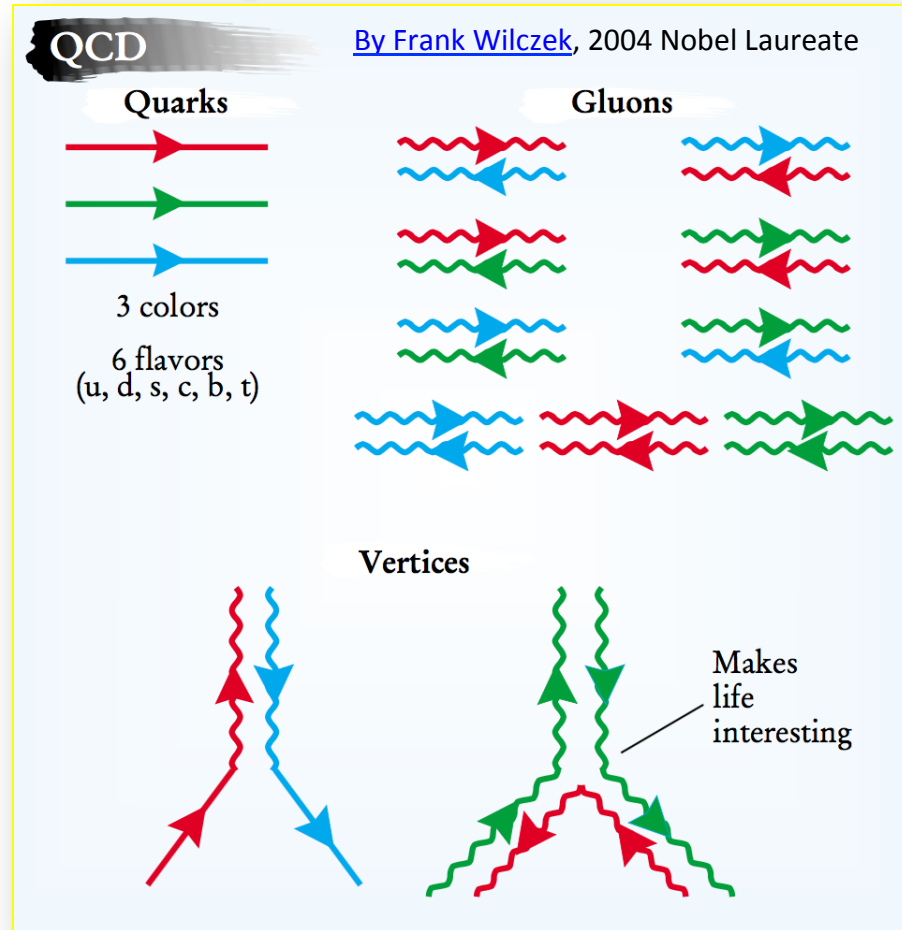
Quantum Chromodynamics, or QCD:
the modern theory of strong
interactions

Originally, its roots are in nuclear
physics and in the description of
ordinary matter.

Nowadays QCD is used to
describe most of what goes on at
high-energy accelerators

About 20-30 years ago, this activity was
commonly called “testing QCD”.

Such is the success of the theory, that
we now speak instead of “calculating
QCD backgrounds” for the investigation
of more speculative phenomena.

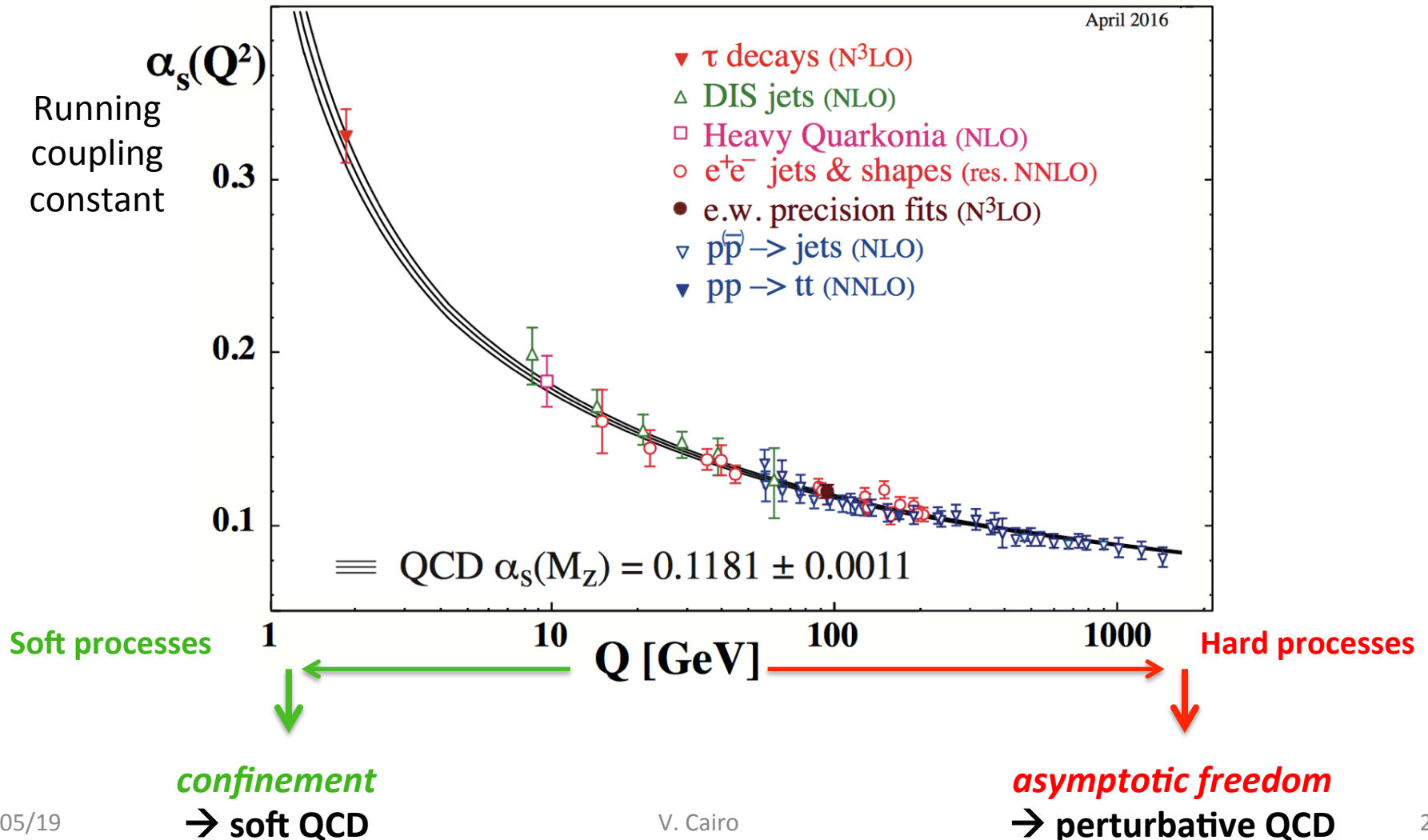


In summary:

QCD is a precise and beautiful theory.
One reflection of this elegance is that the essence
of QCD can be portrayed, without severe
distortions, in the few simple pictures above!

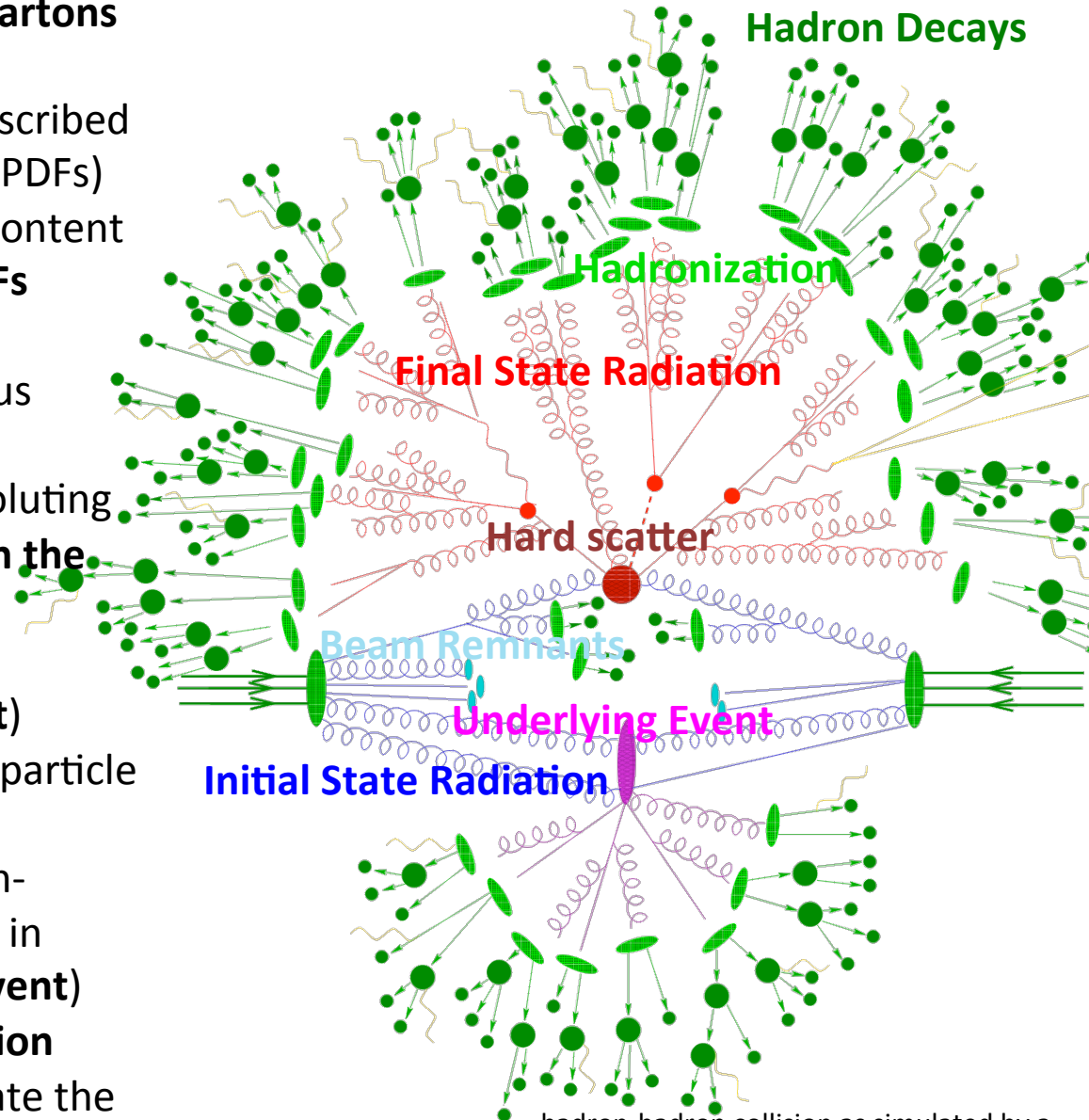
Soft and Perturbative QCD

Differently than the electromagnetic force, which is infinite in range and obeys to the inverse square law, the **strong force** has a **very short range**. The restriction of the strong force to subatomic distances is related to two features called **asymptotic freedom** and **confinement**.



Proton-Proton Interaction Terminology

- Interacting **protons** as “bags” of **partons** (quarks and gluons)
- Parton flavour and momentum described by **Parton Distribution Functions (PDFs)**
- QCD does not predict the parton content of the proton → shapes of the **PDFs determined by a fit to data** from experimental observables in various processes
- **Cross sections** calculated by convoluting the **parton level cross section with the PDFs**
- **Hard scatter (HS)** described by perturbative QCD (**Matrix element**)
- HS partons evolve into collimated particle systems (**jets**)
- Spectator partons interact in a non-perturbative regime and fragment in detectable hadrons (**underlying event**)
- **Initial and final state gluon radiation** (alike Bremsstrahlung) to complicate the picture further



hadron-hadron collision as simulated by a Monte Carlo event generator for a ttH event
(by F.Krauss)

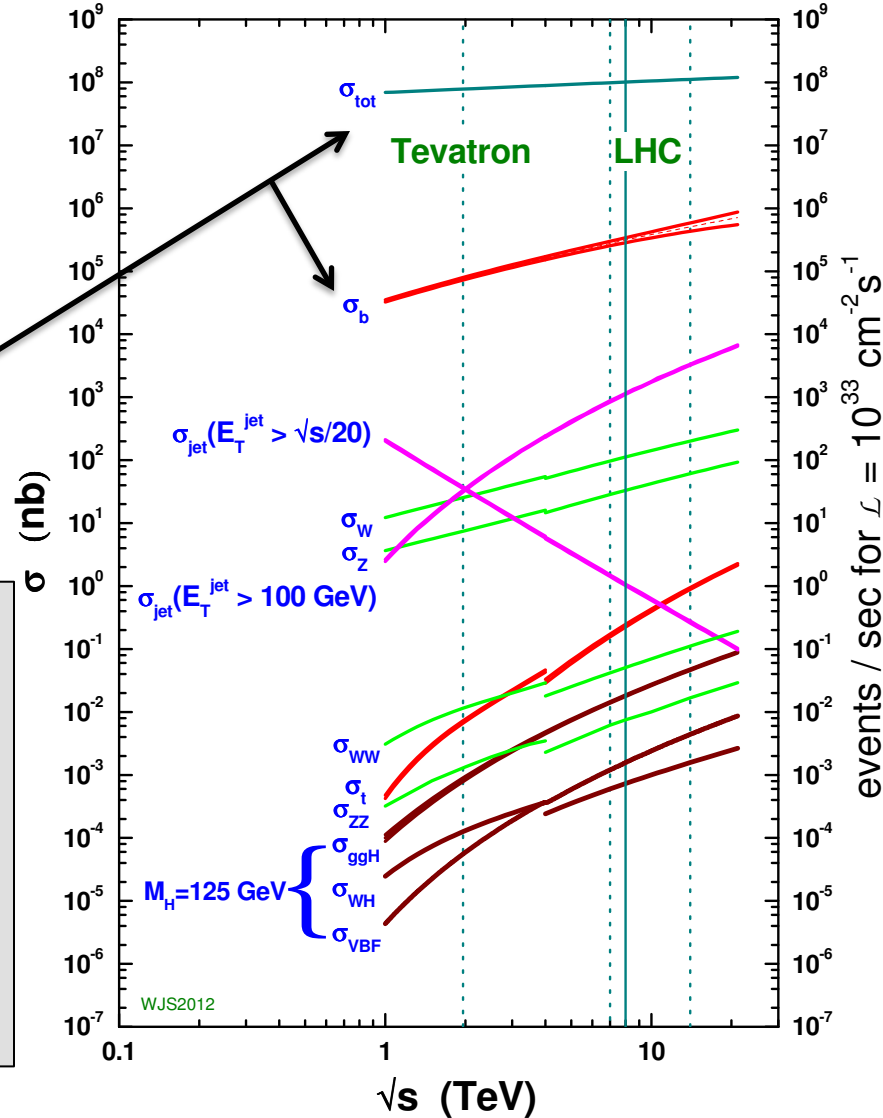
Proton-Proton Interaction Terminology

- Interacting protons as “bags” of partons (quarks and gluons)
- Parton flavour and momentum described by **Parton Distribution Functions (PDFs)**
- QCD does not predict the parton content of the proton → shapes of the **PDFs determined by a fit to data** from experimental observables in various processes
- Cross sections** calculated by convoluting the **parton level cross section with the PDFs**

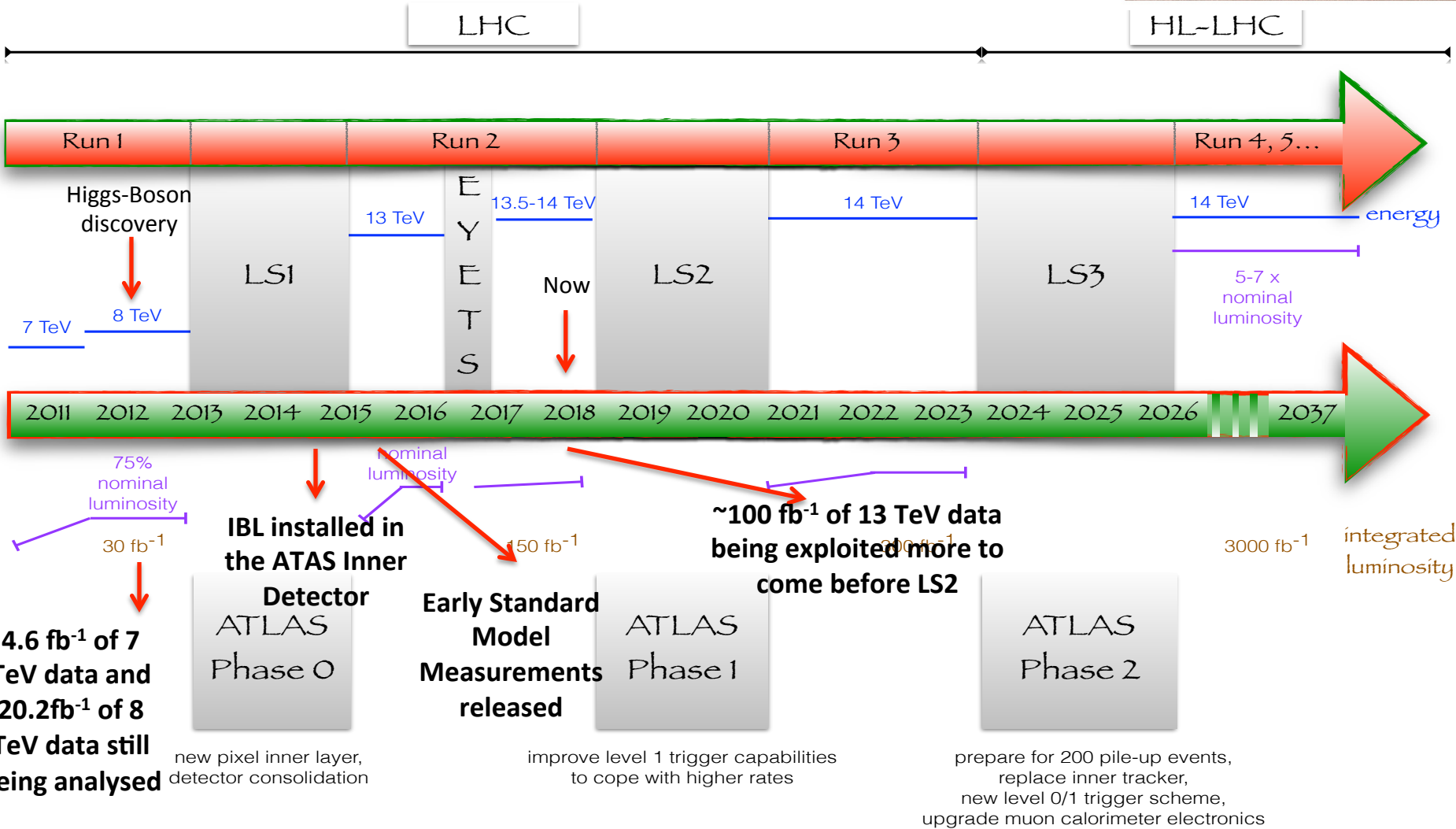
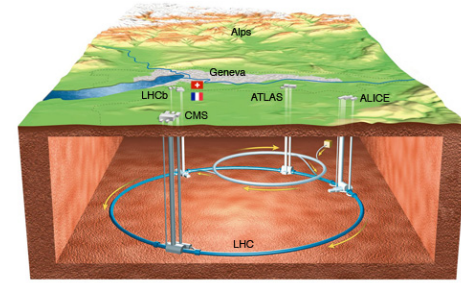
- Hard scatter (HS) described by

Hard QCD events constitute only a tiny fraction of the **total cross-section**, which is then **dominated by soft events** (peripheral processes).
 In fact, the total production cross-section is orders of magnitude larger than very abundant hard QCD processes such as the production of b-quarks

probability that a pair of hadrons undergoes an interaction
proton - (anti)proton cross sections

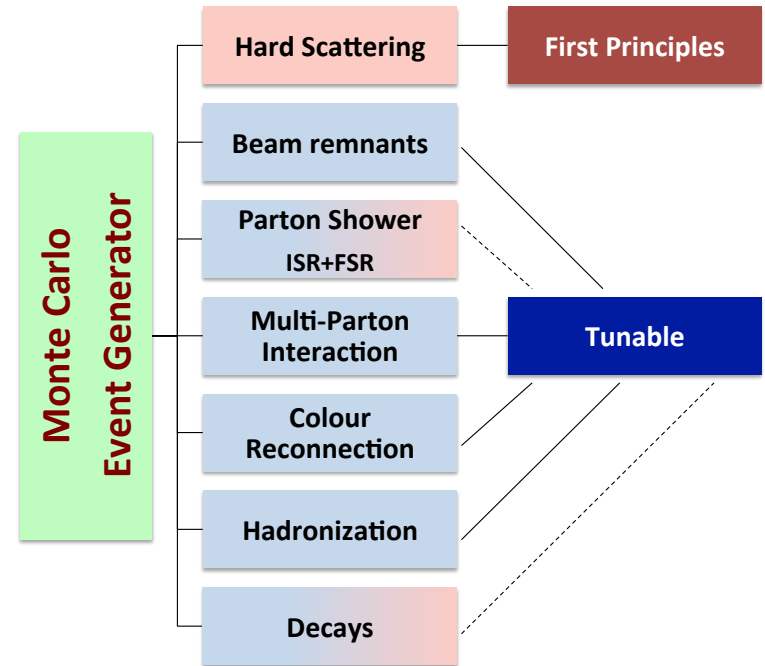


Large Hadron Collider Timeline



Soft QCD and Monte Carlo Tuning

- While hard QCD processes can be studied by means of perturbative approaches, this is not possible for the soft QCD events
- The development of specialised software libraries based on Monte Carlo Methods, Monte Carlo (MC) event generators, to describe phenomenologically particle interactions began shortly after the discovery of the partonic structure of hadrons and the formalisation of QCD as the theory of strong interactions
- Models have to be developed with a set of **tunable parameters** to describe the hadron-level properties of final states dominated by soft QCD
- **Inclusive charged-particle and underlying event measurements** in pp collisions are the ideal test bed to provide insight into the strong interaction in the low energy, non-perturbative QCD region:
 - **Crucial for the tuning** of the Monte Carlo event generator
 - **Essential to understand** and correctly simulate any other more **complex phenomena**
 - **Ideal to study tracking performance** in the “early” stage of a new data taking...



Cross-section

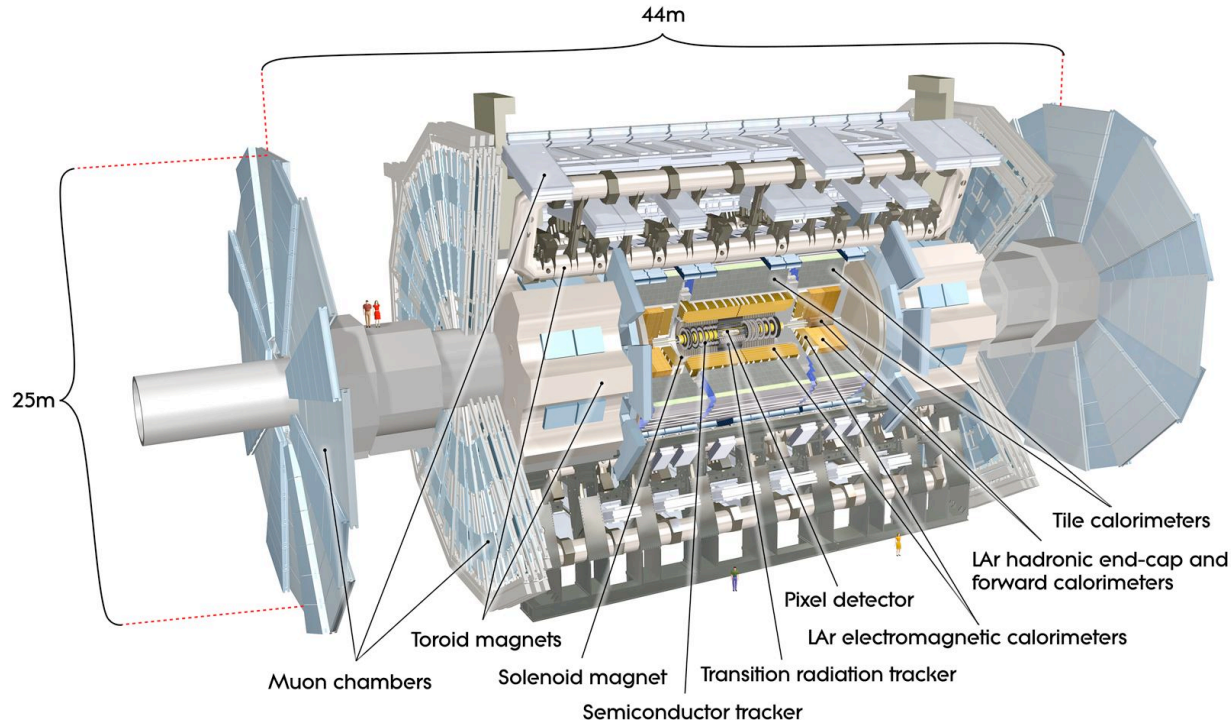
Cross sections for a scattering process
 $ab \rightarrow n$ at hadron colliders

$$\begin{aligned}
 \sigma &= \sum_{a,b} \int_0^1 dx_a dx_b \int \underbrace{f_a^{h_1}(x_a, \mu_F) f_b^{h_2}(x_b, \mu_F)}_{\text{Parton Distribution Functions}} d\hat{\sigma}_{ab \rightarrow n}(\mu_F, \mu_R) \\
 &= \sum_{a,b} \int_0^1 dx_a dx_b \int d\Phi_n \underbrace{f_a^{h_1}(x_a, \mu_F) f_b^{h_2}(x_b, \mu_F)}_{\text{Parton Distribution Functions}} \times \frac{1}{2\hat{s}} |\mathcal{M}_{ab \rightarrow n}|^2(\Phi_n; \mu_F, \mu_R),
 \end{aligned}$$

Renormalization and factorization scales
 ↓
 Matrix Element

ATLAS Experiment

- The ATLAS detector is a multi-purpose detector with a tracking system ideal for the measurement of particles kinematics



- After a 3-year data taking phase (Run 1, 2010-2012) and a 2-year shutdown (LS1, 2013-2014) for repairing and upgrade, the ATLAS Detector is again operational at the LHC Run 2 at $\sqrt{s}=13\text{TeV}$
- Run 2 started in Spring 2015 \rightarrow by the end of 2016 collected $\sim 40 \text{ fb}^{-1}$ of data (about a factor of 2 wrt Run 1 data, which allowed for the discovery of the Higgs Boson)

Single-Diffractive cross-section

- **Hadron level cross-sections: σ vs t , ξ , $\Delta\eta$**
- **Py8 A3 as default** for ND, SD, DD and CD samples
 - Donnachie-Landshoff choice of the pomeron flux factor to describe the ξ and t dependences in the diffractive channels
- **Py8 A2 as alternative** SD sample (Schuler-Sjöstrand model for the Pomeron flux factor, differs from Donnachie-Landshoff mainly in its ξ dependence).
- Both tunes use the **H1 2006 Fit B** diffractive parton densities as an input to model the hadronisation in the diffractive channels.
- **Herwig7** compared to Py8 for uncertainties from hadronisation properties of the dissociation system X

Selection:

L1 trigger: MBTS(A/C) and ALFA(C/A)

ALFA: exactly one reconstructed proton

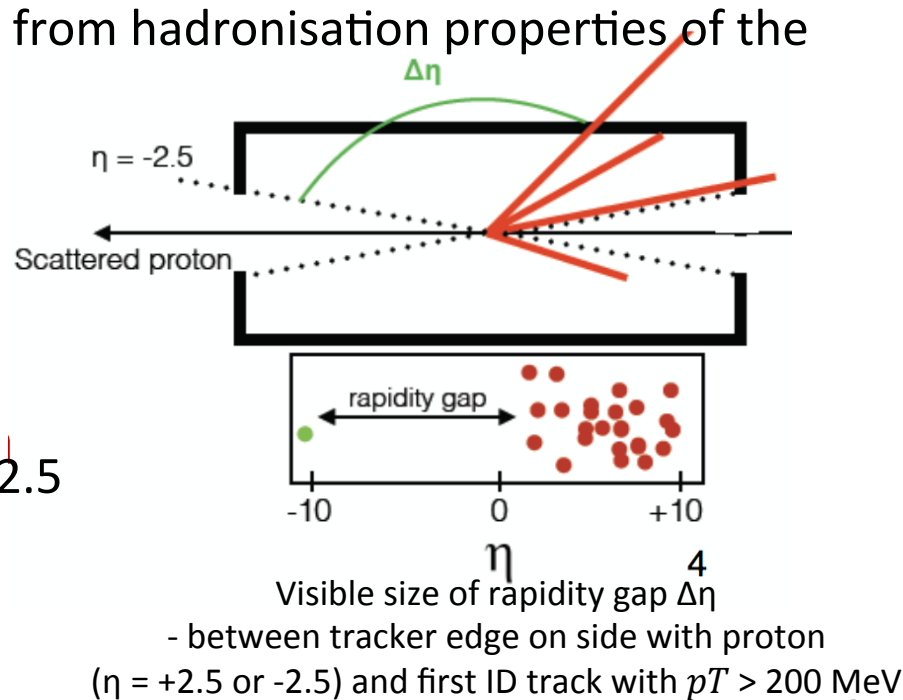
MBTS: at least 5 counters above threshold

ID: at least 1 track with $p_T > 200$ MeV & $|\eta| < 2.5$

Reconstructed vertex

Fiducial region: $0.016 < |t| < 0.43$ GeV²,

$-4.0 < \log_{10}(\xi) < -1.6$, ($80 < MX < 1270$ GeV)



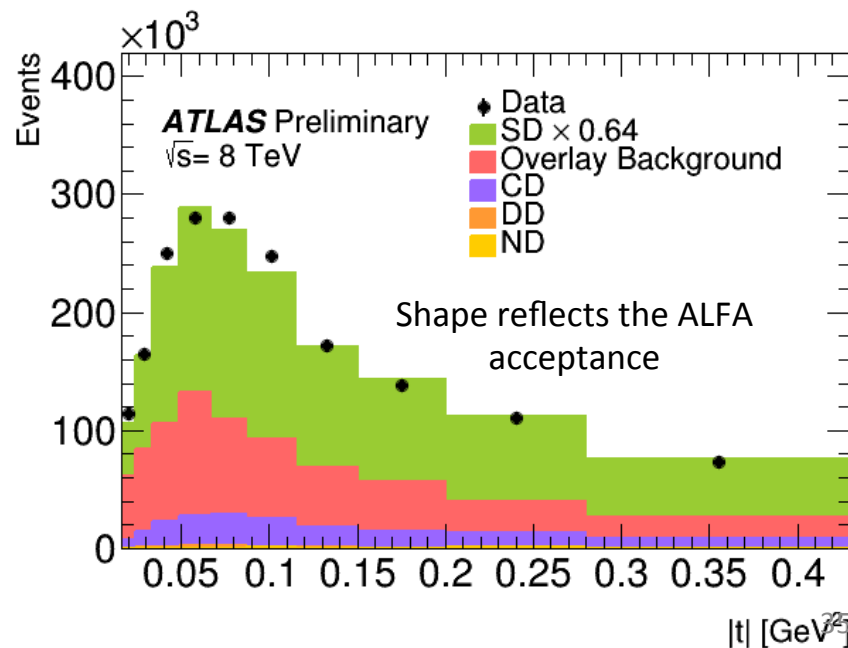
Single-Diffractive cross-section

Background arises from non-SD pp collision processes leading to:

- **Single source** \rightarrow correlated signals in ALFA and the ID
 - dominated by the CD process (forward-going protons and activity in the ID).
 - estimated with MC, reweighted through comparison with data.
 - The probability of a Pythia8 CD event passing the selection criteria is 8.5%. The ND and DD single source contributions are negligible.
- **Overlay Background** \rightarrow coincidences of a signal in ALFA with an uncorrelated signal in the ID
 - signal in the central detector almost always from a ND, DD or SD pp collision, whilst the ALFA signal may occur due to 'pile-up' from real forward going protons in elastic scattering or CD processes, showering in DD or ND events or from beam induced sources (dominantly beam halo).
 - Modelled using a data-driven technique

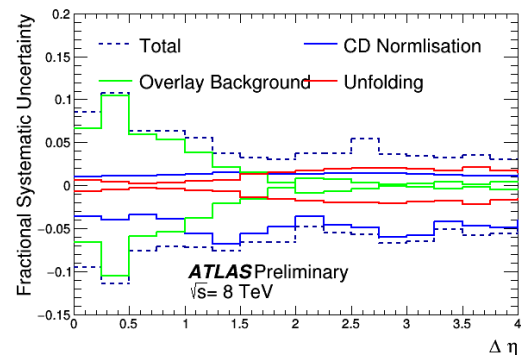
Background subtracted distributions are unfolded at particle level (iterative Bayesian)

Main uncertainty to the measurement from the subtraction of the overlay background!

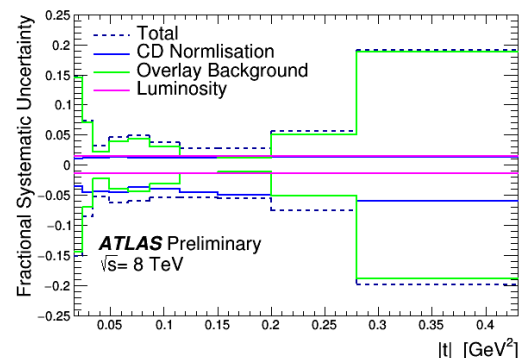


Single-Diffractive cross-section

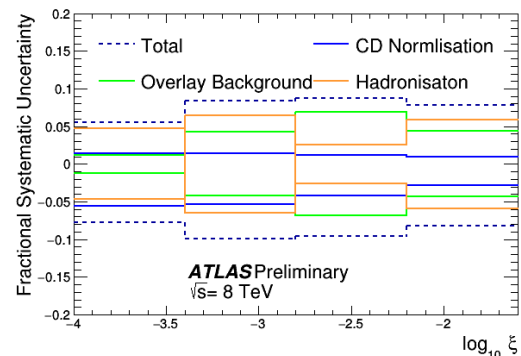
- 1) Overlay background subtraction (from control region)
- 2) Unfolding (residual non-closure in unfolding PYTHIA 8 after reweight to match data using un-reweighted MC)
- 3) Hadronization uncertainty (PYTHIA vs HERWIG at particle level)
- 4) CD background shape (reweight or not) and normalization (CDF data)
- 5) ALFA alignment and reconstruction (followed ALFA elastics analysis from the same data)
- 6) Luminosity (1.5%)
- 7) MBTSthresholds(varythreshold)
- 8) ID track reconstruction
- 9) Trigger efficiencies (vary reference sample)



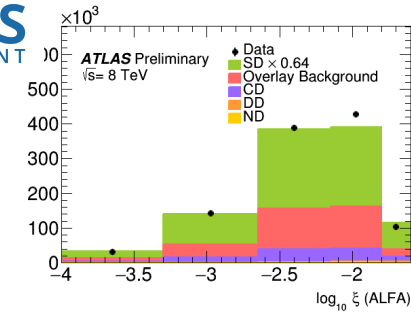
(a)



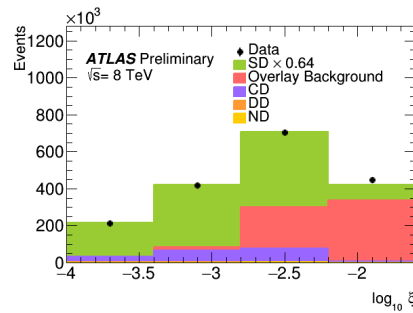
(b)



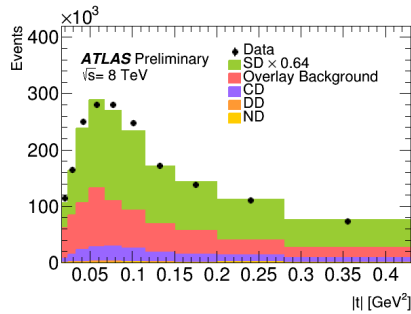
Differential cross sections for single diffraction



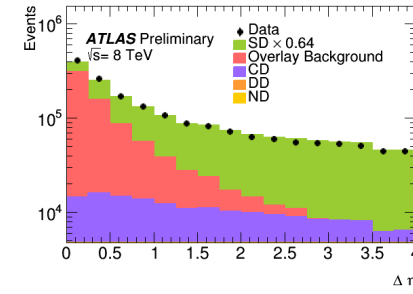
(a) Nominal Sample



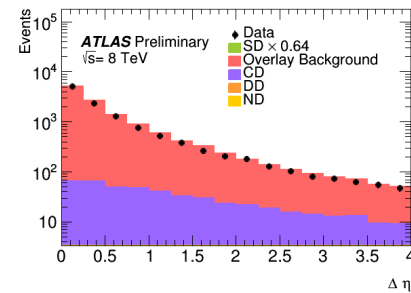
(b) Nominal Sample



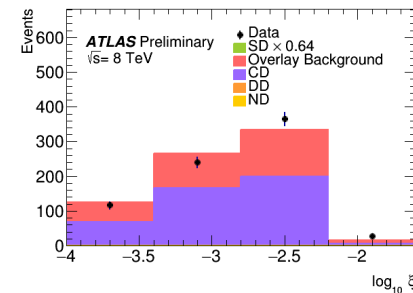
(c) Nominal Sample



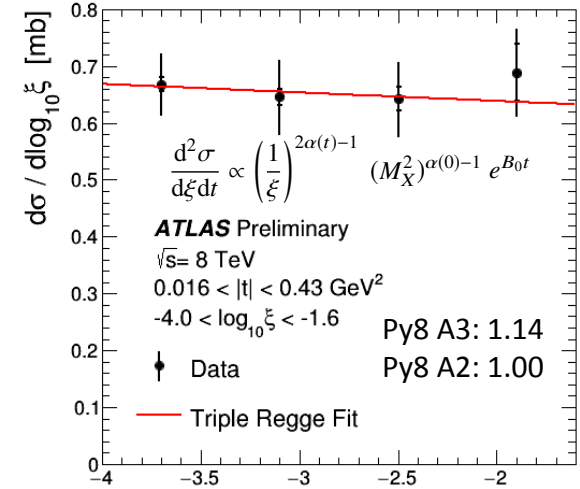
(d) Nominal Sample



(e) Control Region 1

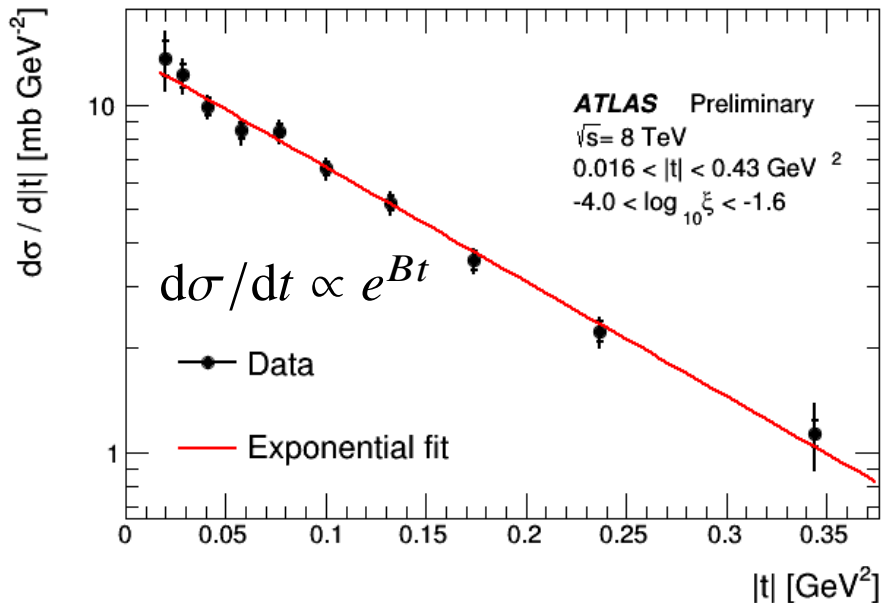
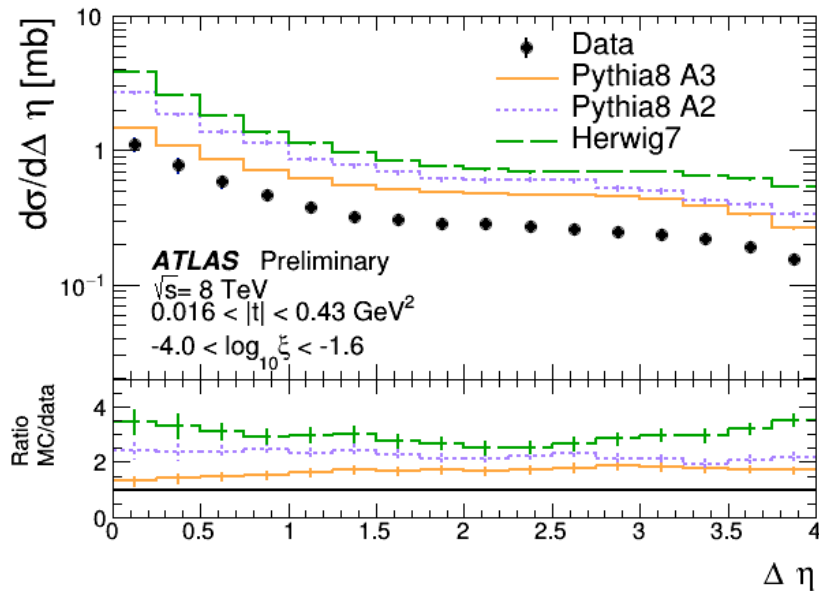


(f) Control Region 2



$$\alpha(0) = 1.07 \pm 0.02 \text{ (stat.)} \pm 0.06 \text{ (syst.)} \pm 0.06 \text{ } (\alpha')$$

Figure 2: Uncorrected (i.e. detector level) distributions of (a) $\log_{10} \xi$ measured in ALFA, (b) $\log_{10} \xi$ measured in the ID, (c) $|t|$ and (d) $\Delta\eta$ for the basic selection of the measurement. (e) Uncorrected $\Delta\eta$ distribution from the control sample in which two proton track segments are required rather than one ('Control Region 1'). (f) Uncorrected distribution in $\log_{10} \xi$ measured in the ID for the control sample in which exactly two proton track segments are required and the MBTS multiplicity is required to be between 2 and 10 ('Control Region 2'). In all distributions, data are compared with the sum of the overlay background model and the PYTHIA8 A3 tune prediction with the SD contribution scaled by 0.64 to match the measurement in this paper. In (f), the CD ξ distribution at the truth level is reweighted as described in the text.



$$B = 7.60 \pm 0.23(\text{stat.}) \pm 0.22(\text{syst.}) \text{ GeV}^{-2}$$

Py8 A3: 7.10 GeV^{-2} (1.6 σ compatibility)

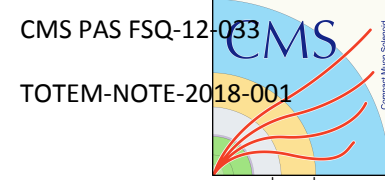
Py8 A2: 7.82 GeV^{-2} (0.7 σ compatibility)

- Diffractive plateau visible
- Shape at low gaps due to stacking up of high- ξ events with small gaps beyond acceptance
- Shape at high gaps due to edge of ξ fiducial region ($\xi = 10^{-4} \rightarrow \Delta\eta \approx 4$)

Distribution	$\sigma_{SD}^{\text{fiducial}(\xi,t)}$ [mb]	$\sigma_{SD}^{t\text{-extrap}}$ [mb]	$\sigma_{SD}^{\xi,t\text{-extrap}}$ [mb]
Data	1.59 ± 0.13	1.88 ± 0.15	6.6
PYTHIA8 A2 (Schüler-Sjostrand)	3.69	4.35	12.48
PYTHIA8 A3 (Donnachie-Landshoff)	2.52	2.98	12.48
HERWIG7	4.96	6.11	24.0

All models overestimate the XS!

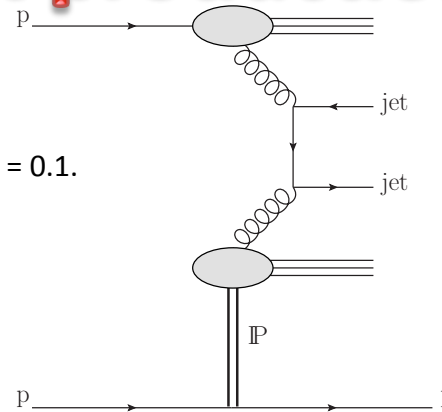
Diffractive di-jet production



SD dijet $d\sigma/dt$, $d\sigma/d\xi$ and $R(x)$

(with $-2.9 \leq \log_{10} x \leq -1.6$)

$$R(x) = \frac{\sigma_{jj}^{pX}(x) / \Delta\xi}{\sigma_{jj}(x)}, \quad \Delta\xi = 0.1.$$



$$\xi_{TOTEM} = 1 - \frac{|p_f|}{|p_i|}$$

$$t = (p_f - p_i)^2$$

$$\xi_{CMS}^{\pm} = \frac{\sum (E^i \pm p_z^i)}{\sqrt{s}}$$

$$\xi_{CMS} - \xi_{TOTEM} \leq 0$$

$$x^{\pm} = \frac{\sum_{jets} (E^{jet} \pm p_z^{jet})}{\sqrt{s}}$$

$$\beta = x / \xi_{TOTEM}$$

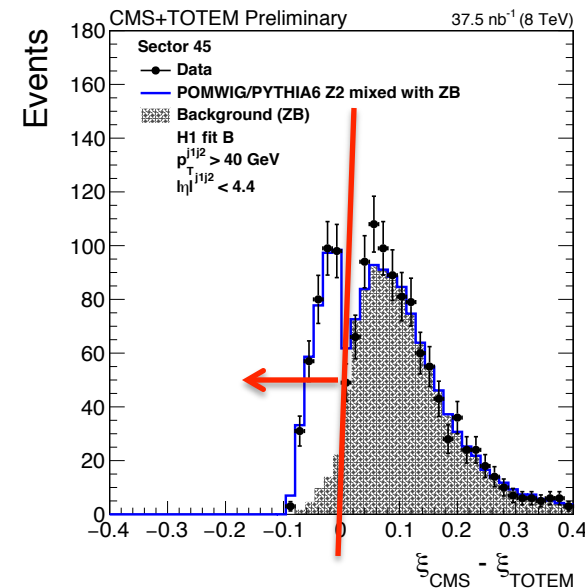
- DATA: 37.5 fb⁻¹ of 8 TeV data (July 2012)
- MC:
 - Py6 (Z2), Py8 (4C, CUETP8M1 and CUETPS8S1) and Hw6 for ND
 - Diffractive di-jets with POMWIG and PY 8 (tune 4C and CUETP8M1 for inclusive diffraction and CUETP8M1 for the Dynamic gap model)
- Events selected by trigger signals delivered simultaneously to the CMS and TOTEM detectors.
 - The CMS orbit-counter reset signal delivered to the TOTEM electronics at the start of the run assures the time synchronisation of the two experiments.

Events combined offline by requiring that both the CMS and TOTEM reconstructed events have the same LHC orbit and bunch numbers.

Selection	Sector 45	Sector 56
At least 2 jets ($p_T > 40 \text{ GeV}$, $ \eta < 4.4$)	427689	
Elastic scattering veto	405112	
Reconstructed proton	9530	
RP and fiducial cuts	2137	3033
$0.03 < t < 1.0 \text{ GeV}^2$, $0 < \xi_{TOTEM} < 0.1$	1393	1806
V. Cairo $\xi_{CMS} - \xi_{TOTEM} \leq 0$	368	420

Diffraction di-jet production

- **Main background:** overlap of a pp collision in CMS and an additional track in the RP stations, from either a beam-halo particle or an outgoing proton from pileup
 - Estimated with a zero-bias sample defined by events from randomly selected non-empty LHC bunch crossings
- Dominant uncertainties from the **jet energy scale** and **horizontal dispersion** (reco ξ depends on the optical functions describing the transport of the protons from the interaction vertex to the Roman Pot stations, specifically the horizontal dispersion, uncertainty calculated by scaling the value of ξ by $\pm 10\%$)



Uncertainty source	$\Delta\sigma/\sigma$
Trigger efficiency	$\pm 2\%$
Calorimeter energy scale	$+1/-2\%$
Jet energy scale and resolution	$+9/-8\%$
Background	$\pm 2\%$
Resolution	$\pm 2\%$
Horizontal dispersion	$+9/-12\%$
Acceptance and unfolding	$\pm 2\%$
Unfolding bias	$\pm 3\%$
Total	$+14/-15\%$

$$\sigma_{jj}^{pX} = 21.7 \pm 0.9 \text{ (stat)}_{-3.3}^{+3.0} \text{ (syst)} \pm 0.9 \text{ (lumi)} \text{ nb}$$

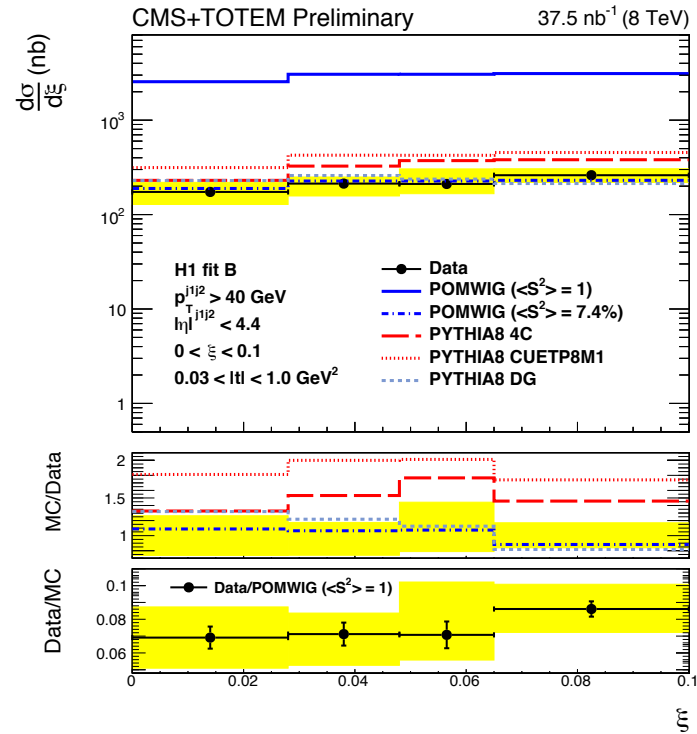
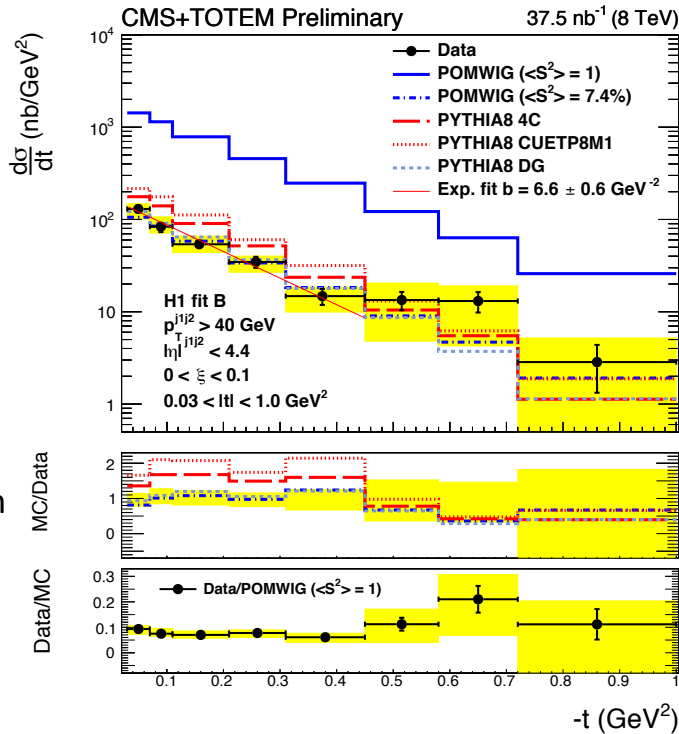
The PYTHIA8 Dynamic Gap cross section is 23.7 nb

Diffraction di-jet production

$$\frac{d\sigma_{jj}^{pX}}{dt} = \mathcal{U} \left\{ \frac{N_{jj}^i}{\mathcal{L} A^i \Delta t^i} \right\}$$

$$\frac{d\sigma_{jj}^{pX}}{d\xi} = \mathcal{U} \left\{ \frac{N_{jj}^i}{\mathcal{L} A^i \Delta \xi^i} \right\}$$

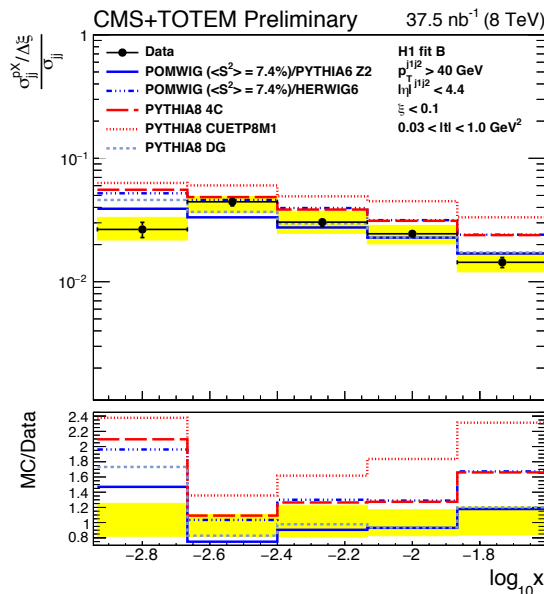
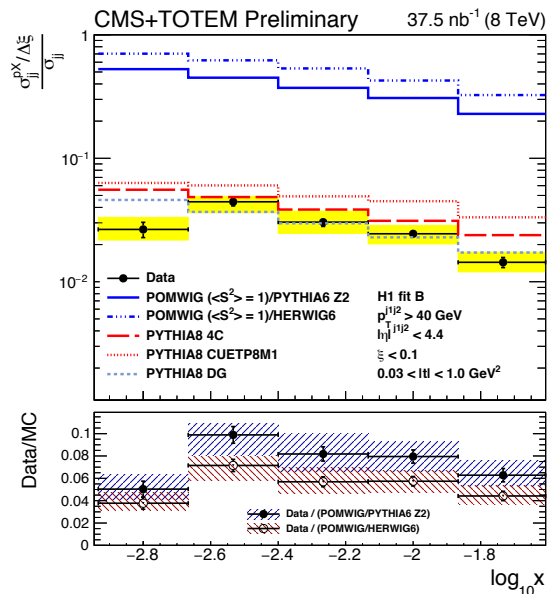
$\langle S^2 \rangle =$
 rapidity gap
 survival
 probability,
 i.e.
 suppression
 of the
 diffractive
 cross section



- **POMWIG** includes the sum of the Pomeron (p_{IP} , $\sigma_{pIP} = 256\text{nb}$), Reggeon (p_{IR} , $\sigma_{pIR} = 31\text{nb}$) and Pomeron-Pomeron (IPIP, $\sigma_{IPIP} = 6.8\text{nb}$) exchange contributions while **PYTHIA8** includes only the Pomeron (p_{IP}) contribution ($\sigma_{pIP} = 280 \text{ nb}$).
- PYTHIA8 4C and PYTHIA8 CUETP8M1 show cross sections higher than the data by up to a factor of two.
- The PYTHIA8 Dynamic Gap model shows overall a good agreement with the data.

Diffractive di-jet production

$$R(x) = \frac{\sigma_{jj}^{pX}(x) / \Delta\xi}{\sigma_{jj}(x)} = \frac{\mathcal{U} \left\{ N_{jj}^{pX} / A_{\text{CMS-TOTEM}} \right\} / \Delta\xi}{\mathcal{U} \left\{ N_{jj} / A_{\text{CMS}} \right\}} \Big| = 0.025 \pm 0.001 (\text{stat}) \pm 0.003 (\text{syst})$$



Uncertainty source	$\Delta R/R$
Calorimeter energy scale	+1/-2 %
Jet energy scale and resolution	± 2 %
Background	± 1 %
Resolution	± 2 %
Horizontal dispersion	+9/-11 %
Acceptance and unfolding	± 2 %
Unfolding bias	± 3 %
Total	+10/-13 %

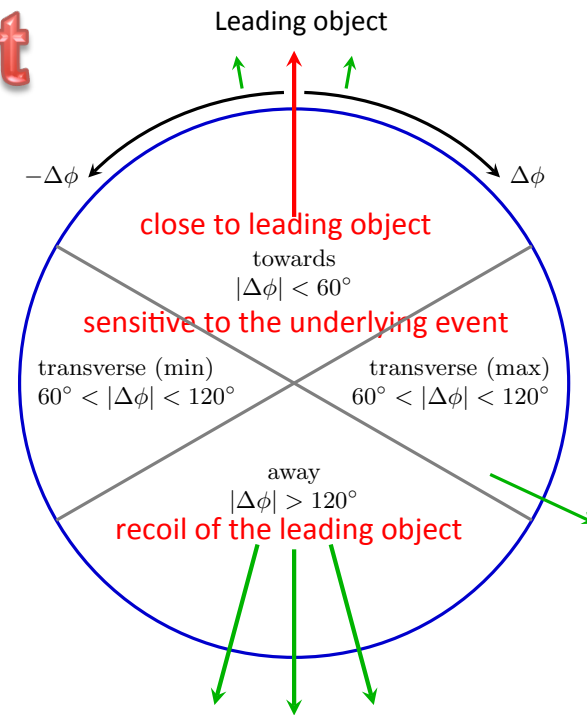
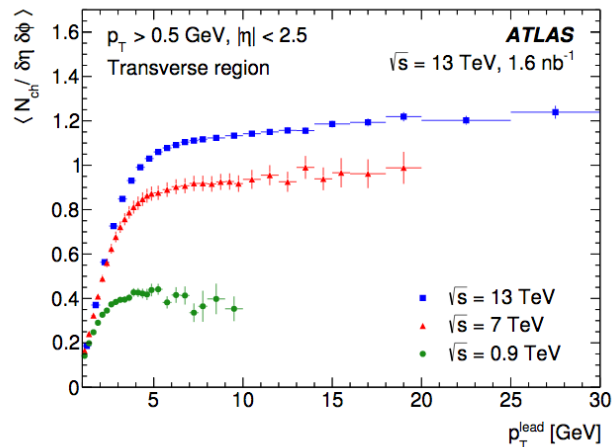
- As before, ~ 1 order of magnitude difference between POMWIG and data
- Suppression in data vs MC not substantially different when using PYTHIA6 or HERWIG6 as ND contribution.
- Good agreement between POMWIG with $\langle S^2 \rangle = 7.4\%$, PYTHIA8 DG and data.
- When HERWIG6 is used for ND the agreement is worse, especially in the lower and higher- x regions.
- The agreement for PYTHIA8 4C is fair in the inter- mediate x region, while it is worse in the lower and higher- x regions.
- The agreement is worse for PYTHIA8 CUETP8M1 with values of the ratio higher than that in the data by up to a factor of two.

Underlying Event

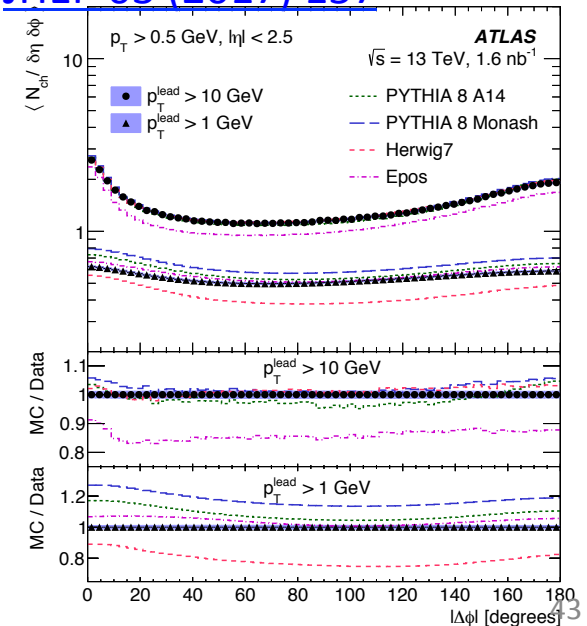
- **First 13 TeV ATLAS analysis based on leading track:**
 - **Same dataset and same event and track selection as the MinBias analysis** with an additional request: leading track with a p_T of at least 1 GeV
 - Monte Carlo Generators:

Generator	Version	Tune	PDF	Focus	From
PYTHIA 8	8.185	A2	MSTW2008 LO	MB	ATLAS
PYTHIA 8	8.185	A14	NNPDF2.3 LO	UE	ATLAS
PYTHIA 8	8.186	Monash	NNPDF2.3 LO	MB/UE	Authors
HERWIG 7	7.0.1	UE-MMHT	MMHT2014 LO	UE/DPS	Authors
EPOS	3.4	LHC	—	MB	Authors

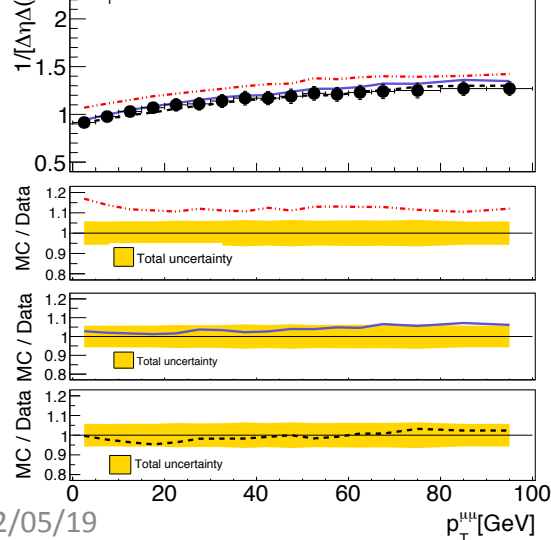
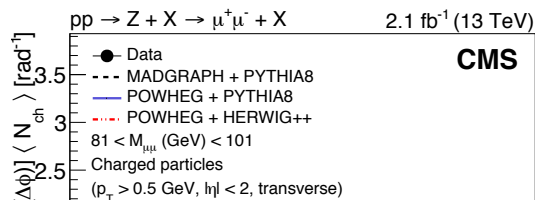
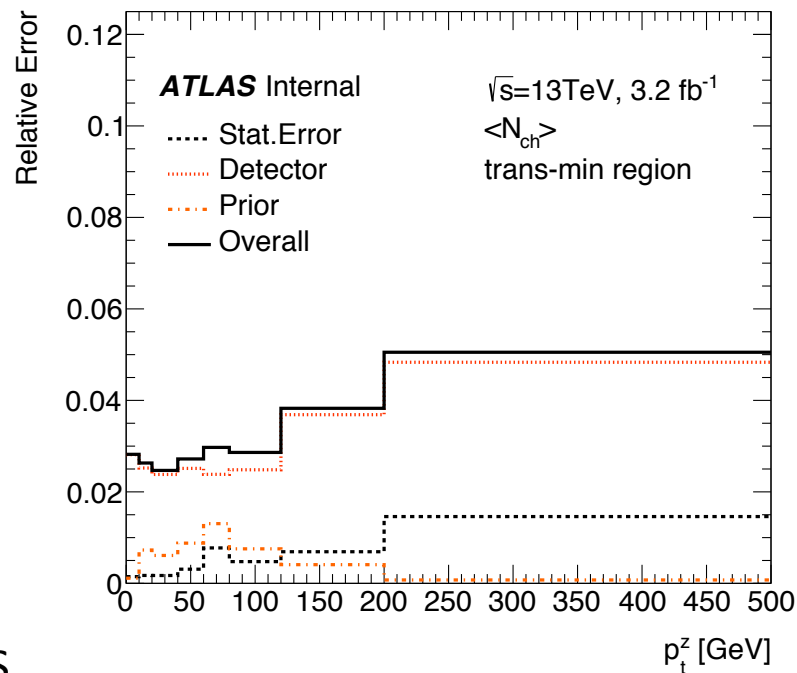
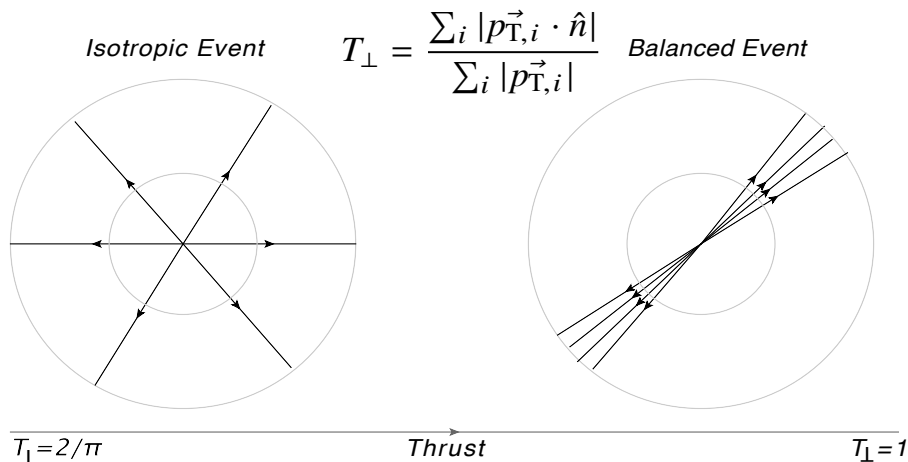
- Results presented at particle level (azimuthal re-orientation of the event was also corrected for)
- **About 20% increase in the UE activity when going from 7 to**



[JHEP 03 \(2017\) 157](#)



Underlying Event in $Z \rightarrow \mu\mu$



CMS

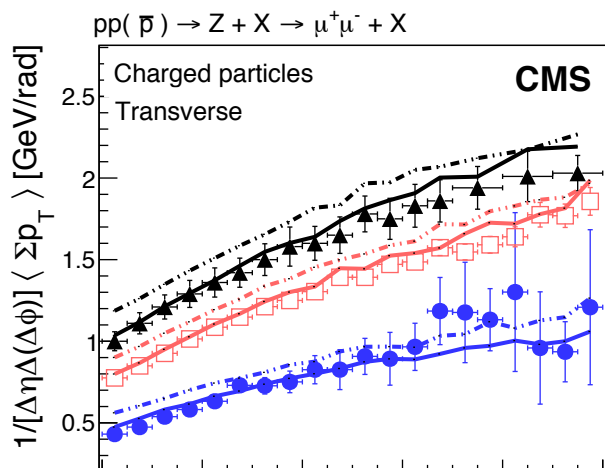
Observable	Uncertainty (%)
Model dependence	2–5
Tracking efficiency	4–6
Pileup	0.5
Trigger	0.1
Physics background	0.5–1
Muon momentum correction	0.4–0.7
Total Uncertainty	4.8–7.8

Underlying Event in $Z \rightarrow \mu\mu$

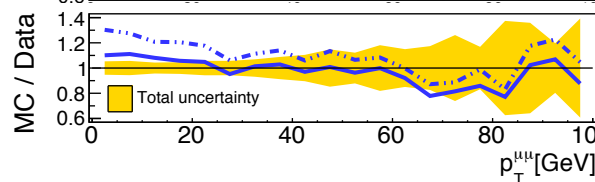
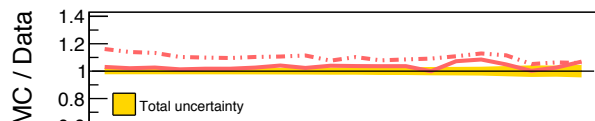
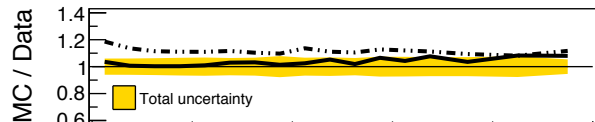
CMS: 2D iterative unfolding, response matrix from MADGRAPH + PYTHIA8 (CUET8PM1 tune)

ATLAS: iterative unfolding in bins of $p_T Z$ and thrust, response matrix from Powheg (CTEQ6L1) + Pythia8 (AZNLO tune)

Largest systematic uncertainties from model dependence

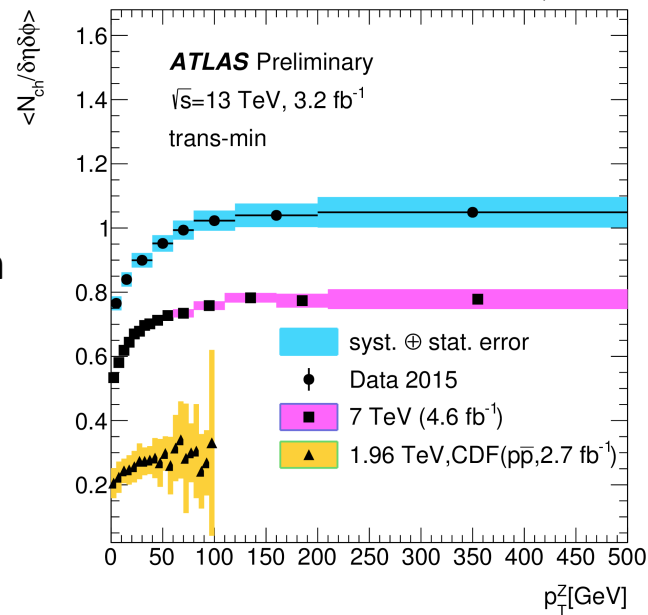
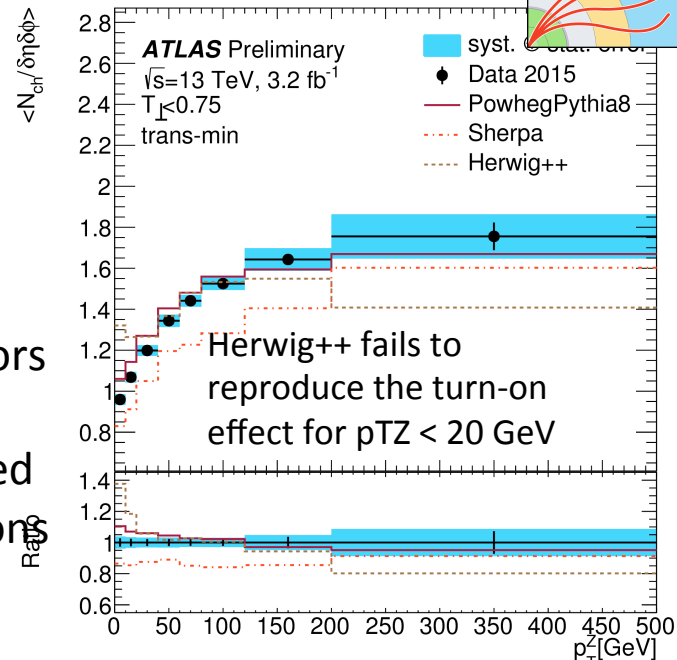


- ▲ CMS, pp, \sqrt{s} = 13 TeV
- ◻ CMS, pp, \sqrt{s} = 7 TeV
- CDF, p \bar{p} , \sqrt{s} = 1.96 TeV
- POWHEG + PYTHIA8, pp, \sqrt{s} = 13 TeV
- POWHEG + PYTHIA8, pp, \sqrt{s} = 7 TeV
- POWHEG + PYTHIA8 p \bar{p} , \sqrt{s} = 1.96 TeV
- - - POWHEG + HERWIG++, pp, \sqrt{s} = 13 TeV
- - - POWHEG + HERWIG++, pp, \sqrt{s} = 7 TeV
- - - POWHEG + HERWIG++, p \bar{p} , \sqrt{s} = 1.96 TeV

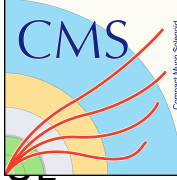


Increase in the underlying event activity with \sqrt{s}

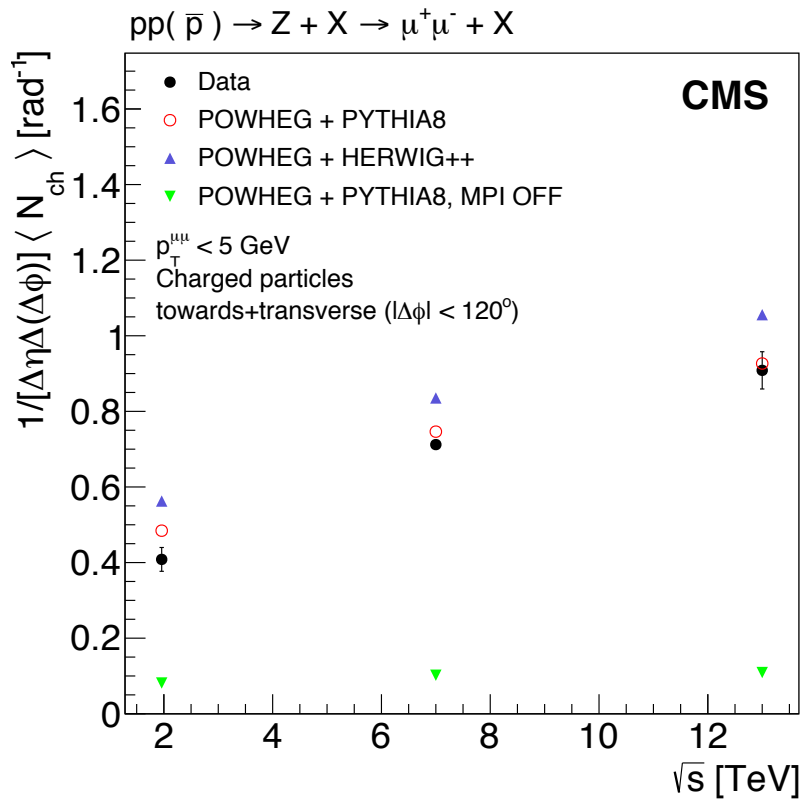
The generators have improved predictions of the mean values compared to the data when focusing on the MPI enriched regions ($T < 0.75$).



Underlying Event in $Z \rightarrow \mu\mu$

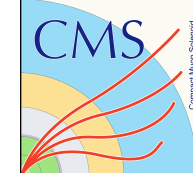


- Setting an upper limit on p_T reduces the ISR and FSR contributions and the remaining activity stems mainly from MPI. Significant increase, by a factor 2–2.5, as the collision energy rises from 1.96 to 13 TeV, which is qualitatively reproduced by POWHEG.

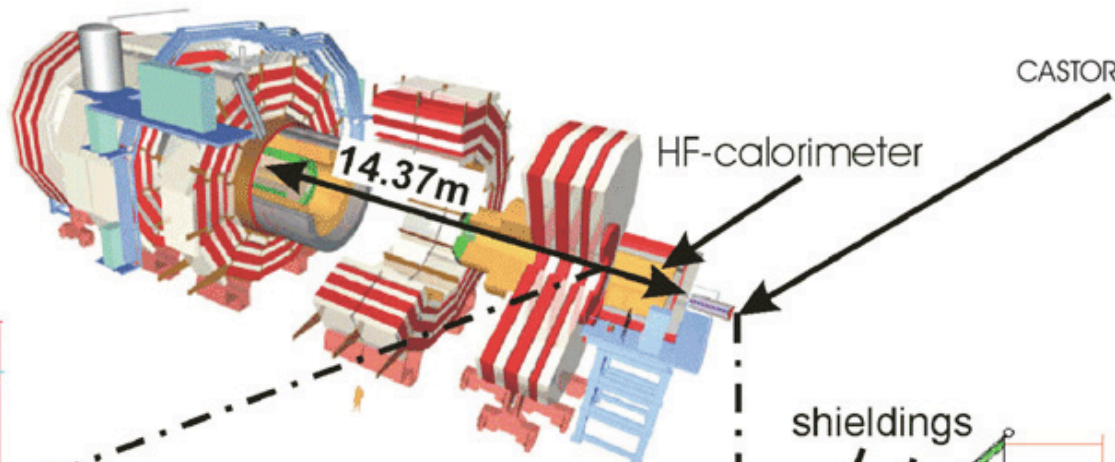


- The energy evolution is better described by POWHEG with PYTHIA8, whereas hadronization with HERWIG++ overestimates the UE activity at all collision energies. The comparison of the distributions with and without MPI indicates that the ISR and FSR contributions, which increase slowly with center-of-mass energy, are small.
- The CUETP8M1 and EE5C tunes employed here are mostly obtained from fits to MinBias measurements and UE measurements with leading jets or leading tracks. The fact that these tunes reproduce globally well the present data supports the hypothesis that the UE activity is independent of the hard process.
- The collision energy dependence of the UE activity is similar for different hard processes. Unlike UE studies with a leading track/jet, the present measurements provide new handles to better understand the evolution of ISR, FSR, and MPI contributions separately, as functions of the event energy scale and the collision energy.

CMS and the forward detectors

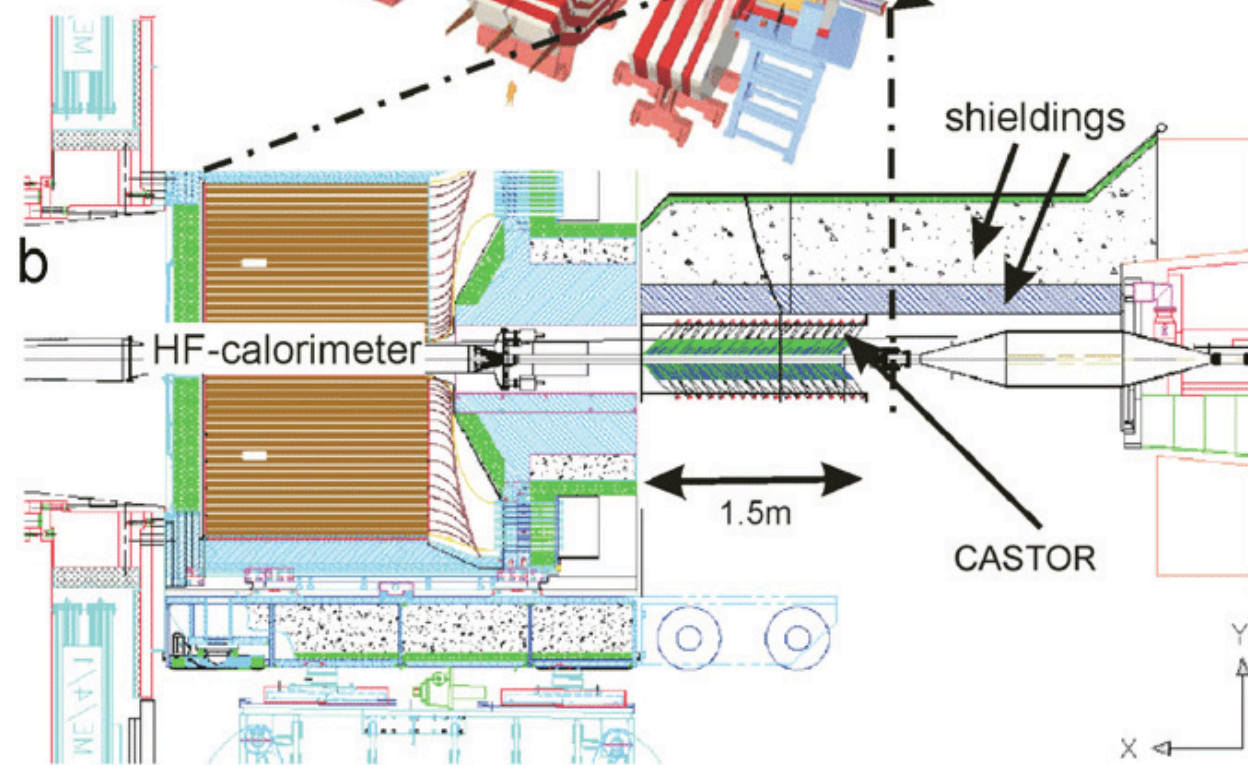


a



The CASTOR Centauro And Strange Object Research detector is located at a distance of 4.4 m from the CMS interaction point right behind the Hadronic Forward HF calorimeter and the T2, a tracking station of the TOTEM experiment, covering the pseudorapidity region $-6.6 < \eta < -5.2$

b



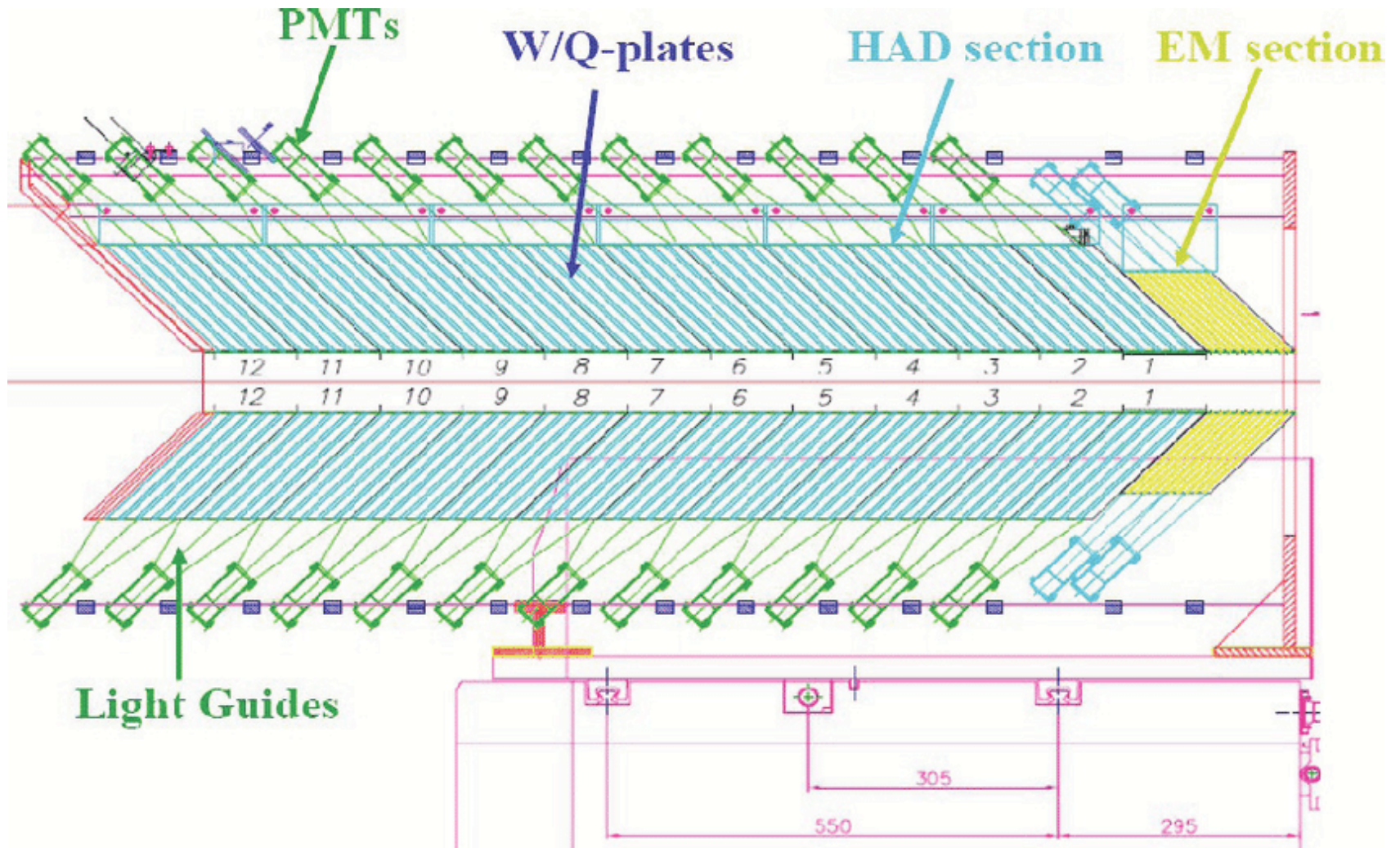
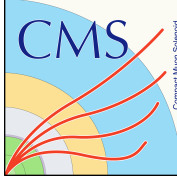
The so called "Centauro" events exhibit:

- Small multiplicity
- Absence or strong suppression of the electromagnetic component
- High mean transverse momentum $\{O(2\text{GeV}/c)\}$

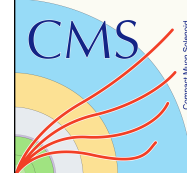
In addition, many hadron rich events are accompanied by a long flying component (abnormally long penetrating particles)

Simulations have shown that these events could not originate from statistical fluctuations of normal hadronic events.

Longitudinal segmentation of CASTOR



UE at forward rapidities

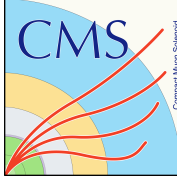


Average total energy as well as the hadronic and electromagnetic components of it are measured with the CMS detector **at $-6.6 < \eta < -5.2$** in pp collisions at 13 TeV and are presented **as a function of the multiplicity of charged particle tracks in the region $|\eta| < 2$**

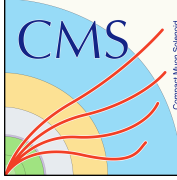
This measurement is **sensitive to correlations induced by the underlying event structure** over very wide pseudorapidity regions.

- CASTOR (Centauro And STRange Object Research) extends ($-6.6 < \eta < -5.2$) the CMS capability to investigate physics processes at very low polar angles and so, providing a **valuable tool to study low-x QCD, diffractive scattering, MPI and UE.**
- Studying low-x ($x = p_{\text{parton}}/p_{\text{hadron}}$) QCD is a key to understand the structure of the proton. At the LHC **the minimum accessible x in pp collisions decreases by a factor of about 10 for each 2 units of rapidity** -> a process with a hard scale of $Q \sim 10$ GeV and within the **CASTOR acceptance can probe quark densities down $x \sim 10^{-6}$** , that has never been achieved before (e.g. production of forward jets and Drell-Yan electron pairs)
- Very useful tool to measure the single-diffractive productions of W and dijets in pp (hard diffractive processes that are sensitive to the quark and gluon content of the low-x proton PDFs, correspondingly)

UE at forward rapidities



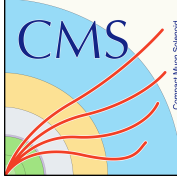
- Data:
 - Low-lumi 13 TeV run in June 2015 (CMS solenoid turned off), 0.22 fb^{-1}
- MC samples:
 - Py8 (version 8.212) with tune CUETP8M1 and 4C, combined with the MBR model to describe diffractive processes.
 - EPOS LHC
 - SIBYLL 2.1.
 - Furthermore, predictions by QGSJETII.04, SIBYLL 2.3c, PYTHIA 8 tune CP5, and HERWIG 7.1 with the default tune for soft interactions are also compared to the data (These simulations are produced only at generator level. A forward folding method is developed to compare generator-level simulations to the data)
- Selection (optimised to select inelastic collision events with minimal bias):
 - Online: unbiased trigger requiring only the presence of two colliding bunches
 - Offline:
 - at least one HF calorimeter tower with the reconstructed $E > 5 \text{ GeV}$ on either the positive or negative η side of the CMS detector
 - at least one track in the CMS tracker with $|\eta| < 2$
 - Reject events with 2 reco vertices is $\Delta Z > 0.5 \text{ cm}$
- Events are classified per track multiplicity (up to 150) and the average total, electromagnetic and hadron energy is measure per track multiplicity bins



UE at forward rapidities

- Statistical uncertainty $< 2\%$
- Measurement dominated by systematic uncertainties
- Most of the uncertainties fully correlated between the total, electromagnetic, and hadronic energy \rightarrow they cancel in ratios between the electromagnetic and hadronic components. Not true for the intercalibration uncertainty: a systematic decrease of the electromagnetic energy causes an increase of the hadronic energy, which leads to an asymmetric uncertainty on the ratio.

Source	Total energy	Electromagnetic energy	Hadronic energy
CASTOR energy scale	17%	17%	17%
CASTOR intercalibration	2–3%	–8%	+15%
HF energy scale	$<0.5\%$	$<0.5\%$	$<0.5\%$
Tracking efficiency	1–5%	1–5%	1–5%
Pileup rejection	1–8%	1–8%	1–10%
Statistical uncertainty	0.05–1.6%	0.06–1.9%	0.06–1.8%
Total	18–19%	18–20%	20–26%



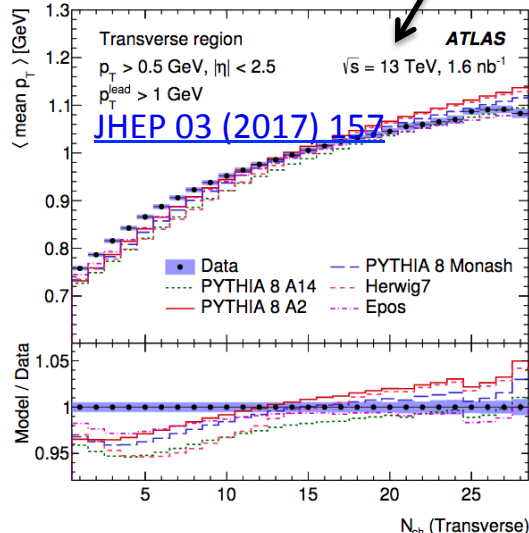
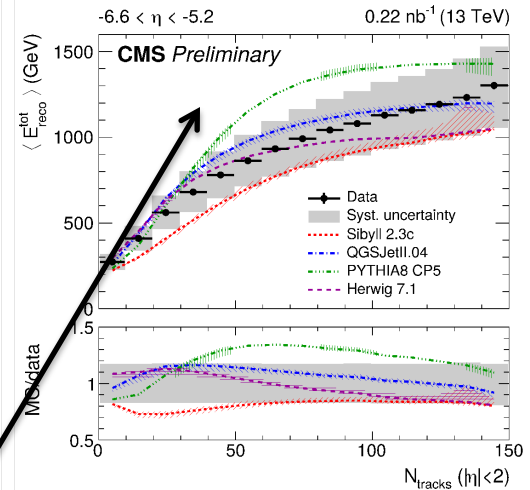
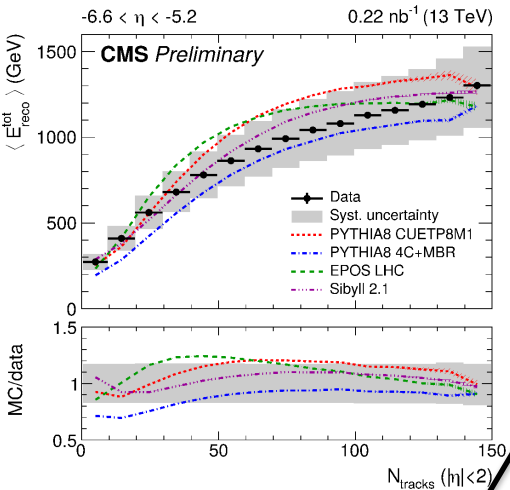
UE at forward rapidities

Full detector simulation

Forward folding method (consistent with full det. sim. To better than 1%)

- PYTHIA8 CUETP8M1
- .-.- PYTHIA8 4C+MBR
- .-.- EPOS LHC
- .-.- Sibyll 2.1

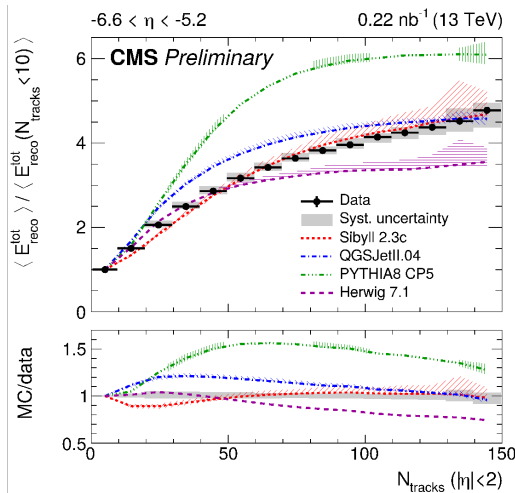
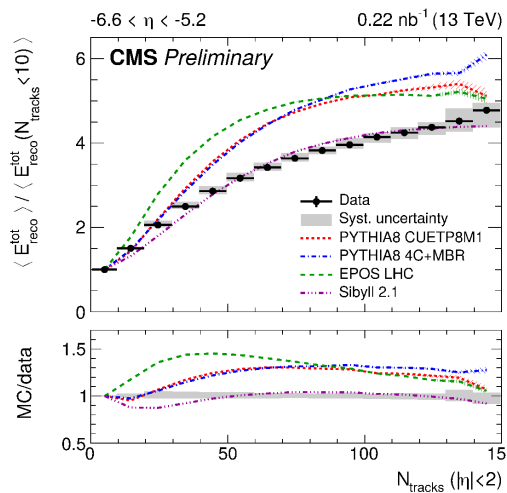
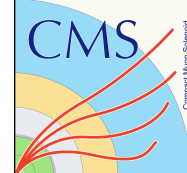
- Sibyll 2.3c
- .-.- QGSJetII.04
- .-.- PYTHIA8 CP5
- .-.- Herwig 7.1



- Average total energy increases with multiplicity, consistent with the general behaviour of the underlying event measured at central rapidities
- This shape can be associated to an initial correlation of central-to-forward event activity, which is dampened by energy conservation towards more violent collisions.
- All models describe these data with minor tensions only.
- Thus, the model parameter tunes for the underlying event, as determined at central rapidities, are consistent with the very forward data within experimental uncertainties.

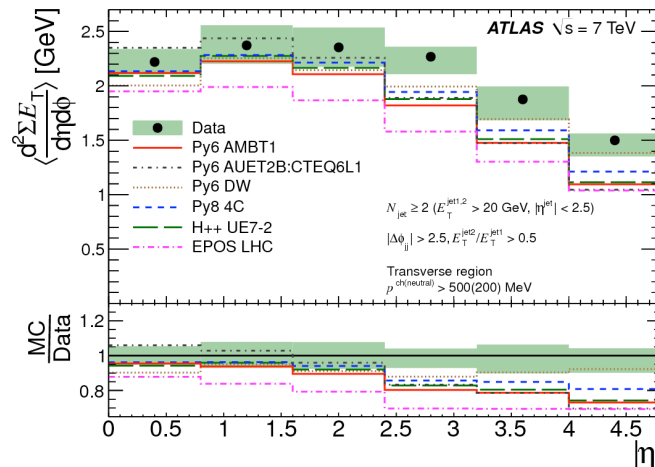
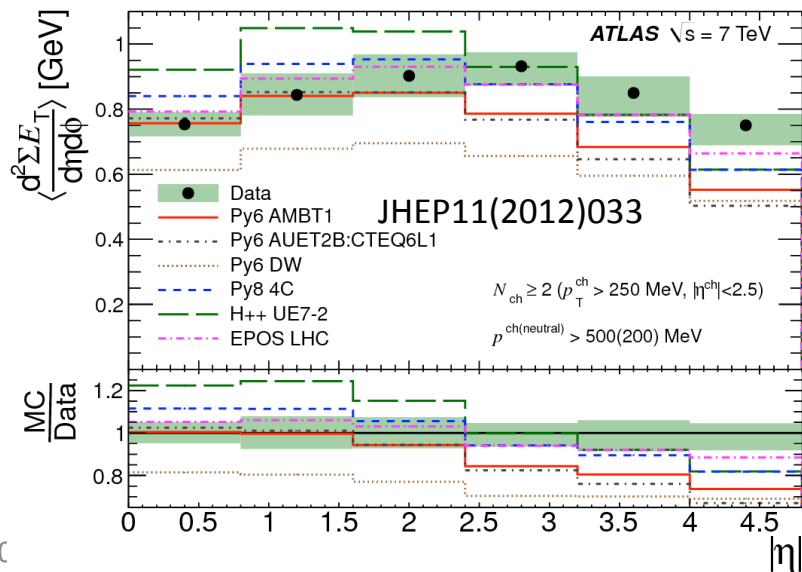
PYTHIA 8 4C+MBR and SIBYLL 2.3c underestimate data at low Nch
 PYTHIA 8 CP5 predicts average energies larger than those observed at intermediate Nch

UE at forward rapidities

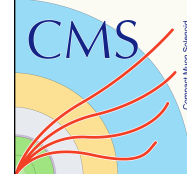


• These normalized results indicate some interesting potential to further improve the underlying event model predictions in the very forward direction!

- Distributions normalised to the first Nch bin (Nch<10) → systematic uncertainty dominated by the energy scale correlated in Nch bins, is reduced
- Relative increase is steep at low multiplicities and becomes softer at higher multiplicities.
- Py 8 tunes have very similar shapes, inconsistent with that observed in the data (worst for Py8 CP5, optimised for UE at central rapidity)
- All the other generators see a saturation at about Nch 80, not visible in data
- Both versions of SIBYLL provide predictions in agreement with the data.



UE at forward rapidities

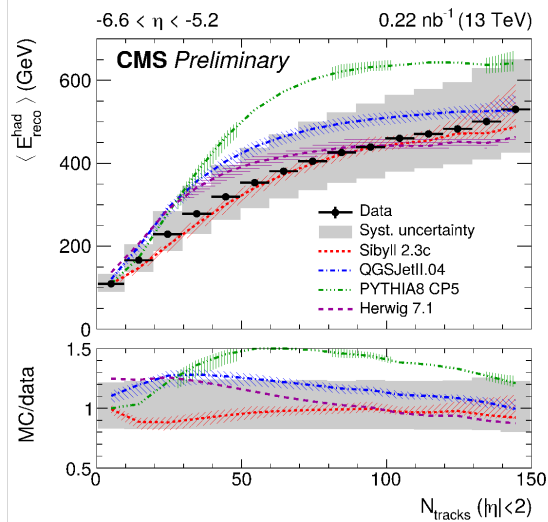
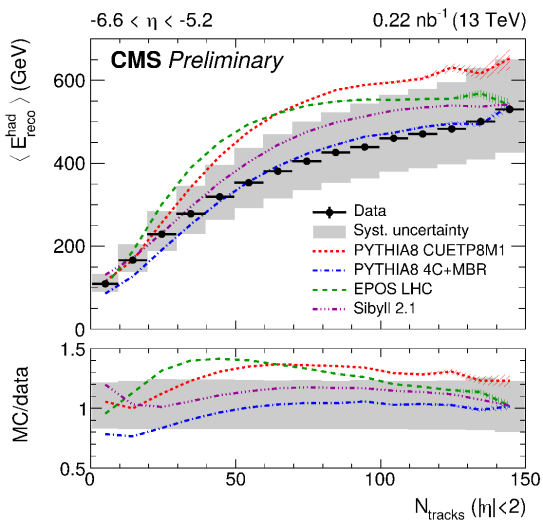
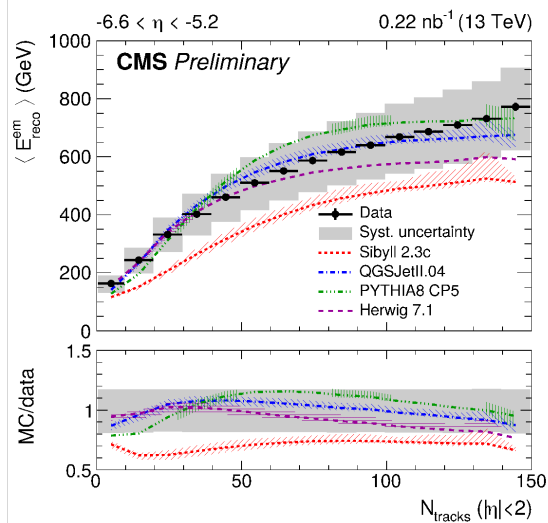
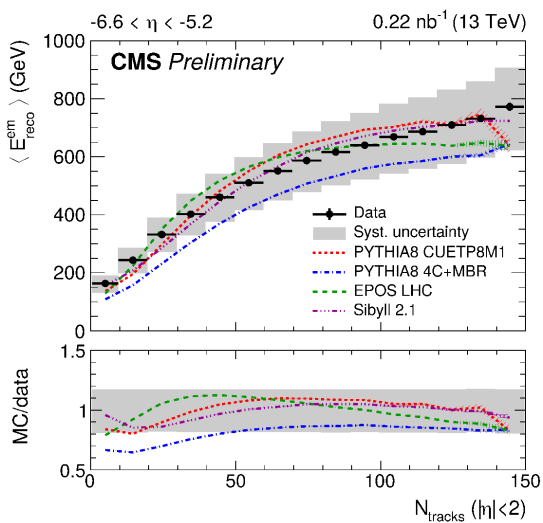


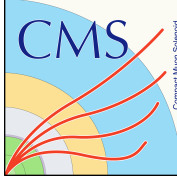
Useful to study different underlying particle production mechanisms, since the el is mostly due to decaying neutral pions, and the hadr is related to the production of non-resonant hadrons; most commonly charged pions.

- All models, with the exception of SIBYLL 2.3c, describe the electromagnetic component well. Also PYTHIA 8 4C+MBR slightly underestimates the electromagnetic energy at low multiplicities.
- Most models tend to overestimate the hadronic component, again with the exception of SIBYLL 2.3c and PYTHIA 8 4C+MBR.

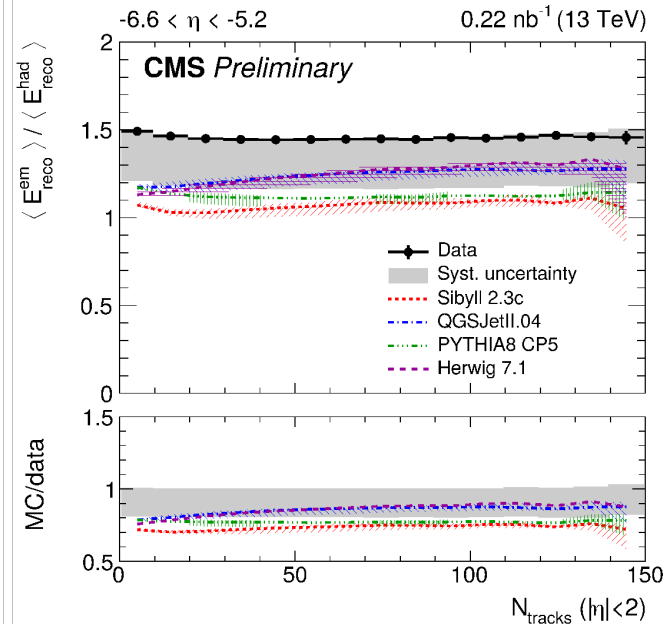
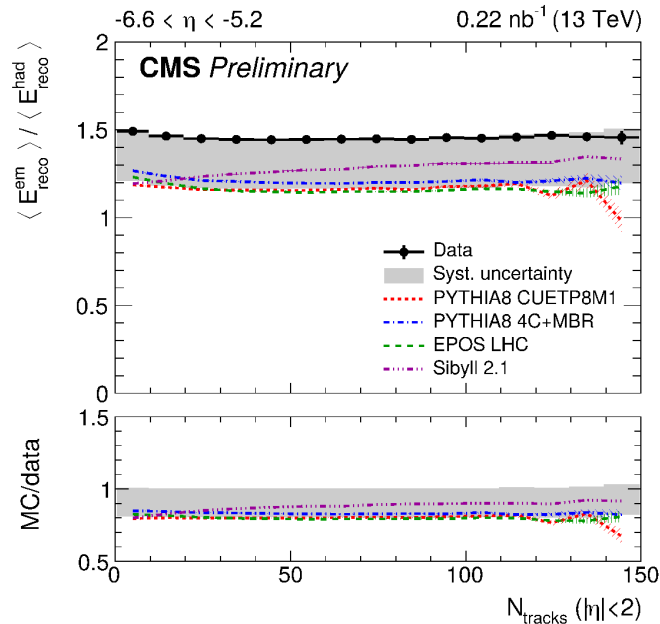
These data can be in particular relevant in the context of the simulation of cosmic ray induced extensive air showers since they point to the accuracy of the modelling of the production of neutral pions versus charged pions or other non-resonant hadrons.

As the energies in $-6.6 < \eta < -5.2$ are already close to the peak of the forward-directed energy flow, this will have an important impact on modelling of complete extensive air shower cascades.



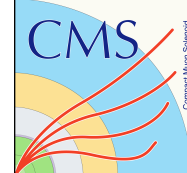


UE at forward rapidities



- Relative calibration of the electromagnetic and hadronic section is the main source of uncertainty and results in a highly asymmetric uncertainty band.
- The measured ratio is approximately constant over the whole multiplicity range.
- This measured ratio depends on the details of hadronization in the observed phase space. Deviations of model predictions from the data hint on underlying differences of final state hadron production mechanisms contributing to the observed average energies.
- The contribution of string fragmentation, remnant fragmentation, initial- or final-state radiation, or eventual effects of a very dense hydrodynamical phase have to be considered to understand these data.
- Also the decay of short-lived resonances has an important impact on this ratio.
- The observed independence of the measured ratio from track multiplicity indicates that no dramatic change of the particle production mechanism is observed at this very forward pseudorapidity.
- All model predictions are lower than the data, specifically those of the modern tunes, PYTHIA 8 CP5 and SIBYLL 2.3c, whereas the QGSJETII.04, SIBYLL 2.1, and HERWIG 7.1 models give the best description of the ratio within the systematic uncertainties.

UE at forward rapidities



- The average energy per event in the pseudorapidity region $-6.6 < \eta < -5.2$ has been measured as a function of the observed central track multiplicity ($|\eta| < 2$) in proton-proton collision at a centre-of-mass energy of 13 TeV. Data recorded during the first days of the LHC Run 2, with low beam intensities, are used. The measurement is presented in terms of the total energy as well as its electromagnetic and hadronic components. The very forward region covered by the data contains the highest energy densities studied in proton-proton collisions at the LHC. This makes the data in particular relevant for improving the modeling of multiparticle production in event generators used for the simulation of ultra-high energy cosmic ray air showers.
- The observables introduced provide a new approach to characterise particle production, and to study the properties of the underlying event. The measured average total energy as function of the track multiplicity is described with only minor tension by all models. This is a very good indication that underlying event parameter tunes performed at mid-rapidity can be extrapolated to the very forward direction within experimental uncertainties. However, it is also found that in a shape analysis of the same data we see very significant model differences and partly large deviations from the data. Thus, there is remaining opportunity to further improve the particle production models in this very forward phase space. Among all models, SIBYLL 2.1 shows the best reproduction of the measured multiplicity dependence of the average total energy.
- The data is also presented separately for the average electromagnetic and hadronic energy per event as a function of central track multiplicity. This is useful to study different underlying particle production mechanisms, since the former is mostly due to decaying neutral pions, and the latter related to the production of non-resonant hadrons; most commonly charged pions. We find a general good description of all models of the electromagnetic energy – with the exception of SIBYLL 2.3c. Notably, the predicted energy in hadrons reveals a significantly larger spread compared to the electromagnetic energy between the different models.
- The data are also presented in terms of the ratio between the electromagnetic and hadronic energies. The data exhibit a larger fraction of electromagnetic energy compared to the models, and disagree with the two most recent model tunes, SIBYLL 2.3c and PYTHIA 8 CP5. This deficiency implies an increased difficulty to solve the muon deficit in ultra-high energy air shower simulations since more energy will be channelled into the electromagnetic part of the cascade and will subsequently be lost for the generation of further hadrons .

SPS qq 4l: Powheg-Box at NLO

QCD (qg incl. in the NLO)

gg: LO MCFM, with NLO
corrections

On-shell gg H and VBF H:

Powheg-Box at NLO QCD

On-shell VH and ttH: LO Py8

off-shell VBF/VBS H: LO

MadGraph

All showered with Py8 (MG with
Py6)

DPS 4l: Py8 LO

Background from Z + jets

(AlpGen), $t\bar{t}$, dibosons (Sherpa),
tribosons (MG), VH (Py8), Z+top
(MG)

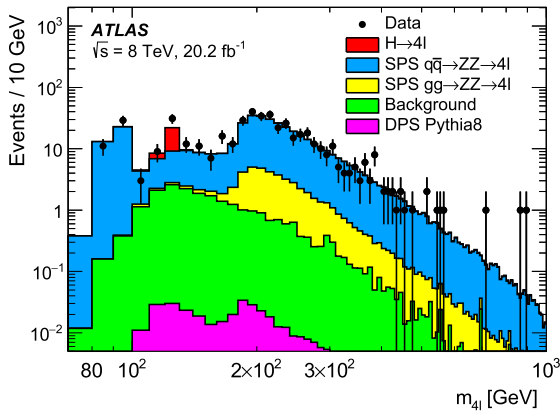
Signal: Py8 and, for cross
checks, with Hw++

WZ: Powheg (central
predictions), MADGRAPH5
aMC@NLO (kinematics
studies)

$W\gamma$: MADGRAPH 5; $Z\gamma$:
MADGRAPH5 aMC@NLO
FxFx and MLM merging
schemes for NLO and LO,
resp.

$W\gamma^*$, SHS WW, and ZZ at
NLO with the POWHEG
All showered with Py8

DPS in inclusive four-lepton production

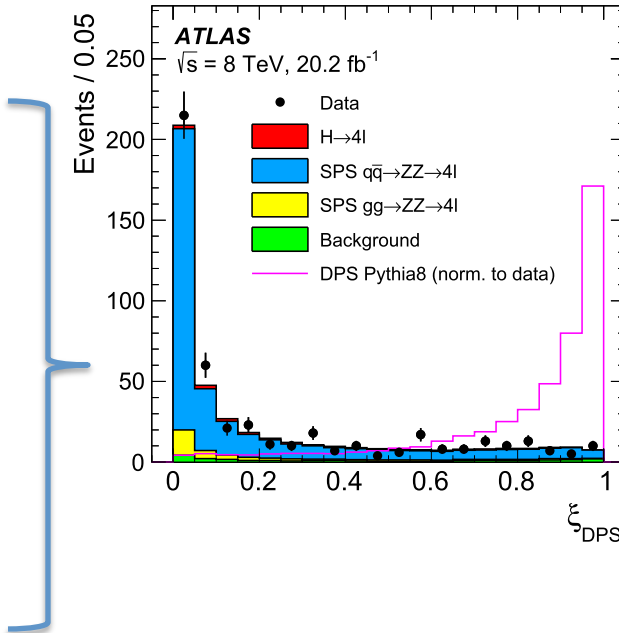
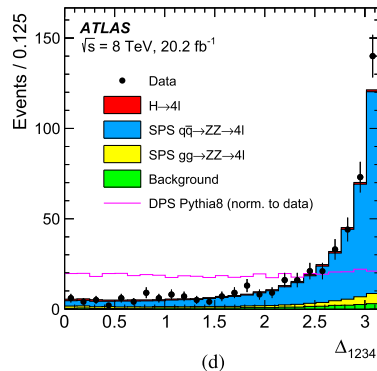
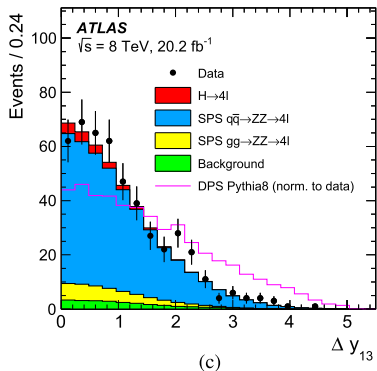
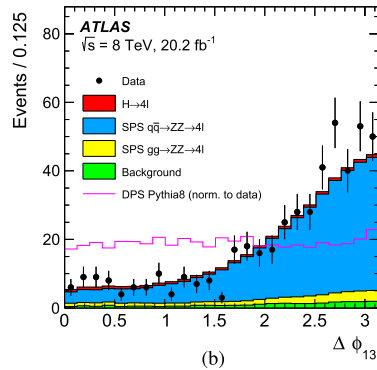
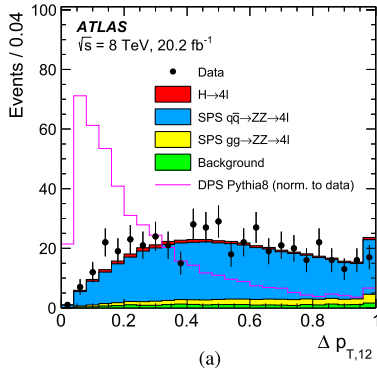


- In the DPS 4l final states, the two leptons of each dilepton will tend to be balanced in pT and back-to-back in ϕ , due to the dominance of low-pT Z(*) production.
- In the SPS case, the leading and sub-leading pairs are expected to balance each other in pT.

$$\Delta p_{T,ij} = \frac{|\vec{p}_{T,i} + \vec{p}_{T,j}|}{p_{T,i} + p_{T,j}}, \quad \Delta \phi_{ij} = |\phi_i - \phi_j|,$$

$$\Delta y_{ij} = |y_i - y_j|, \quad i, j = 1, 2, 3, 4, \quad i \neq j$$

$$\Delta i_{jkm} = |\phi_{i+j} - \phi_{k+m}|, \quad ijkm = 1234, 1324, 1423.$$



$$f_{\text{DPS}} = \frac{N_{\text{DPS},4\ell}}{N_{\text{SPS},4\ell} + N_{\text{DPS},4\ell}}$$

$$= -0.009 \pm 0.017$$

Consistent with zero

DPS in inclusive 4l production

$$\frac{1}{\sigma_{\text{eff}}} = \frac{f_{\text{DPS}} \sigma^{4\ell}}{\frac{k}{2} \sigma_{\text{SPS}}^A \sigma_{\text{SPS}}^B},$$

$$\sigma_{4\ell} = 32.0 \pm 1.6 \text{ (stat.)} \pm 0.7 \text{ (syst.)} \pm 0.9 \text{ (lumi.) fb.}$$

$$\frac{k}{2} \sigma_A \sigma_B = (13.9 \pm 0.1 \text{ (stat)} \pm 3.6 \text{ (syst)}) \cdot 10^{11} \text{ fb}^2.$$

DPS in same-sign WW

Backgrounds:

- processes with genuine same-charge lepton pairs from leptonic decays of bosons produced at the hard scattering
 - Mainly WZ process. Other such processes include $W\gamma^*$, $W\gamma$, $Z\gamma$, and ZZ production, as well as to a lesser extent SHS $W^\pm W^\pm$ and WWW processes .
- Non-prompt lepton backgrounds in which one or two of the selected leptons do not originate from the decay of a massive boson from the hard scattering (W+jets, QCD MJ, ttbar to a a smaller extend).
- charge misidentification, arises from the misassignment of the electric charge to an electron (main such background from Z-> tautau, when both τ leptons de- cay leptonically to form an electron-muon pair.)

Dominant contributions from WZ (very similar kinematics to that of the signal, i.e. no hadronic activity in form of high pt jet, but Lorentz boost sharing along z-axis for WZ) and non prompt leptons (kinematics differences larger, but also much larger cross-sections)

11 variables used to train 2 BTDs against these backgrounds (MC for the WZ and data-driven control sample for non-prompt leptons) \rightarrow 2D classifier with 15 bins to optimize the constraining power of the maximum likelihood fit

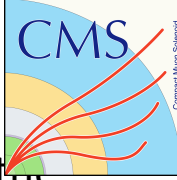
DPS in same-sign WW

Systematic uncertainties: overall normalization and shape uncertainties

- Largest uncertainty from the method used to evaluate non-prompt leptons, up to 40% normalization uncertainty and 10% shape uncertainty
- 30% norm. unc. on charge mis-id
- Normalization uncertainties for the main backgrounds estimated from simulation are derived in dedicated 3-lepton (4-lepton) control regions for the WZ (ZZ) processes. The background components are fit to the data in these regions. Norm unc. of 16 (6)% is applied.
- A 50% normalization uncertainty is applied to all other simulation-derived backgrounds
- Pile up modelling 1% unc.
- Lumi 2.5 (2.3)% for the 2016 (2017)
- Trigger and jet energy scale at % level
- Model dependence in signal (Py8 vs H++) → small variations in BDT

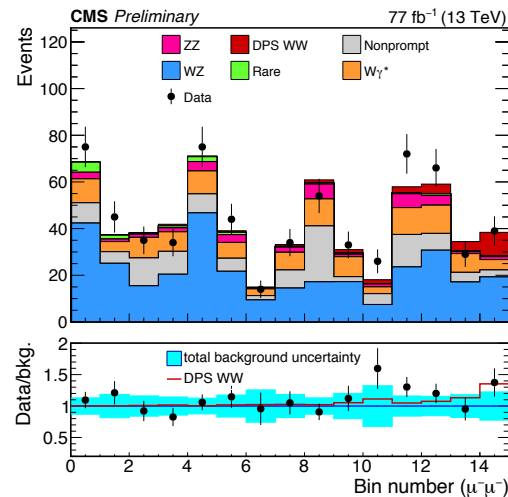
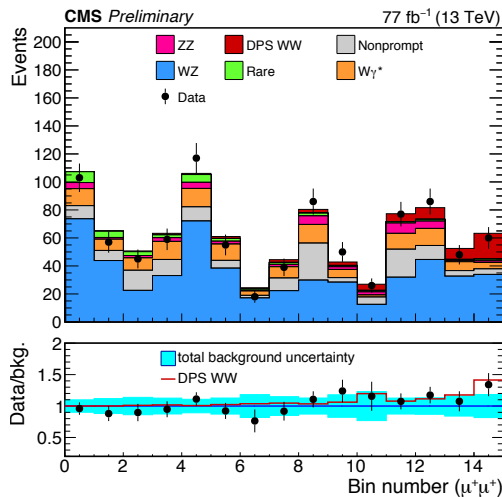
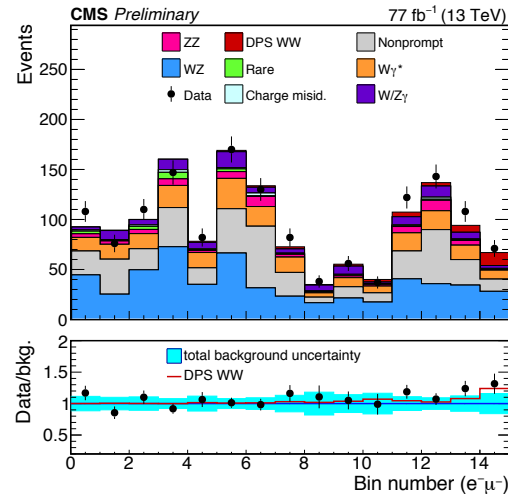
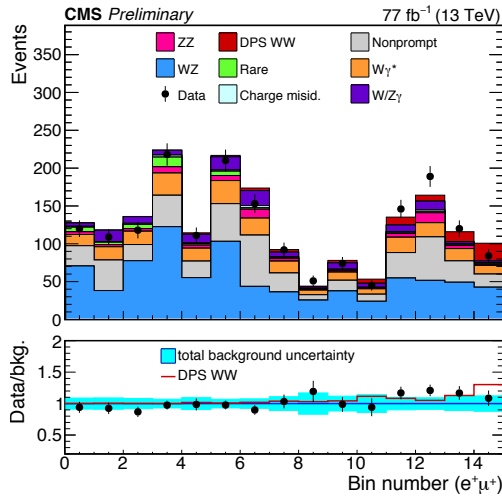
	$\mu^+\mu^+$	$\mu^-\mu^-$	$e^+\mu^+$	$e^-\mu^-$
Nonprompt	141.8 ± 11.9	117.7 ± 10.9	461.7 ± 21.5	411.2 ± 20.3
WZ	537.0 ± 23.2	328.5 ± 18.1	833.5 ± 28.9	543.1 ± 23.3
ZZ	43.6 ± 6.6	37.7 ± 6.1	71.0 ± 8.4	65.7 ± 8.1
$W\gamma^*$	133.1 ± 11.5	118.0 ± 10.9	255.5 ± 16.0	226.9 ± 15.1
Rare	34.7 ± 5.9	13.5 ± 3.7	48.4 ± 7.0	23.2 ± 4.8
$W/Z\gamma$	—	—	17.0 ± 4.1	17.1 ± 4.1
Charge misid.	—	—	131.4 ± 11.5	104.2 ± 10.2
Total background	890.2 ± 29.8	615.3 ± 24.8	1818.5 ± 42.6	1391.4 ± 37.3
DPS WW	56.8 ± 7.5	28.9 ± 5.4	76.5 ± 8.8	40.1 ± 6.3
Data	926	675	1840	1480

Given the fact that the signal process is enhanced in the l+l+ configuration and the background processes show more symmetry between the two charges, the classification into the two charge configurations increases the sensitivity of the analysis



DPS in same-sign WW

The uncertainty in the extrapolation from the measurement phase space to the inclusive phase space is assumed to be negligible.



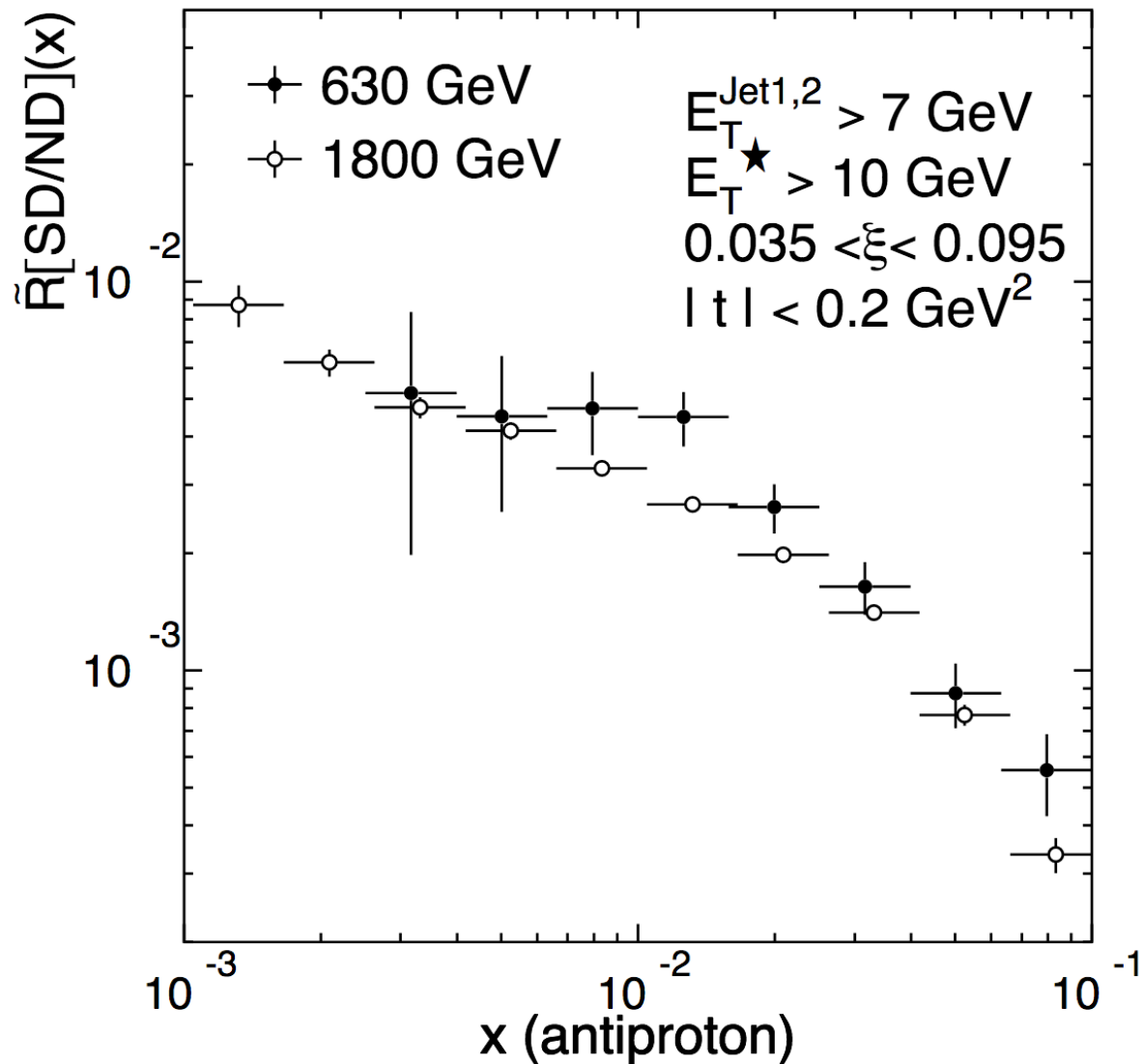
Totem

ALFA

vertically oriented 'Roman pot station' insertions to the beam-pipe at 237 m and 241 m from the interaction point on both sides of ATLAS, housing movable scintillating fibre detectors.

Diffractive di-jet production

Phys. Rev. Lett. 88 (2002) 151802



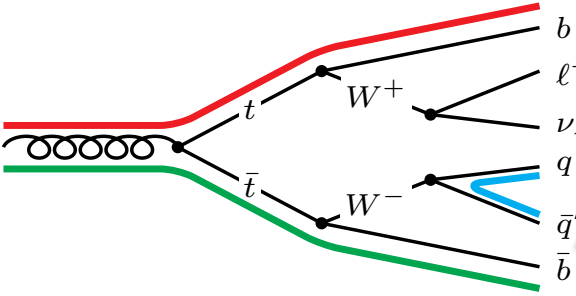
Measurement of colour flow using jet-pull observables with Top-pairs

CERN-EP-2018-041, Submitted to EPJC

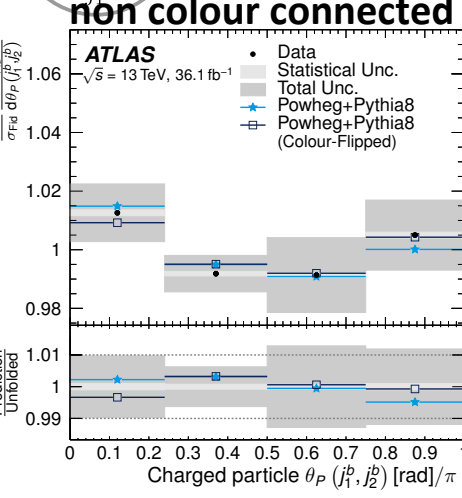
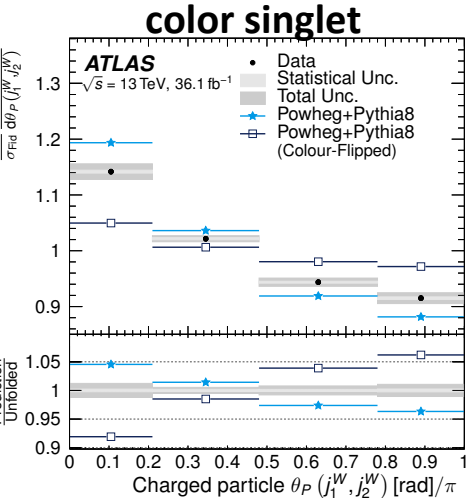
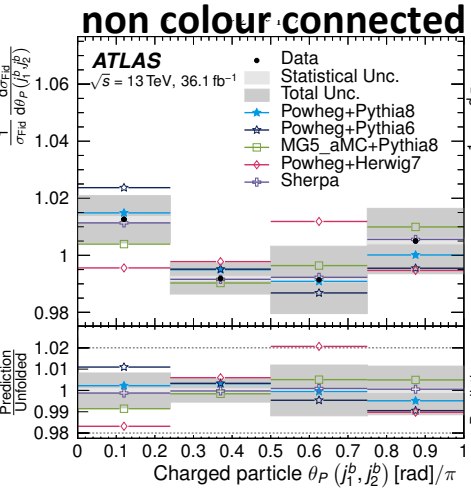
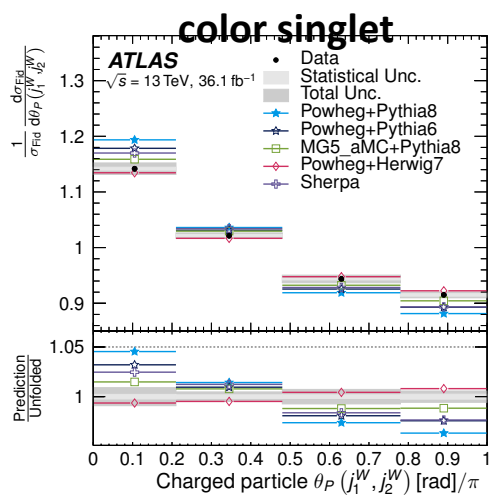
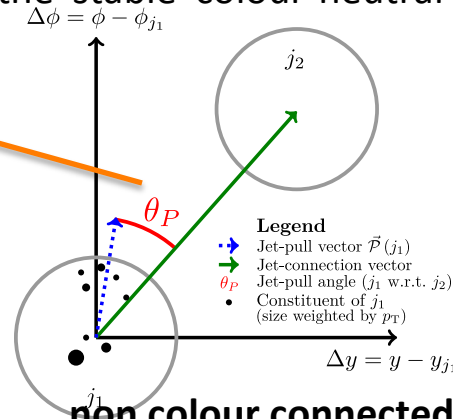
In the decay chain of a hard-scatter event, the colour charge “flows” from the initial state towards stable particles:



As colour charge is conserved, connections exist between initial particles and the stable colour-neutral hadrons.



normalised **jet-pull angle** measured for two different systems of dijets:
Color singlet and non-colour connected

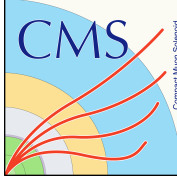


Powheg+H7 describes data better than Powheg+Py8

Good predictions by Sherpa, worst predictions by Powheg+H7

Data prefer SM color flow predictions

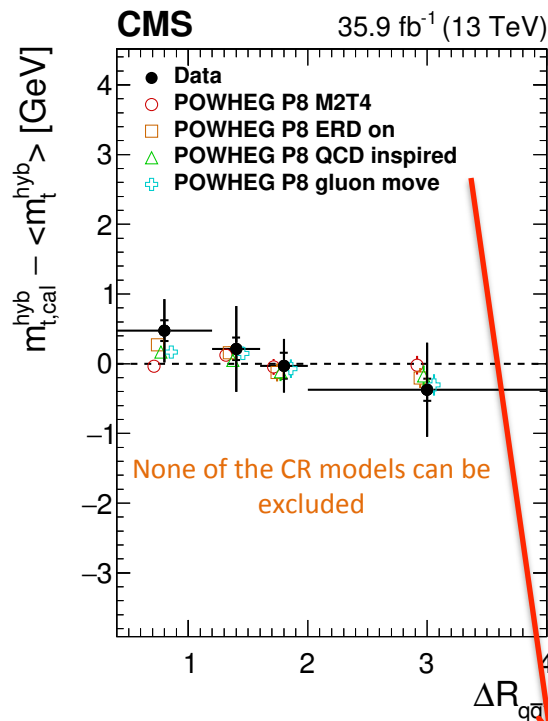
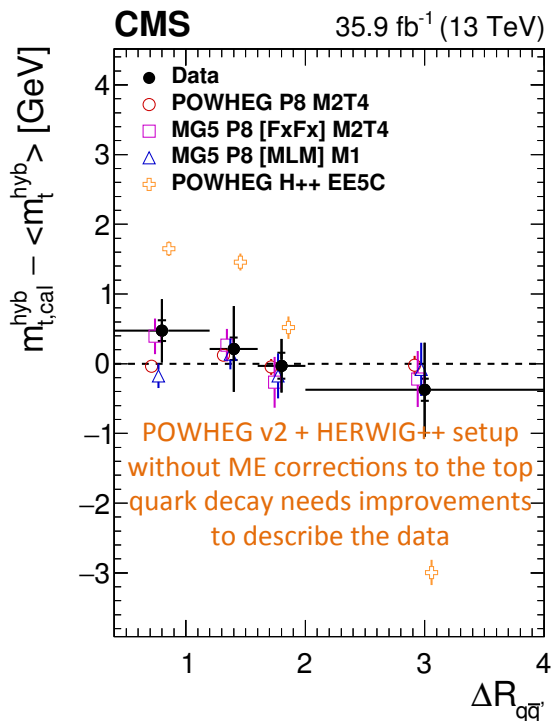
Predictions within the uncertainties



Still on PS and Colour reconnection...

Measurement of the **top quark mass with lepton+jets** final states using pp collisions at @ 13 TeV

- **Mass extraction closely follows** the strategy of the most precise **CMS Run 1** measurement
- But **new simulations** describe the data better and allow a more refined estimation of the **modeling uncertainties**
- Renormalization and factorization scales in the **ME calculation** and the **PS scales** are now varied separately for the evaluation of systematic effects. Impacts of different **models of CR** (that were not available for the Run 1 measurements) are also tested



	2D approach δm_t^{2D} [GeV]	1D approach δm_t^{1D} [GeV]	Hybrid δm_t^{hyb} [GeV]	δJSF^{hyb} [%]
<i>Experimental uncertainties</i>				
Method calibration	0.05	<0.1	0.05	0.05
JEC (quad. sum)	0.13	0.2	0.83	0.18
- InterCalibration	(-0.02)	(<0.1)	(+0.16)	(+0.04)
- MPFIInSitu	(-0.01)	(<0.1)	(+0.23)	(+0.07)
- Uncorrelated	(-0.13)	(+0.2)	(+0.78)	(+0.16)
Jet energy resolution	-0.08	+0.1	+0.04	-0.04
b tagging	+0.03	<0.1	+0.01	+0.03
Pileup	-0.08	+0.1	+0.02	-0.05
Non-fit background	+0.04	-0.1	-0.02	+0.02
<i>Modeling uncertainties</i>				
JEC Flavor (linear sum)	0.42	0.1	0.31	0.39
- light quarks (uds)	(+0.10)	(-0.1)	(-0.01)	(+0.06)
- charm	(+0.02)	(<0.1)	(-0.01)	(+0.01)
- bottom	(-0.32)	(<0.1)	(-0.31)	(-0.32)
- gluon	(-0.22)	(+0.3)	(+0.02)	(-0.15)
b jet modeling (quad. sum)	0.13	0.1	0.09	0.12
- b frag. Bowler-Lund	(-0.07)	(+0.1)	(-0.01)	(-0.05)
- b frag. Peterson	(+0.04)	(<0.1)	(+0.05)	(+0.04)
- semileptonic B decays	(+0.11)	(<0.1)	(+0.08)	(+0.10)
PDF	0.02	<0.1	0.02	0.02
Ren. and fact. scales	0.02	0.1	0.02	0.01
ME/PS matching	-0.08	+0.1	+0.03	-0.05
ME generator	+0.19 ± 0.14	+0.1	+0.29 ± 0.08	+0.22 ± 0.11
ISR PS scale	+0.07 ± 0.09	+0.1	+0.10 ± 0.05	+0.06 ± 0.07
FSR PS scale	+0.24 ± 0.06	-0.4	-0.22 ± 0.04	+0.13 ± 0.05
Top quark p _T	+0.02	-0.1	-0.06	-0.01
Underlying event	-0.10 ± 0.08	+0.1	+0.01 ± 0.05	-0.07 ± 0.07
Early resonance decays	-0.22 ± 0.09	+0.8	+0.42 ± 0.05	-0.03 ± 0.07
Color reconnection	+0.34 ± 0.09	-0.1	+0.23 ± 0.06	+0.31 ± 0.08
Total systematic	0.72	1.0	1.09	0.62
Statistical (expected)	0.09	0.1	0.06	0.08
Total (expected)	0.72	1.0	1.09	0.62

$$m_t^{hyb} = 172.25 \pm 0.08 \text{ (stat+JSF)} \pm 0.62 \text{ (syst)} \text{ GeV}$$

CR modelling contributes one of the largest sources of uncertainty!

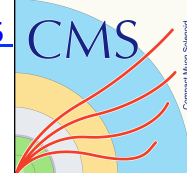


Studies of Underlying Event in Top-pairs

Table 1: Monte Carlo setups used for the comparisons with the differential cross section measurements of the UE. The table lists the main characteristics and values used for the most relevant parameters of the generators. The row labeled as “Setup designation” is used to define the abbreviation to be used throughout this paper.

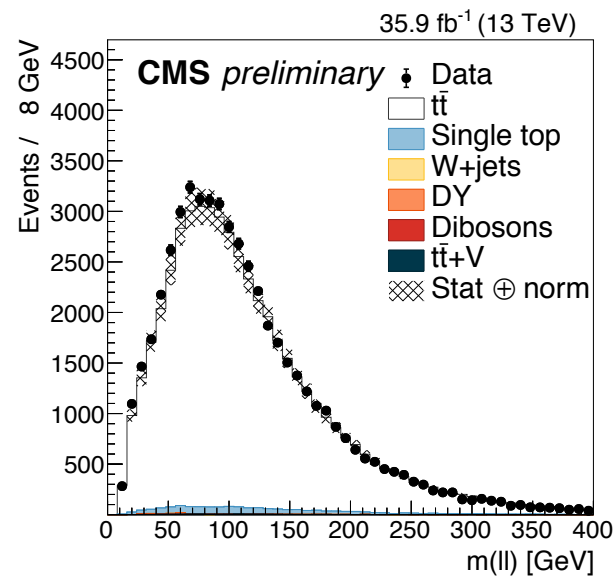
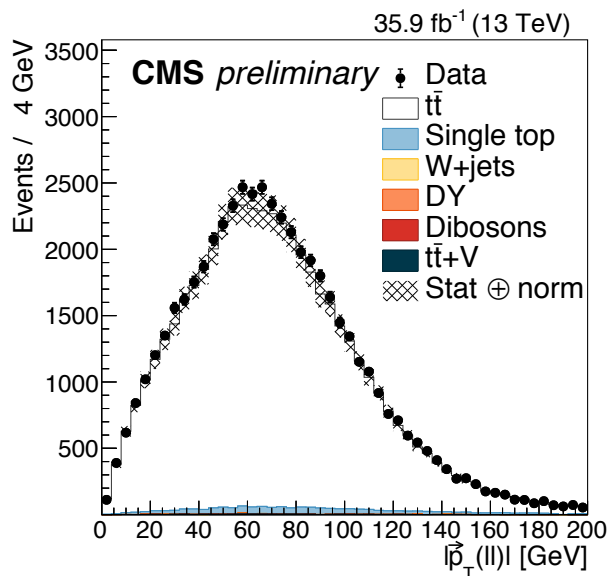
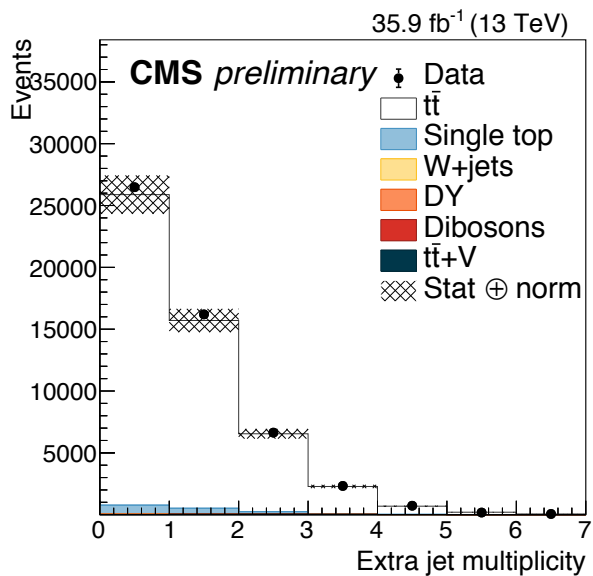
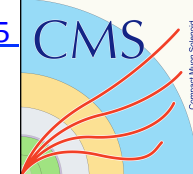
Event generator	POWHEG (v2)	MG5_aMC@NLO	SHERPA 2.2.4
<i>Matrix element characteristics</i>			
Mode	hvq	FxFx Merging	OPENLOOPS
QCD scales (μ_R, μ_F)	m_T^{\dagger}	$\sum_{t,\bar{t}} m_T/2$	
α_S	0.118	0.118	0.118
PDF	NNPDF3.0 NLO	NNPDF3.0 NLO	NNPDF3.0 NNLO
pQCD accuracy	t \bar{t} [NLO] 1 jet [LO]	t \bar{t} +0,1,2 jets [NLO] 3 jets [LO]	t \bar{t} [NLO]
<i>Parton shower</i>			
Setup designation	PW+PY8	aMC@NLO+PY8	SHERPA
PS		PYTHIA 8.219	CS
Tune(s)		CUETP8M2T4	default
PDF		NNPDF2.3 LO	NNPDF3.0 NNLO
($\alpha_S^{ISR}, \alpha_S^{FSR}$)		(0.1108,0.1365)	(0.118,0.118)
ME Corrections		on	n/a
Setup designation	PW+HW++	PW+HW7	
PS	HERWIG++	HERWIG 7	
Tune(s)	EE5C	Default	
PDF	CTEQ6L1	MMHT2014lo68cl	
($\alpha_S^{ISR}, \alpha_S^{FSR}$)	(0.1262,0.1262)	(0.1262,0.1262)	
ME Corrections	off	on	

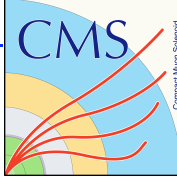
Studies of Underlying Event in Top-pairs



Parameter	Pw+Py8 simulation setups										
	CUETP8M2T4	Extreme variations		Fine grain variations							
		no MPI	no CR	MPI/CR	Parton shower scale			CR including $t\bar{t}$			
				UE up/down	ISR up/down	FSR up/down	ERD on	QCD based [32]	Gluon move [4]	Rope (no CR) [33, 34]	
PartonLevel MPI	on	off									
SpaceShower renormMultFac alphaSvalue	1.0 0.1108				4/0.25			0.2521			
TimeShower renormMultFac alphaSvalue	1.0 0.1365					4/0.25		0.2521			
MultipartonInteractions pT0Ref ecmPow expPow	2.2 0.2521 1.6			2.20/2.128 1.711/1.562				2.174 0.2521 1.312	2.3 1.35		
ColorReconnection reconnect range mode junctionCorrection timeDilationPar m0 flipMode m2Lambda fracGluon dLambdaCut	on 6.59 0		off	6.5/8.7				1 0.1222 15.86 1.204	2 0 1.89 1 0	(off)	
PartonVertex setVertex										on	
Ropewalk RopeHadronization doShoving doFlavour										on on on	
PartonLevel earlyResDec	off						on	on	on	on	

Studies of Underlying Event in Top-pairs

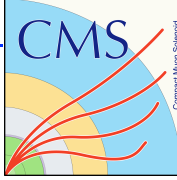




Studies of Underlying Event in Top-pairs

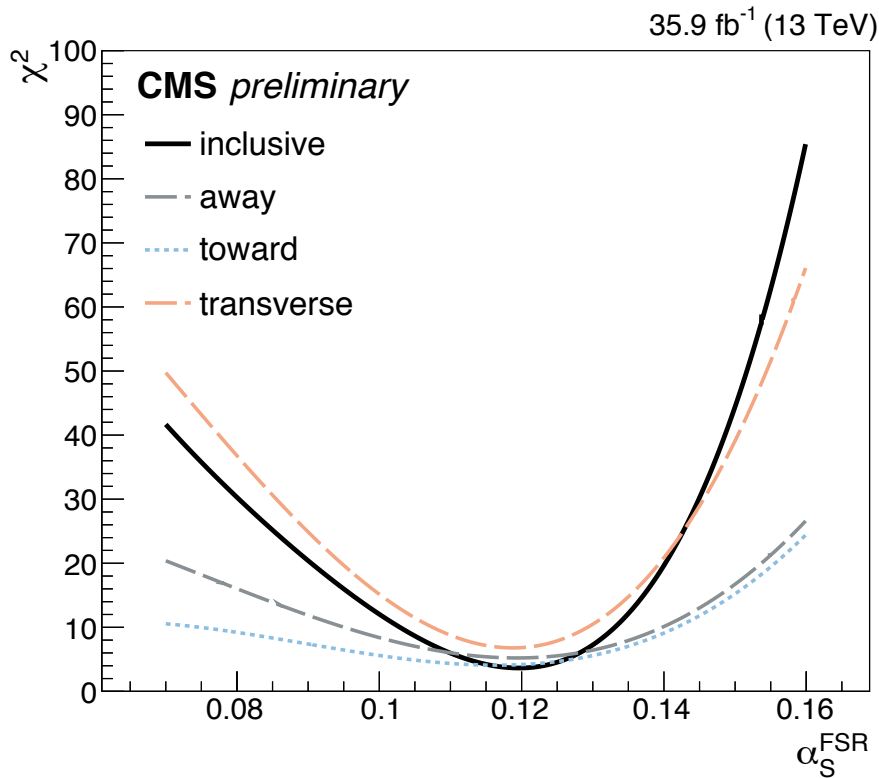
Source	Variable									
	N_{ch}	$\sum p_T$	$\sum p_z$	\bar{p}_T	\bar{p}_z	$ \vec{p}_T $	Sphericity	Aplanarity	C	D
Statistical	0.1	0.2	0.4	0.2	0.2	0.3	0.1	0.2	0.1	0.2
Experimental										
Background	1.2	1.6	1.8	0.4	0.7	1.6	0.2	0.7	0.3	0.6
Trk. eff.	4.4	4.2	4.9	0.8	0.4	4.0	0.5	0.7	0.3	0.7
Theory										
μ_R / μ_F	0.5	0.8	1.0	0.3	0.3	1.0	0.1	0.2	0.1	0.1
Resummation scale	0.2	0.8	0.5	1.1	0.2	1.6	0.8	1.1	0.7	1.0
α_S^{FSR}	0.5	0.7	0.7	0.8	1.7	0.7	0.2	1.5	0.2	0.9
α_S^{ISR}	0.1	0.3	1.1	1.2	0.7	0.4	0.3	0.5	0.2	0.4
UE model	0.1	0.1	0.2	1.0	0.4	0.5	0.4	1.3	0.2	0.5
m_t	0.4	0.7	1.5	0.6	0.9	0.5	0.3	1.4	0.3	1.0
$p_T(t)$	1.4	4.4	4.5	2.8	2.1	6.7	0.3	0.7	0.4	0.7
Total	4.9	6.5	7.3	3.7	3.1	8.2	1.2	3.0	1.0	2.2

Largest systematics from top p_T modelling



Studies of Underlying Event in Top-pairs

While no sensitivity has been found to α_{SR} , most observables are influenced by the choice of α_{FSR} . The most sensitive distribution is found to be \vec{p}_T



$ \vec{p}_T(\ell\ell) $ region	Inclusive	Away	Toward	Transverse
Best fit α_S^{FSR}	0.120	0.119	0.116	0.119
68% CI	[-0.006,+0.006]	[-0.011,+0.010]	[-0.013,+0.011]	[-0.006,+0.006]
95.45% CI	[-0.013,+0.011]	[-0.022,+0.019]	[-0.030,+0.021]	[-0.013,+0.012]

A value of $\alpha_{\text{FSR}} = 0.120 \pm 0.006$ is obtained, which is lower than the one obtained in the Monash tune and used in the CUETP8M2T4 tune.